Modelling Chemical Kinetics and Vibrational Excitation in Plasma Discharges

Carlos Daniel Pintassilgo

Faculdade de Engenharia, Universidade do Porto, Portugal

Instituto de Plasmas e Fusão Nuclear, Instituto Superior Técnico, Universidade de Lisboa, Portugal

OUTLINE

Fundamentals

coupling between electron, chemical and vibrational kinetics

Typical examples

pulsed discharges (dry air, N_2)

Application to DBD discharges

N_2-O_2-H_2O plasmas (humid air)

OUTLINE

Fundamentals

coupling between electron, chemical and vibrational kinetics

Typical examples

pulsed discharges (dry air, N_2)

Application to DBD discharges

N_2-O_2-H_2O plasmas (humid air)

$$\frac{d}{du}\left[\left(\frac{eE}{N}\right)^2 \frac{u}{3\sigma_m^e}\frac{df_e^0}{du} + \frac{2m}{M}u^2\,\sigma_m\left(f_e^0 + k_B T_o\,\frac{df_e^o}{du}\right) + 4B_0\sigma_0\,u\,f_e^0\right]$$

$$+\sum_{i,j}\delta_i\left\{(u+u_{ij})\,\sigma_{ij}(u+u_{ij})\,f_e^0(u+u_{ij}) - u\,\sigma_{ij}(u)\,f_e^0(u)\right\}$$

$$+\sum_{j,i}\delta_j\left\{(u-u_{ij})\,\sigma_{ji}(u-u_{ij})\,f_e^0(u-u_{ij}) - u\,\sigma_{ji}(u)\,f_e^0(u)\right\} = 0\,.$$

$$\frac{d}{du}\left[\left(\frac{eE}{N}\right)^2 \frac{u}{3\sigma_m^e}\frac{df_e^0}{du} + \frac{2m}{M}u^2\,\sigma_m\left(f_e^0 + k_B T_o \frac{df_e^o}{du}\right) + 4B_0\sigma_0\, u\, f_e^0\right]$$

$$+\sum_{i,j}\delta_i\left\{(u+u_{ij})\,\sigma_{ij}(u+u_{ij})\,f_e^0(u+u_{ij}) - u\,\sigma_{ij}(u)\,f_e^0(u)\right\}$$

$$+\sum_{j,i}\delta_j\left\{(u-u_{ij})\,\sigma_{ji}(u-u_{ij})\,f_e^0(u-u_{ij}) - u\,\sigma_{ji}(u)\,f_e^0(u)\right\} = 0\,.$$

$$f(u) = \frac{1}{n_e}\frac{4\pi}{m}\sqrt{\frac{2}{m}}f_e^0(u)$$

$$\int_0^\infty f(u)\,\sqrt{u}\,du = 1$$

$$\frac{d}{du}\left[\left(\frac{eE}{N}\right)^2 \frac{u}{3\sigma_m^e}\frac{df_e^0}{du} + \frac{2m}{M}u^2\,\sigma_m\left(f_e^0 + k_B T_o \frac{df_e^o}{du}\right) + 4B_0\sigma_0\, u\, f_e^0\right]$$
$$+\sum_{i,j}\delta_i\left\{(u+u_{ij})\,\sigma_{ij}(u+u_{ij})\,f_e^0(u+u_{ij}) - u\,\sigma_{ij}(u)\,f_e^0(u)\right\}$$
$$+\sum_{j,i}\delta_j\left\{(u-u_{ij})\,\sigma_{ji}(u-u_{ij})\,f_e^0(u-u_{ij}) - u\,\sigma_{ji}(u)\,f_e^0(u)\right\} = 0\,.$$

$\delta_i = n_i/N$

fractional populations of molecules in vibrationally or electronically excited states *i*

$$\frac{d}{du}\left[\left(\frac{eE}{N}\right)^2 \frac{u}{3\sigma_m^e}\frac{df_e^0}{du} + \frac{2m}{M}u^2\,\sigma_m\left(f_e^0 + k_B T_o \frac{df_e^o}{du}\right) + 4B_0\sigma_0\,u\,f_e^0\right]$$

$$+\sum_{i,j}\delta_i\left\{(u+u_{ij})\,\sigma_{ij}(u+u_{ij})\,f_e^0(u+u_{ij}) - u\,\sigma_{ij}(u)\,f_e^0(u)\right\}$$

$$+\sum_{j,i}\delta_j\left\{(u-u_{ij})\,\sigma_{ji}(u-u_{ij})\,f_e^0(u-u_{ij}) - u\,\sigma_{ji}(u)\,f_e^0(u)\right\} = 0\,.$$

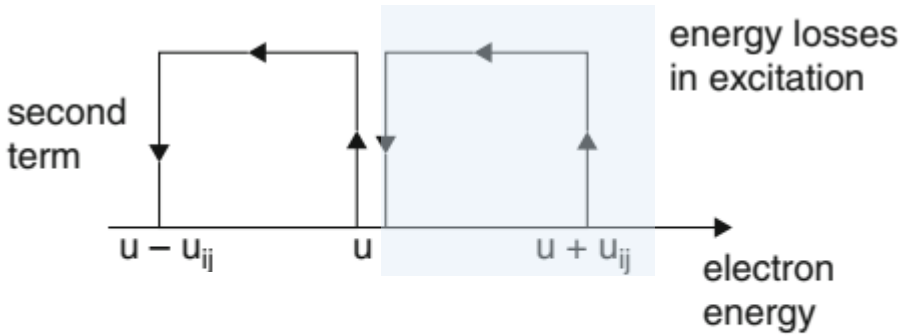

$\delta_i = n_i/N$

fractional populations of molecules in vibrationally or electronically excited states *i*

$$\frac{d}{du}\left[\left(\frac{eE}{N}\right)^2 \frac{u}{3\sigma_m^e}\frac{df_e^0}{du} + \frac{2m}{M}u^2\,\sigma_m\left(f_e^0 + k_B T_o \frac{df_e^o}{du}\right) + 4B_0\sigma_0\,u\,f_e^0\right]$$

$$+\sum_{i,j}\delta_i\left\{(u+u_{ij})\,\sigma_{ij}(u+u_{ij})\,f_e^0(u+u_{ij}) - u\,\sigma_{ij}(u)\,f_e^0(u)\right\}$$

$$+\sum_{j,i}\delta_j\left\{(u-u_{ij})\,\sigma_{ji}(u-u_{ij})\,f_e^0(u-u_{ij}) - u\,\sigma_{ji}(u)\,f_e^0(u)\right\} = 0\,.$$

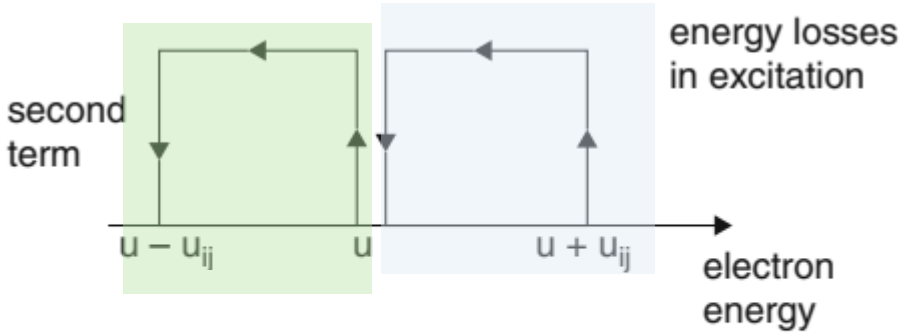

$\delta_i = n_i/N$

fractional populations of molecules in vibrationally or electronically excited states *i*

$$\frac{d}{du}\left[\left(\frac{eE}{N}\right)^2 \frac{u}{3\sigma_m^e}\frac{df_e^0}{du} + \frac{2m}{M}u^2\,\sigma_m\left(f_e^0 + k_B T_o \frac{df_e^o}{du}\right) + 4B_0\sigma_0\, u\, f_e^0\right]$$

$$+\sum_{i,j}\delta_i\left\{(u+u_{ij})\,\sigma_{ij}(u+u_{ij})\,f_e^0(u+u_{ij}) - u\,\sigma_{ij}(u)\,f_e^0(u)\right\}$$

$$+\sum_{j,i}\delta_j\left\{(u-u_{ij})\,\sigma_{ji}(u-u_{ij})\,f_e^0(u-u_{ij}) - u\,\sigma_{ji}(u)\,f_e^0(u)\right\} = 0\,.$$

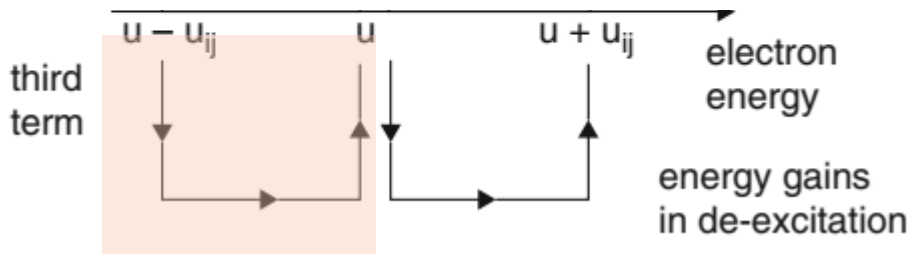

$\delta_j = n_j/N$

fractional populations of molecules in vibrationally or electronically excited states *j*

$$\frac{d}{du}\left[\left(\frac{eE}{N}\right)^2 \frac{u}{3\sigma_m^e}\frac{df_e^0}{du} + \frac{2m}{M}u^2\,\sigma_m\left(f_e^0 + k_B T_o \frac{df_e^o}{du}\right) + 4B_0\sigma_0\, u\, f_e^0\right]$$

$$+\sum_{i,j}\delta_i\left\{(u+u_{ij})\,\sigma_{ij}(u+u_{ij})\,f_e^0(u+u_{ij}) - u\,\sigma_{ij}(u)\,f_e^0(u)\right\}$$

$$+\sum_{j,i}\delta_j\left\{(u-u_{ij})\,\sigma_{ji}(u-u_{ij})\,f_e^0(u-u_{ij}) - u\,\sigma_{ji}(u)\,f_e^0(u)\right\} = 0\,.$$

$$\delta_j = n_j/N$$

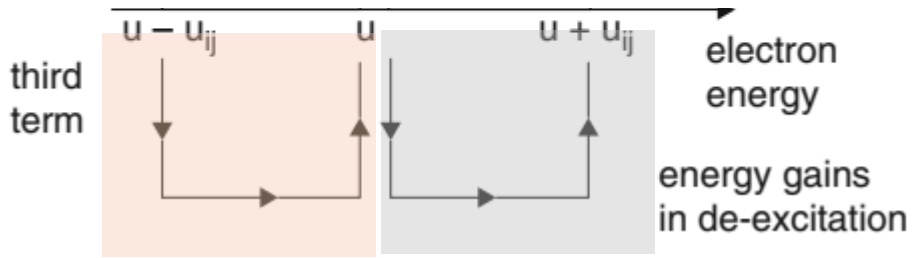

fractional populations of molecules in vibrationally or electronically excited states *j*

$$\frac{d}{du}\left[\left(\frac{eE}{N}\right)^2 \frac{u}{3\sigma_m^e}\frac{df_e^0}{du} + \frac{2m}{M}u^2\,\sigma_m\left(f_e^0 + k_B T_o \frac{df_e^o}{du}\right) + 4B_0\sigma_0\,u\,f_e^0\right]$$

$$+ \sum_{i,j}\delta_i\left\{(u+u_{ij})\,\sigma_{ij}(u+u_{ij})\,f_e^0(u+u_{ij}) - u\,\sigma_{ij}(u)\,f_e^0(u)\right\}$$

$$+ \sum_{j,i}\delta_j\left\{(u-u_{ij})\,\sigma_{ji}(u-u_{ij})\,f_e^0(u-u_{ij}) - u\,\sigma_{ji}(u)\,f_e^0(u)\right\} = 0\,.$$

$\delta_i = n_i/N$

$\delta_j = n_j/N$

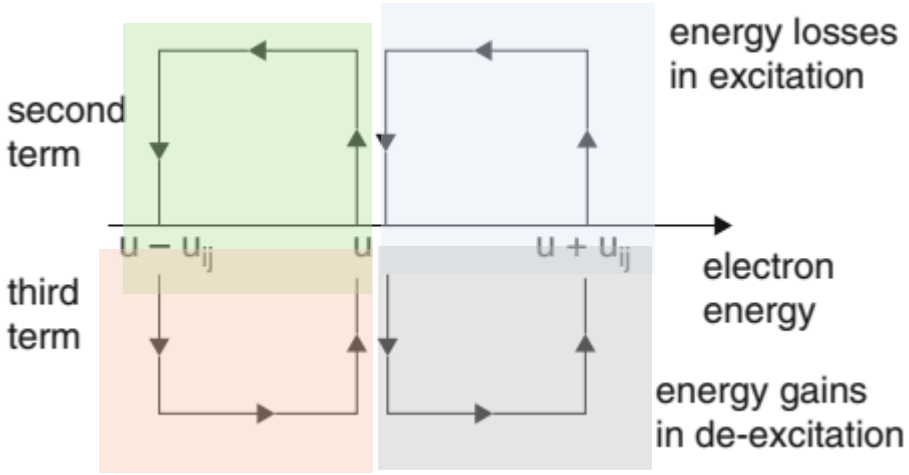

$$\frac{d}{du}\left[\left(\frac{eE}{N}\right)^2 \frac{u}{3\sigma_m^e}\frac{df_e^0}{du} + \frac{2m}{M}u^2\,\sigma_m\left(f_e^0 + k_B T_o \frac{df_e^o}{du}\right) + 4B_0\sigma_0\,u\,f_e^0\right]$$

$$+ \sum_{i,j} \delta_i \left\{(u+u_{ij})\,\sigma_{ij}(u+u_{ij})\,f_e^0(u+u_{ij}) - u\,\sigma_{ij}(u)\,f_e^0(u)\right\}$$

$$+ \sum_{j,i} \delta_j \left\{(u-u_{ij})\,\sigma_{ji}(u-u_{ij})\,f_e^0(u-u_{ij}) - u\,\sigma_{ji}(u)\,f_e^0(u)\right\} = 0\,.$$

$\delta_i = n_i/N$

$\delta_j = n_j/N$

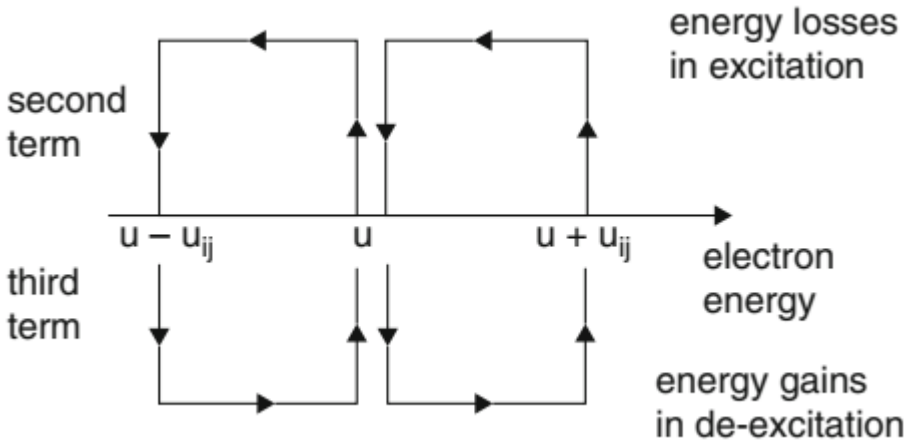

$$\frac{d}{du}\left[\left(\frac{eE}{N}\right)^2 \frac{u}{3\sigma_m^e}\frac{df_e^0}{du} + \frac{2m}{M}u^2\,\sigma_m\left(f_e^0 + k_B T_o \frac{df_e^o}{du}\right) + 4B_0\sigma_0\, u\, f_e^0\right]$$

$$+ \sum_{i,j} \delta_i \left\{(u+u_{ij})\,\sigma_{ij}(u+u_{ij})\,f_e^0(u+u_{ij}) - u\,\sigma_{ij}(u)\,f_e^0(u)\right\}$$

$$+ \sum_{j,i} \delta_j \left\{(u-u_{ij})\,\sigma_{ji}(u-u_{ij})\,f_e^0(u-u_{ij}) - u\,\sigma_{ji}(u)\,f_e^0(u)\right\} = 0\,.$$

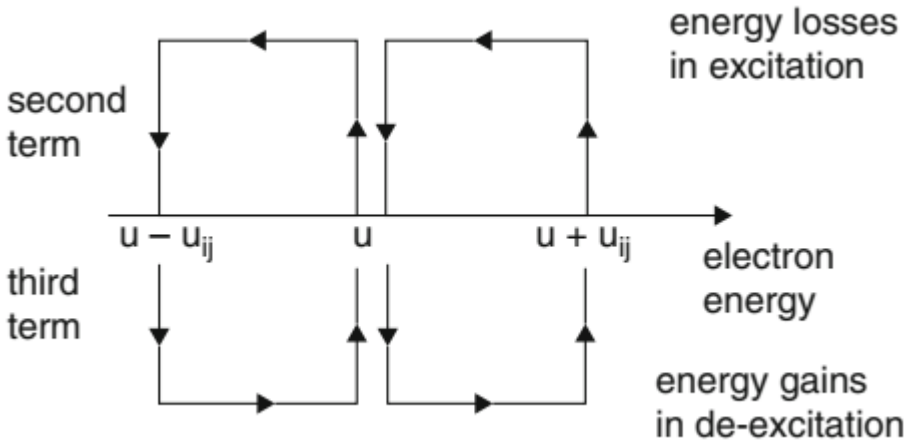

$\delta_i = n_i/N$

$\delta_j = n_j/N$

In most situations, the fractional populations of electronically excited states are negligible, but the same does not occur in molecular gases.

$$\frac{d}{du}\left[\left(\frac{eE}{N}\right)^2 \frac{u}{3\sigma_m^e}\frac{df_e^0}{du} + \frac{2m}{M}u^2\,\sigma_m\left(f_e^0 + k_B T_o \frac{df_e^o}{du}\right) + 4B_0\sigma_0\, u\, f_e^0\right]$$

$$+ \sum_{i,j} \delta_i \left\{(u+u_{ij})\,\sigma_{ij}(u+u_{ij})\,f_e^0(u+u_{ij}) - u\,\sigma_{ij}(u)\,f_e^0(u)\right\}$$

$$+ \sum_{j,i} \delta_j \left\{(u-u_{ij})\,\sigma_{ji}(u-u_{ij})\,f_e^0(u-u_{ij}) - u\,\sigma_{ji}(u)\,f_e^0(u)\right\} = 0\,.$$

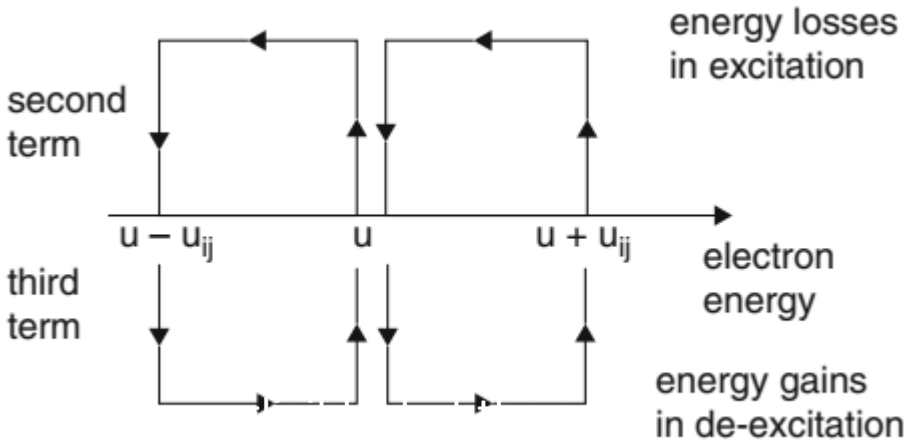

$\delta_i = n_i/N$

$\delta_j = n_j/N$

Therefore, **to solve the electron Boltzmann equation**, we need to **know the fractional population of the vibrational levels**.

$$\frac{dn_v}{dt} =$$

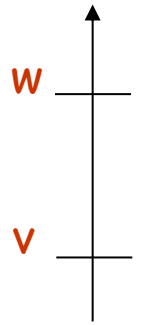

$$\frac{dn_v}{dt} =$$

e-V

$$e + N_2(X, v) \rightleftharpoons e + N_2(X, w)$$

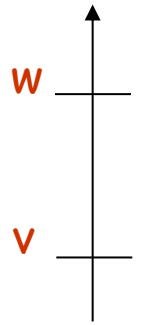

$$\frac{dn_v}{dt} =$$

e-V

$$e + N_2(X, v) \rightleftharpoons e + N_2(X, w)$$

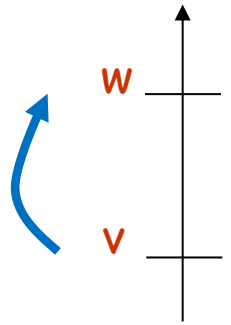

$$\frac{dn_v}{dt} = \qquad - n_e n_v \sum_{w \neq v} C_v^w$$

e-V

$$e + N_2(X, v) \rightleftharpoons e + N_2(X, w)$$

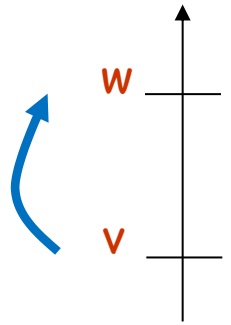

$$\frac{dn_v}{dt} = - n_e n_v \sum_{w \neq v} C_v^w$$

$$C_v^w = \sqrt{\frac{2}{m}} \int \sigma_{v,w} f(u) u du$$

e-V $$e + N_2(X, v) \rightleftharpoons e + N_2(X, w)$$

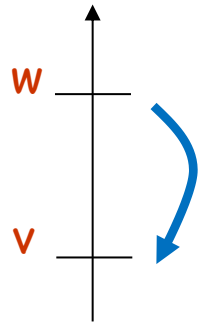

$$\frac{dn_v}{dt} = n_e \sum_{w \neq v} n_w C_w^v -$$

$$C_v^w = \sqrt{\frac{2}{m}} \int \sigma_{v,w} f(u) u du$$

$$\sigma_{w,v}(u) = \frac{g_v}{g_w} \frac{u + u_{v,w}}{u} C_{v,w}(u + u_{v,w})$$

e-V $$e + N_2(X, v) \rightleftharpoons e + N_2(X, w)$$

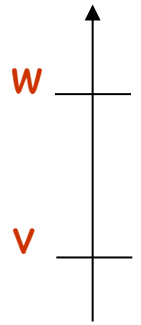

$$\frac{dn_v}{dt} = n_e \sum_{w \neq v} n_w C_w^v - n_e n_v \sum_{w \neq v} C_v^w$$

$$C_v^w = \sqrt{\frac{2}{m}} \int \sigma_{v,w} f(u) u du$$

$$\sigma_{w,v}(u) = \frac{g_v}{g_w} \frac{u + u_{v,w}}{u} C_{v,w}(u + u_{v,w})$$

e-V $e + N_2(X, v) \rightleftharpoons e + N_2(X, w)$

V-V $N_2(X, v) + N_2(X, w) \rightleftharpoons N_2(X, v-1) + N_2(X, w+1)$

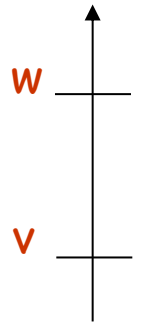

$$\frac{dn_v}{dt} = n_e \sum_{w \neq v} n_w C_w^v - n_e n_v \sum_{w \neq v} C_v^w$$

$$C_v^w = \sqrt{\frac{2}{m}} \int \sigma_{v,w} f(u) u du$$

$$\sigma_{w,v}(u) = \frac{g_v}{g_w} \frac{u + u_{v,w}}{u} C_{v,w}(u + u_{v,w})$$

e-V $$e + N_2(X, v) \rightleftharpoons e + N_2(X, w)$$

V-V $$N_2(X, v) + N_2(X, w) \rightleftharpoons N_2(X, v-1) + N_2(X, w+1)$$

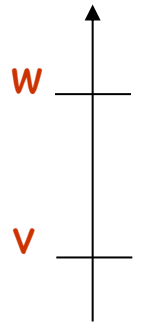

$$\frac{dn_v}{dt} = n_e \sum_{w \neq v} n_w C_w^v - n_e n_v \sum_{w \neq v} C_v^w + n_{v-1} \sum_w n_{w+1} Q_{v-1,v}^{w+1,w}$$

$$+ n_{v+1} \sum_w n_w Q_{v+1,v}^{w,w+1}$$

$$C_v^w = \sqrt{\frac{2}{m}} \int \sigma_{v,w} f(u) u du$$

$$\sigma_{w,v}(u) = \frac{g_v}{g_w} \frac{u + u_{v,w}}{u} C_{v,w}(u + u_{v,w})$$

e-V	$e + N_2(X, v) \rightleftharpoons e + N_2(X, w)$
V-V	$N_2(X, v) + N_2(X, w) \rightleftharpoons N_2(X, v-1) + N_2(X, w+1)$
V-T N_2-N_2	$N_2(X, v) + N_2 \rightleftharpoons N_2(X, v-1) + N_2$

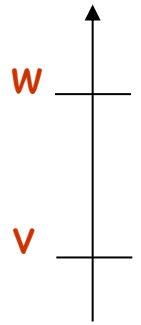

$$\frac{dn_v}{dt} = n_e \sum_{w \neq v} n_w C_w^v - n_e n_v \sum_{w \neq v} C_v^w + n_{v-1} \sum_w n_{w+1} Q_{v-1,v}^{w+1,w}$$

$$+ n_{v+1} \sum_w n_w Q_{v+1,v}^{w,w+1}$$

$$C_v^w = \sqrt{\frac{2}{m}} \int \sigma_{v,w} f(u) u du$$

$$\sigma_{w,v}(u) = \frac{g_v}{g_w} \frac{u + u_{v,w}}{u} C_{v,w}(u + u_{v,w})$$

e-V	$e + N_2(X, v) \rightleftharpoons e + N_2(X, w)$
V-V	$N_2(X, v) + N_2(X, w) \rightleftharpoons N_2(X, v-1) + N_2(X, w+1)$
V-T N_2-N_2	$N_2(X, v) + N_2 \rightleftharpoons N_2(X, v-1) + N_2$

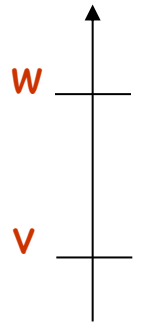

$$\frac{dn_v}{dt} = n_e \sum_{w \neq v} n_w C_w^v - n_e n_v \sum_{w \neq v} C_v^w + n_{v-1} \sum_w n_{w+1} Q_{v-1,v}^{w+1,w}$$

$$+ n_{v+1} \sum_w n_w Q_{v+1,v}^{w,w+1} + n_{v-1}[N_2] P_{v,v-1} + n_{v+1}[N_2] P_{v+1,v}$$

$$C_v^w = \sqrt{\frac{2}{m}} \int \sigma_{v,w} f(u) u du$$

$$\sigma_{w,v}(u) = \frac{g_v}{g_w} \frac{u + u_{v,w}}{u} C_{v,w}(u + u_{v,w})$$

e-V	$e + N_2(X, v) \rightleftharpoons e + N_2(X, w)$
V-V	$N_2(X, v) + N_2(X, w) \rightleftharpoons N_2(X, v-1) + N_2(X, w+1)$
V-T N_2-N_2	$N_2(X, v) + N_2 \rightleftharpoons N_2(X, v-1) + N_2$

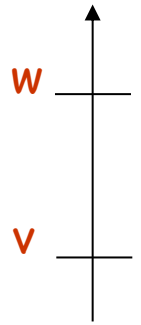

$$\frac{dn_v}{dt} = n_e \sum_{w \neq v} n_w C_w^v - n_e n_v \sum_{w \neq v} C_v^w + n_{v-1} \sum_w n_{w+1} Q_{v-1,v}^{w+1,w}$$

$$+ n_{v+1} \sum_w n_w Q_{v+1,v}^{w,w+1} + n_{v-1}[N_2] P_{v,v-1} + n_{v+1}[N_2] P_{v+1,v}$$

$$C_v^w = \sqrt{\frac{2}{m}} \int \sigma_{v,w} f(u) u du$$

$$\sigma_{w,v}(u) = \frac{g_v}{g_w} \frac{u + u_{v,w}}{u} C_{v,w}(u + u_{v,w})$$

e-V	$e + N_2(X, v) \rightleftharpoons e + N_2(X, w)$
V-V	$N_2(X, v) + N_2(X, w) \rightleftharpoons N_2(X, v-1) + N_2(X, w+1)$
V-T N_2-N_2	$N_2(X, v) + N_2 \rightleftharpoons N_2(X, v-1) + N_2$

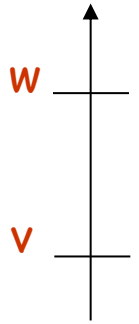

$$\frac{dn_v}{dt} = n_e \sum_{w \neq v} n_w C_w^v - n_e n_v \sum_{w \neq v} C_v^w + n_{v-1} \sum_w n_{w+1} Q_{v-1,v}^{w+1,w}$$

$$+ n_{v+1} \sum_w n_w Q_{v+1,v}^{w,w+1} + n_{v-1}[N_2] P_{v,v-1} + n_{v+1}[N_2] P_{v+1,v}$$

$$C_v^w = \sqrt{\frac{2}{m}} \int \sigma_{v,w} f(u) u du$$

$$\sigma_{w,v}(u) = \frac{g_v}{g_w} \frac{u + u_{v,w}}{u} C_{v,w}(u + u_{v,w})$$

$$\frac{d}{du}\left[\left(\frac{eE}{N}\right)^2 \frac{u}{3\sigma_m^e}\frac{df_e^0}{du} + \frac{2m}{M}u^2\,\sigma_m\left(f_e^0 + k_B T_o \frac{df_e^o}{du}\right) + 4B_0\sigma_0\, u\, f_e^0\right]$$
$$+\sum_{i,j}\delta_v\,(u+u_{ij})\,\sigma_{ij}(u+u_{ij})\,f_e^0(u+u_{ij}) - u\,\sigma_{ij}(u)\,f_e^0(u)\}$$
$$+\sum_{j,i}\delta_w\{(u-u_{ij})\,\sigma_{ji}(u-u_{ij})\,f_e^0(u-u_{ij}) - u\,\sigma_{ji}(u)\,f_e^0(u)\} = 0\,.$$

$$\delta_v = n_v/N \qquad \delta_w = n_w/N$$

$$\frac{d}{du}\left[\left(\frac{eE}{N}\right)^2 \frac{u}{3\sigma_m^e}\frac{df_e^0}{du} + \frac{2m}{M}u^2\,\sigma_m\left(f_e^0 + k_B T_o \frac{df_e^o}{du}\right) + 4B_0\sigma_0\, u\, f_e^0\right]$$

$$+ \sum_{i,j} \delta_v \{(u+u_{ij})\,\sigma_{ij}(u+u_{ij})\,f_e^0(u+u_{ij}) - u\,\sigma_{ij}(u)\,f_e^0(u)\}$$

$$+ \sum_{j,i} \delta_w \{(u-u_{ij})\,\sigma_{ji}(u-u_{ij})\,f_e^0(u-u_{ij}) - u\,\sigma_{ji}(u)\,f_e^0(u)\} = 0\,.$$

$\delta_v = n_v/N$ $\qquad$ $\delta_w = n_w/N$

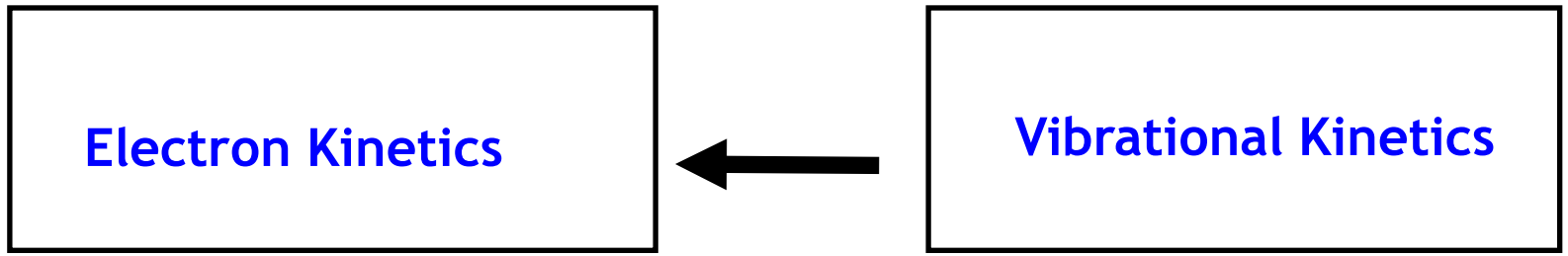
Electron Kinetics
Vibrational Kinetics

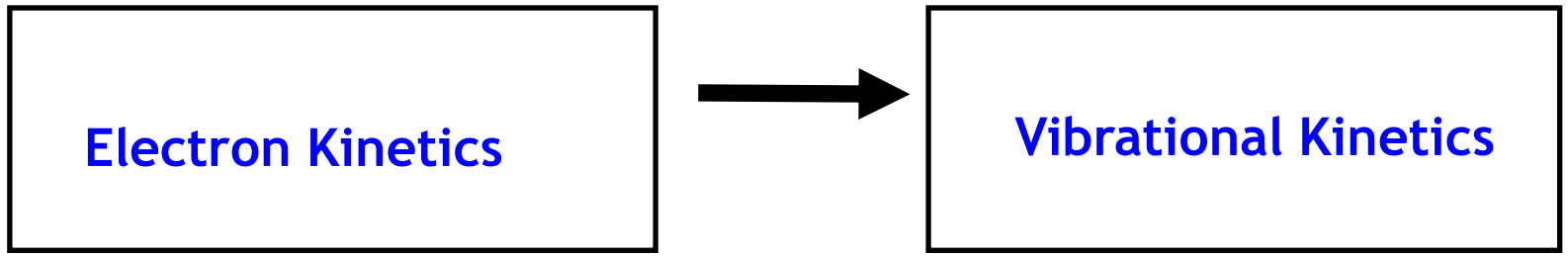
Electron Kinetics
Vibrational Kinetics

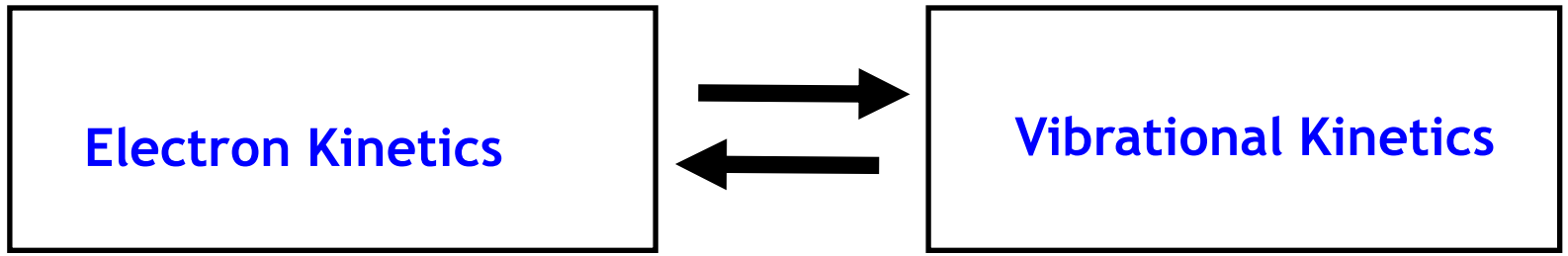
Electron Kinetics
Vibrational Kinetics

J. Phys. D: Appl. Phys. **19** (1986) 17–35. Printed in Great Britain

Coupled electron energy and vibrational distribution functions in stationary N_2 discharges

J Loureiro and C M Ferreira

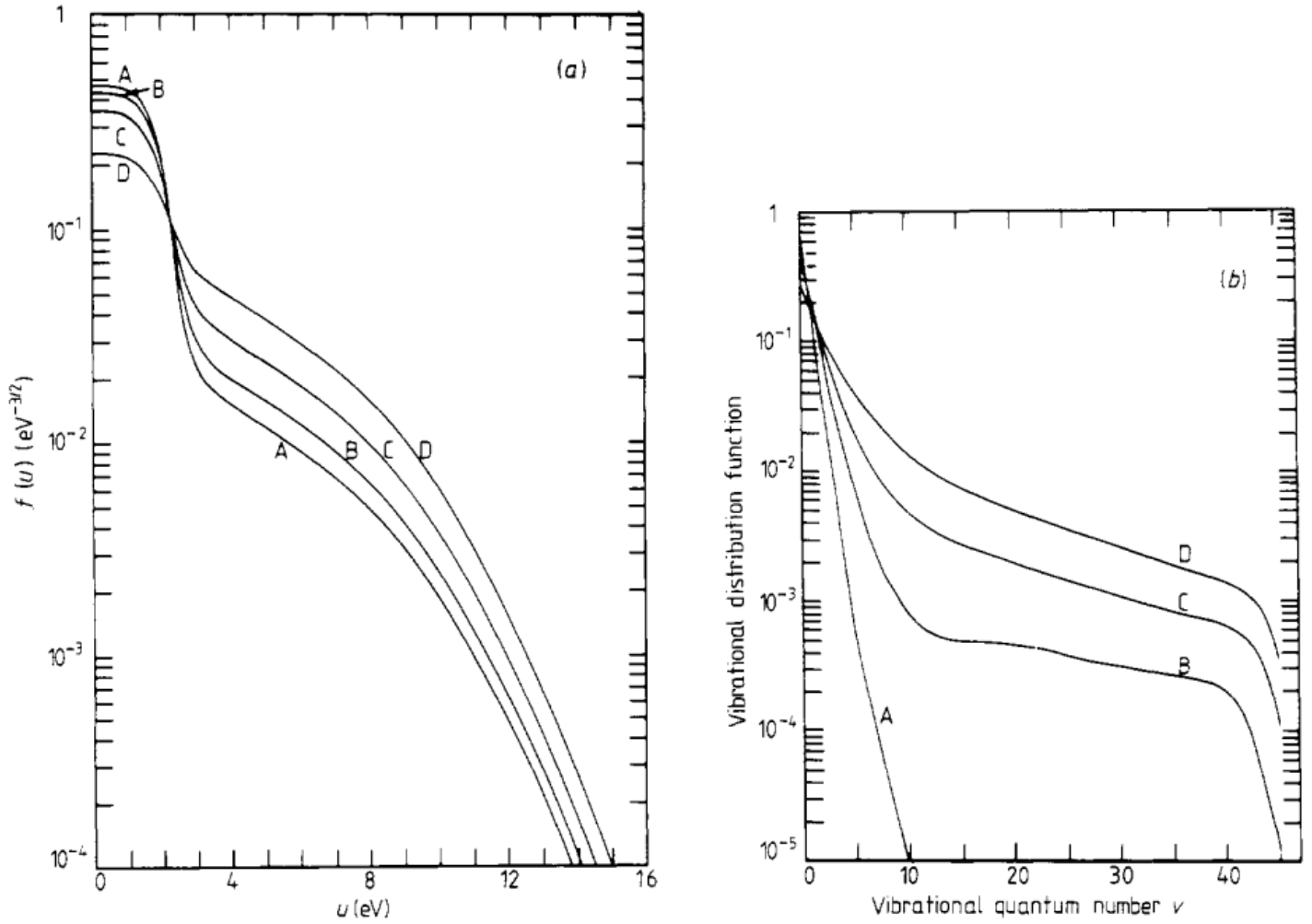

Figure 2. (*a*) Electron energy distribution function for $E/N = 10^{-15}$ V cm^2 and the following values of θ in 10^3 K: (A) 2; (B) 3; (C) 4; (D) 6. (*b*) Vibrational distribution function for the same conditions as in figure 2(*a*).

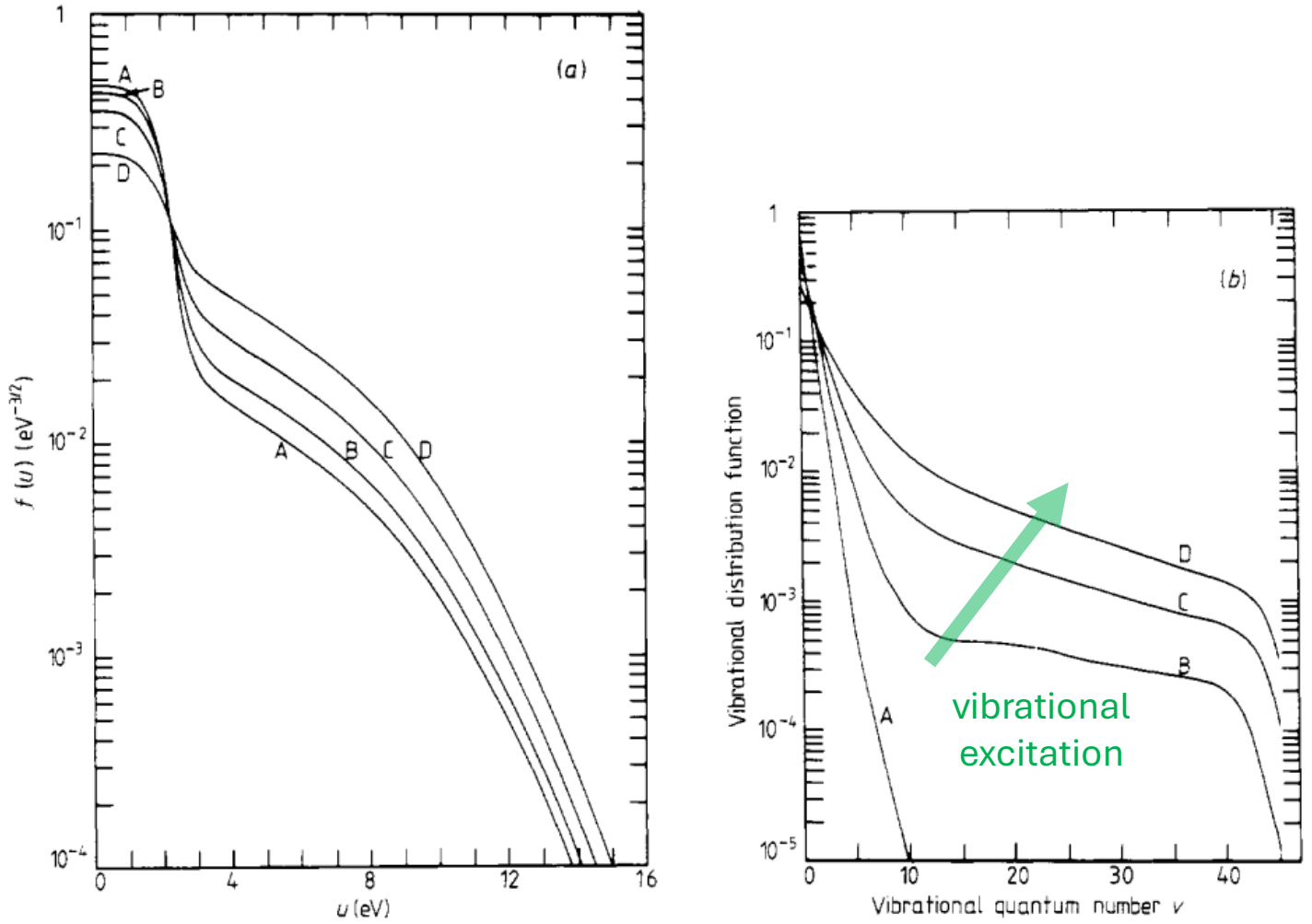

Figure 2. (*a*) Electron energy distribution function for $E/N = 10^{-15}$ V cm^2 and the following values of θ in 10^3 K: (A) 2; (B) 3; (C) 4; (D) 6. (*b*) Vibrational distribution function for the same conditions as in figure 2(*a*).

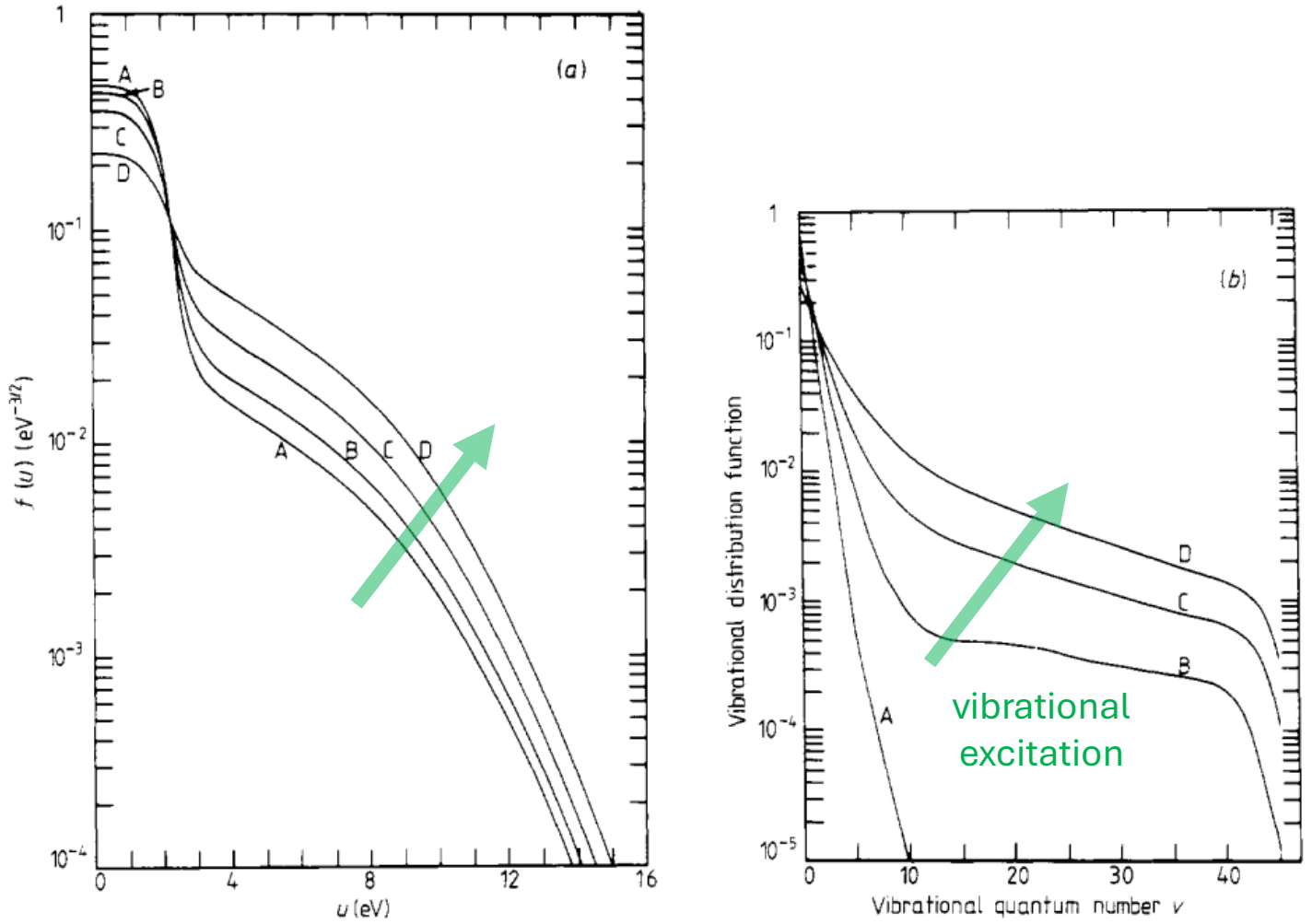

Figure 2. (*a*) Electron energy distribution function for $E/N = 10^{-15}$ V cm^2 and the following values of θ in 10^3 K: (A) 2; (B) 3; (C) 4; (D) 6. (*b*) Vibrational distribution function for the same conditions as in figure 2(*a*).

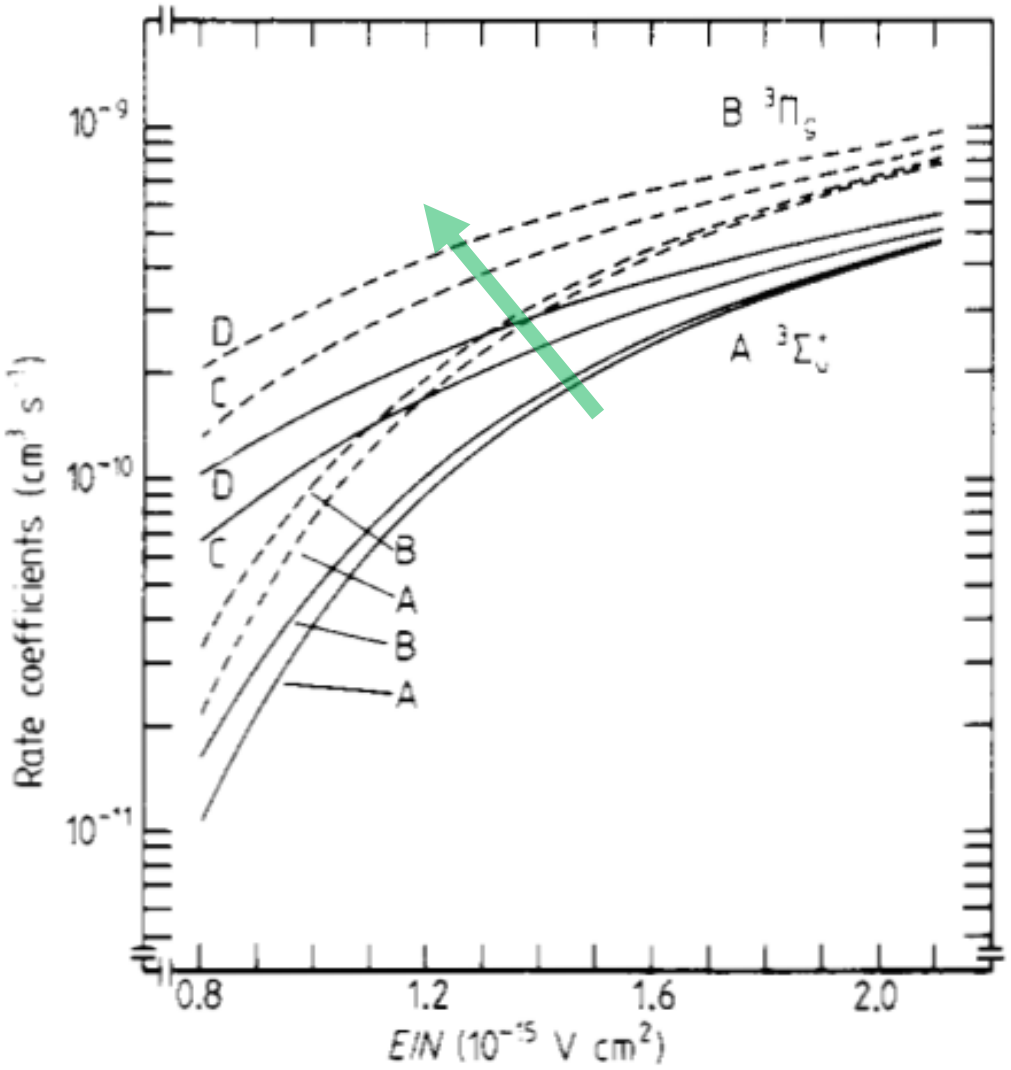
B $^3\Pi_g$
A $^3\Sigma_u^+$
D
C
D
C
B
A
B
A
10^{-9}
10^{-10}
10^{-11}
Rate coefficients ($cm^3 s^{-1}$)
0.8
1.2
1.6
2.0
E/N (10^{-15} V cm^2)

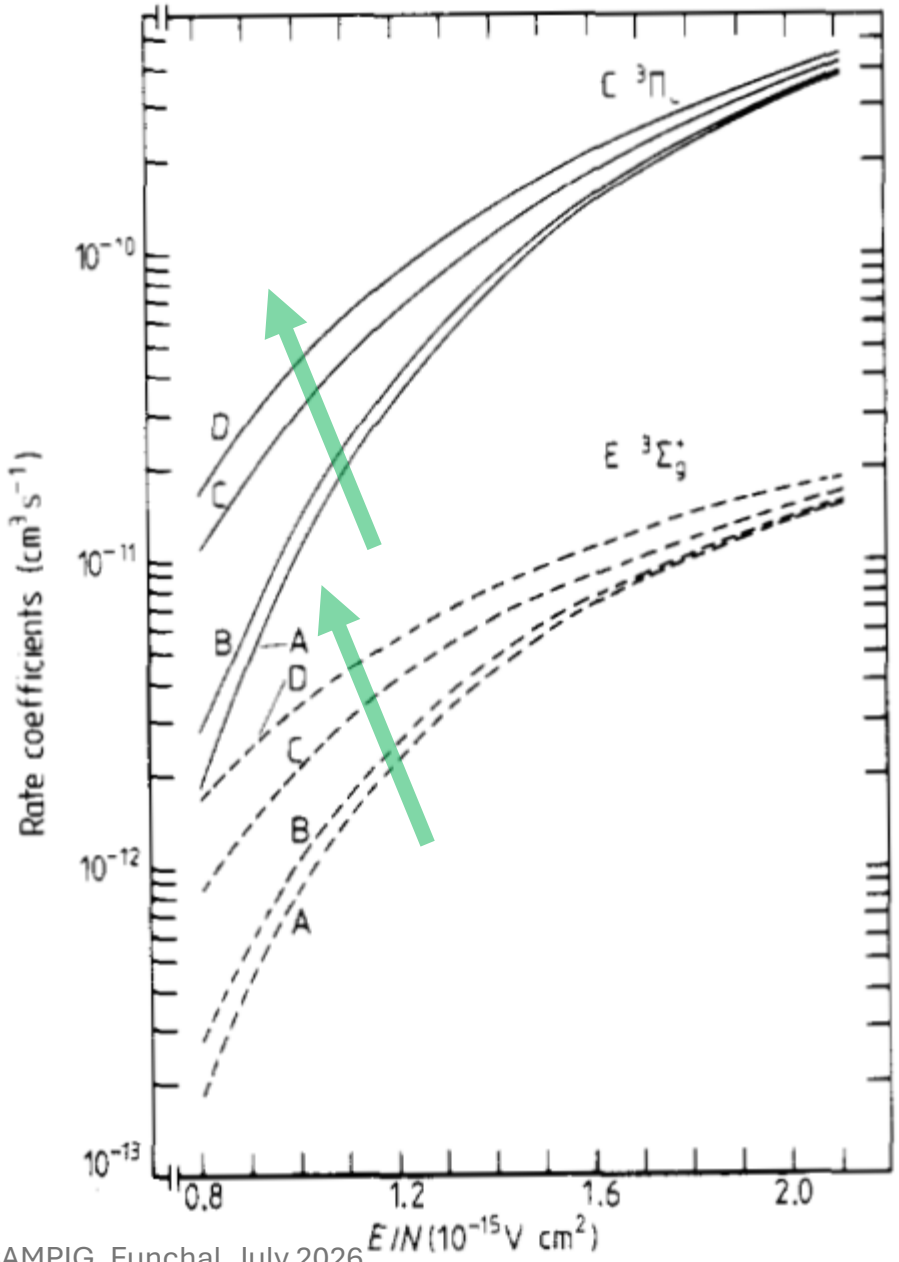
C $^3\Pi_u$
E $^3\Sigma_g^+$
D
C
B
A
D
C
B
A
10^{-10}
10^{-11}
10^{-12}
10^{-13}
Rate coefficients ($cm^3 s^{-1}$)
0.8
1.2
1.6
2.0
E/N (10^{-15} V cm^2)

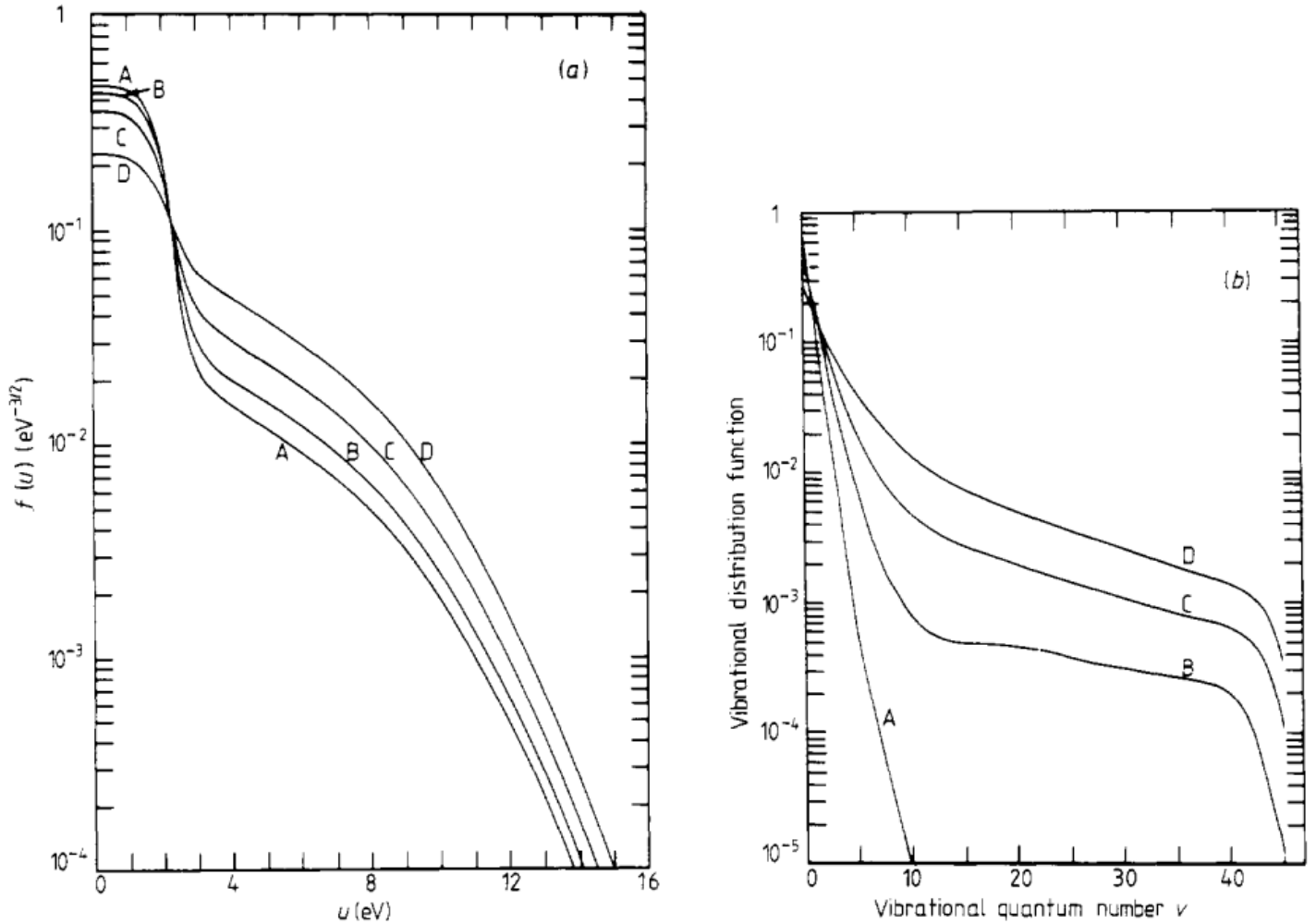

Figure 2. (a) Electron energy distribution function for $E/N = 10^{-15}$ V cm^2 and the following values of θ in 10^3 K: (A) 2; (B) 3; (C) 4; (D) 6. (b) Vibrational distribution function for the same conditions as in figure 2(a).

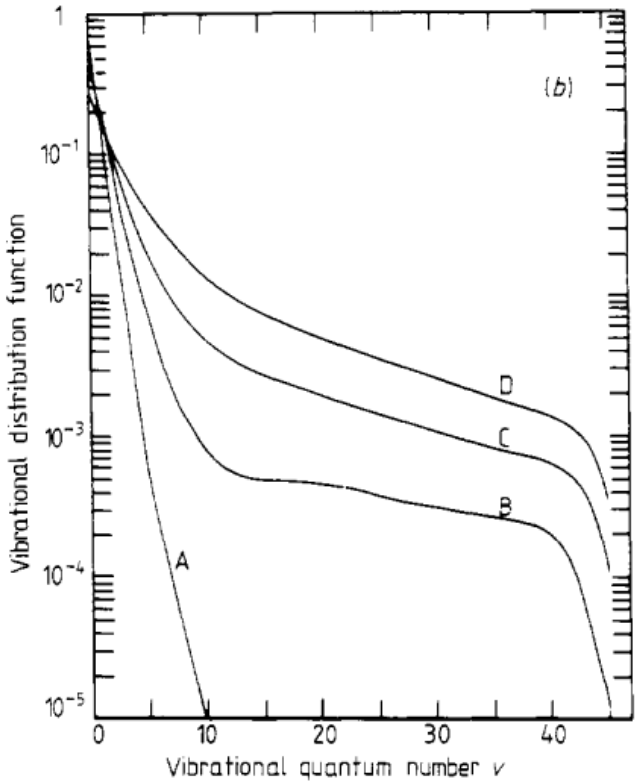
(b)
Vibrational distribution function
Vibrational quantum number v
A
B
C
D
1
10^{-1}
10^{-2}
10^{-3}
10^{-4}
10^{-5}
0
10
20
30
40

e-V	$e + N_2(X, v) \rightleftharpoons e + N_2(X, w)$

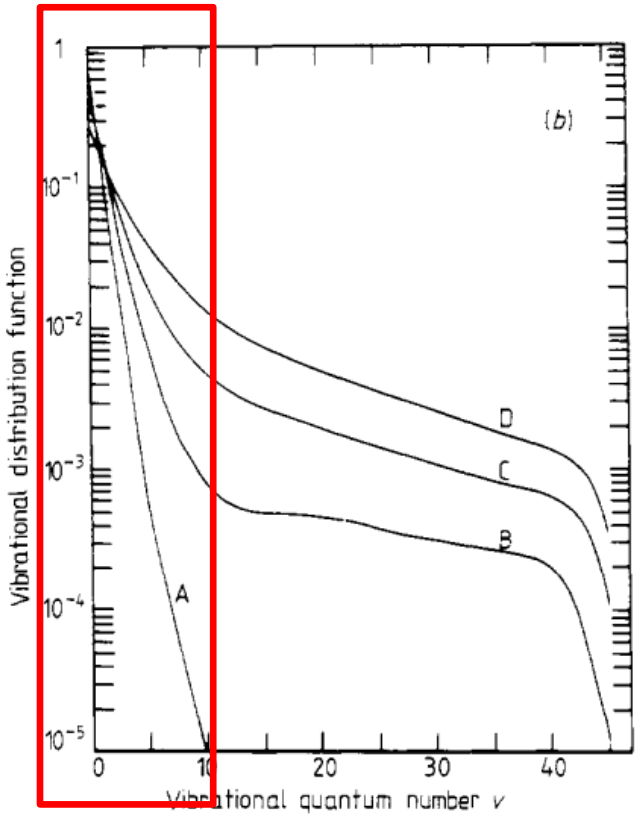

e-V	$e + N_2(X, v) \rightleftharpoons e + N_2(X, w)$
V-V	$N_2(X, v) + N_2(X, w) \rightleftharpoons N_2(X, v-1) + N_2(X, w+1)$
V-T N_2-N_2	$N_2(X, v) + N_2 \rightleftharpoons N_2(X, v-1) + N_2$

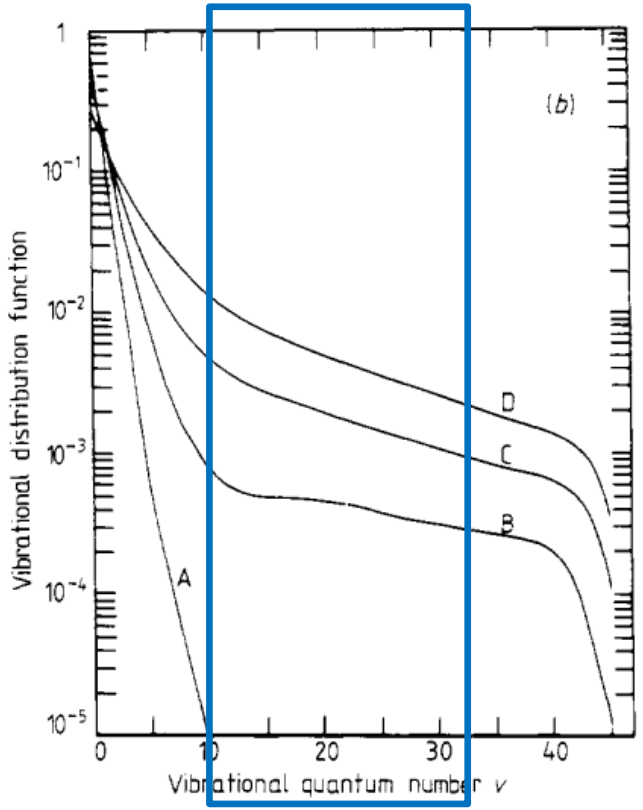

e-V	$e + N_2(X, v) \rightleftharpoons e + N_2(X, w)$
V-V	$N_2(X, v) + N_2(X, w) \rightleftharpoons N_2(X, v-1) + N_2(X, w+1)$
V-T N_2-N_2	$N_2(X, v) + N_2 \rightleftharpoons N_2(X, v-1) + N_2$

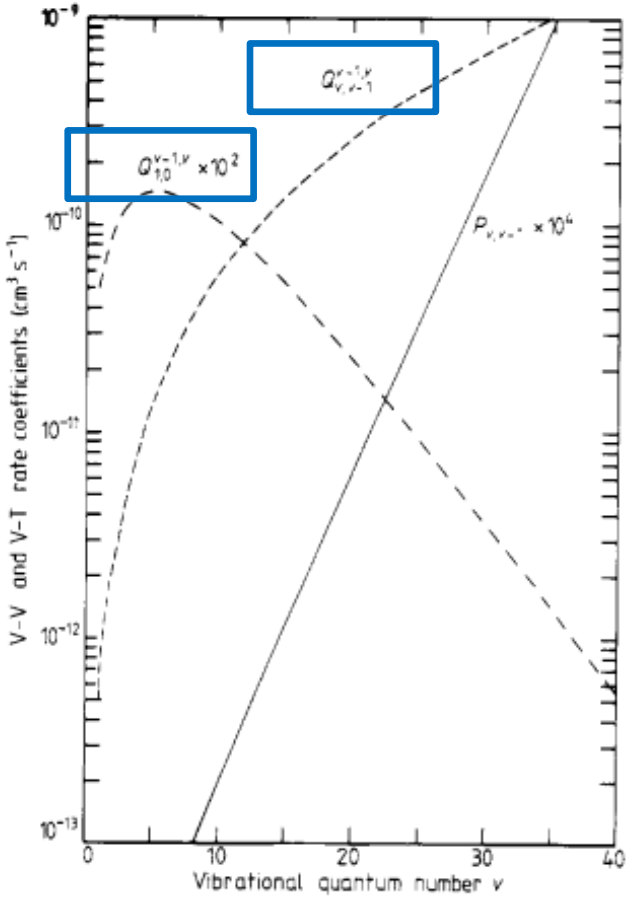

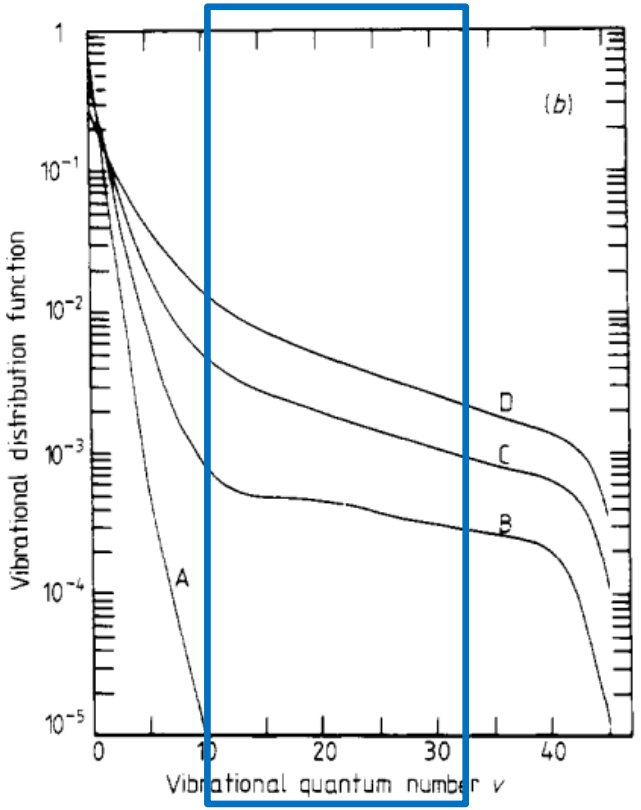

e-V	$e + N_2(X, v) \rightleftharpoons e + N_2(X, w)$
V-V	$N_2(X, v) + N_2(X, w) \rightleftharpoons N_2(X, v-1) + N_2(X, w+1)$
V-T N_2-N_2	$N_2(X, v) + N_2 \rightleftharpoons N_2(X, v-1) + N_2$

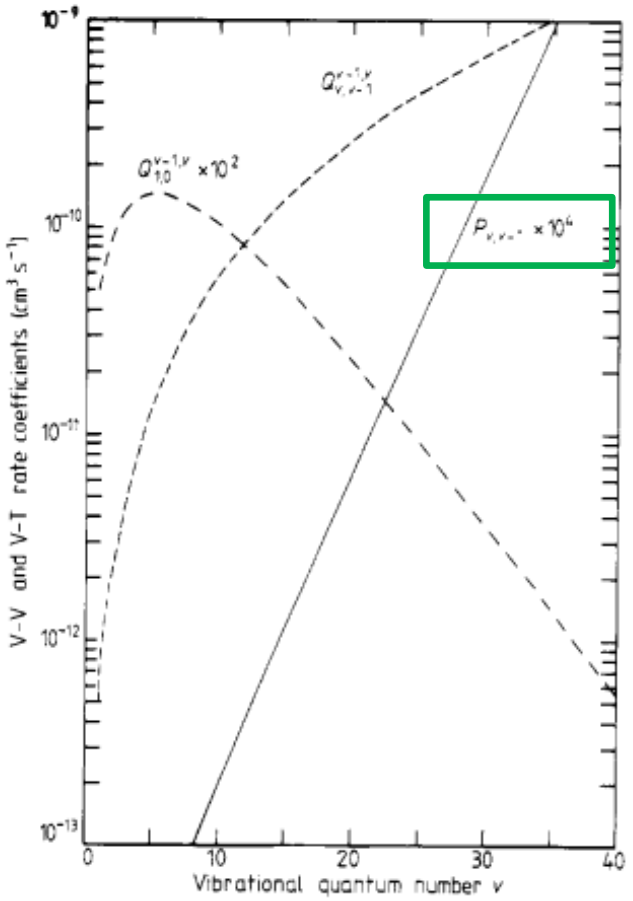

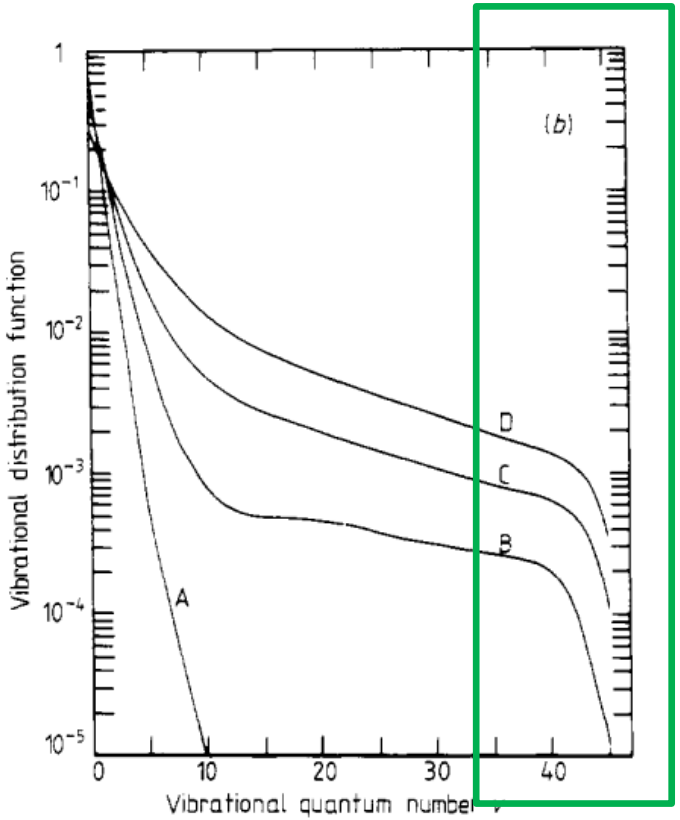

J Loureiro and C M Ferreira 1989 *J. Phys. D: Appl. Phys.* **22** 1680

H_2

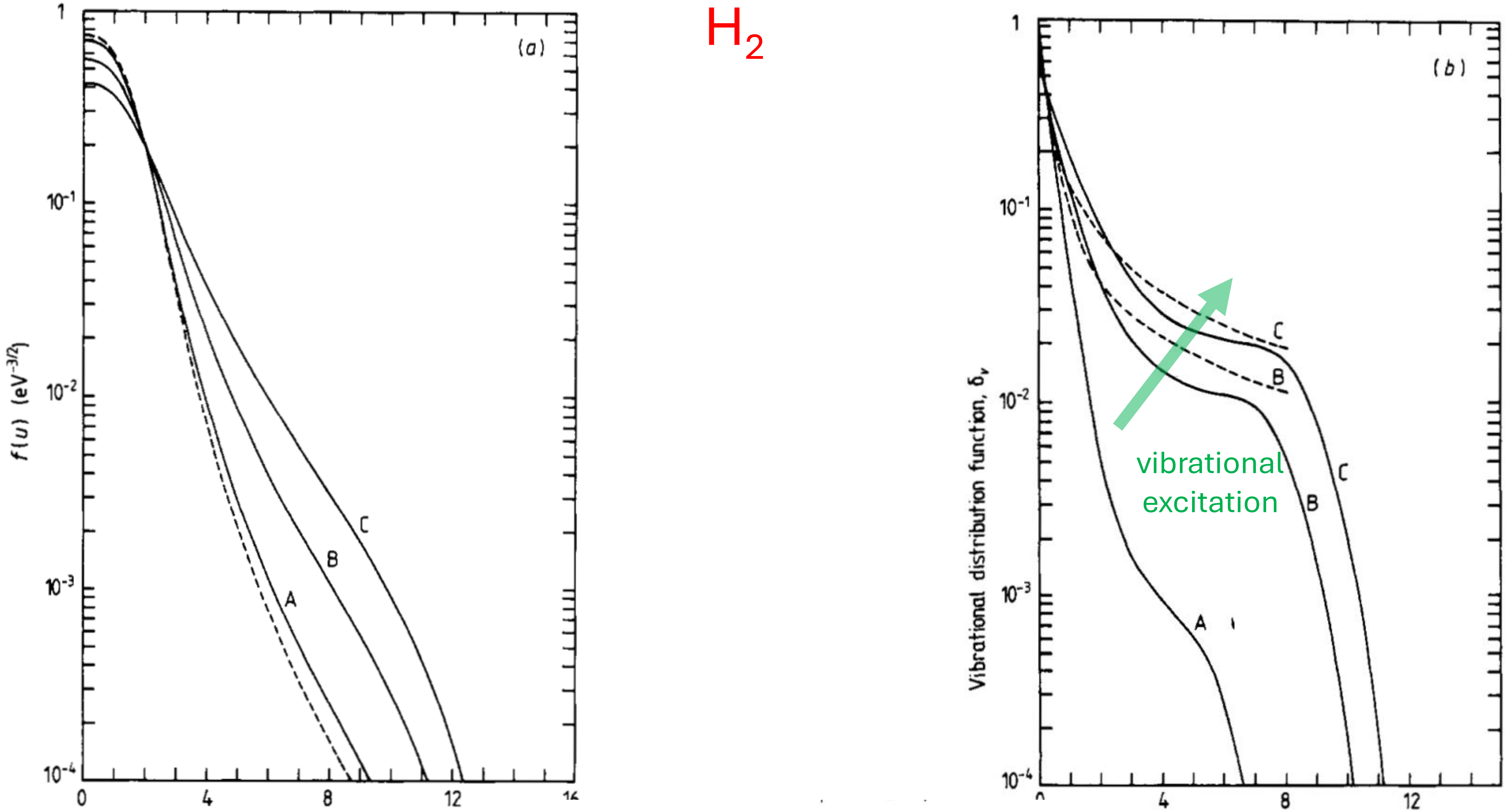

Figure 3. (*a*) Electron energy distribution functions for $E/N = 3 \times 10^{-16}$ V cm^2, $\delta_a = 0$ and the following constant values of T_v in K: A, 2000; B, 3000; C, 4000. (*b*) Vibrational distribution functions for the same conditions as in (*a*). The broken curves represent EDF for $T_v = T_g = 400$ K (figure 3(*a*)); modified Treanor distributions for $T_v = 3000$ (B) and 4000 K (C) (figure 3(*b*)).

J Loureiro and C M Ferreira 1989 *J. Phys. D: Appl. Phys.* **22** 1680

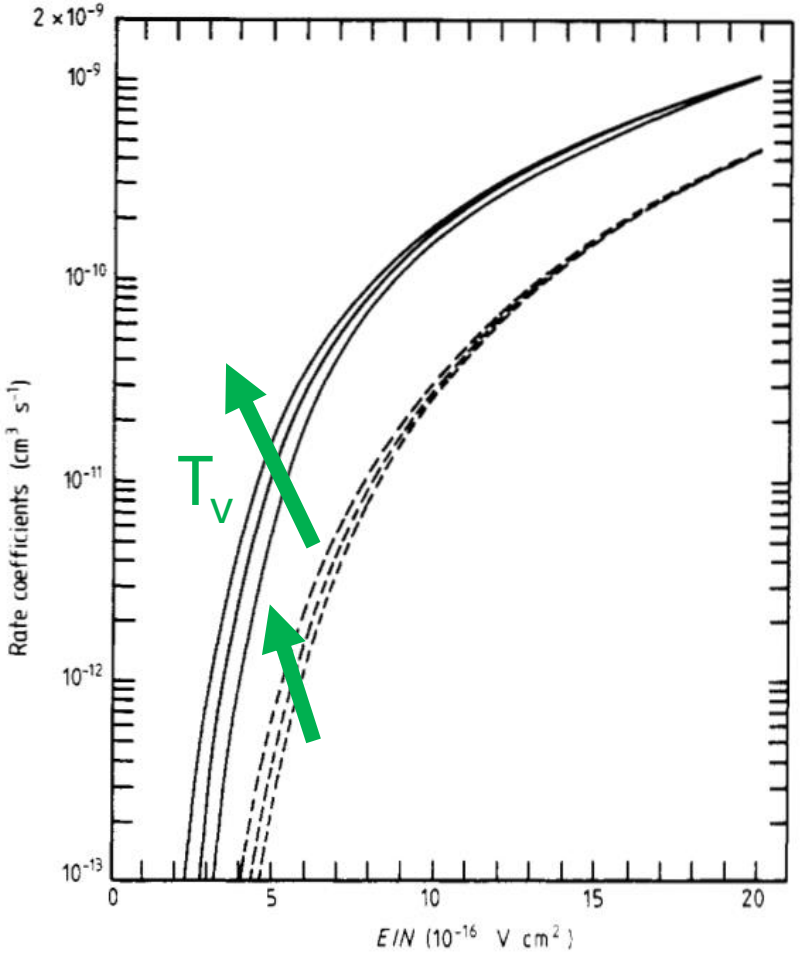

Figure 12. As in figure 10 but for the total rate coefficient for emission of radiation (full curves) and ionisation (broken curves).

H_2

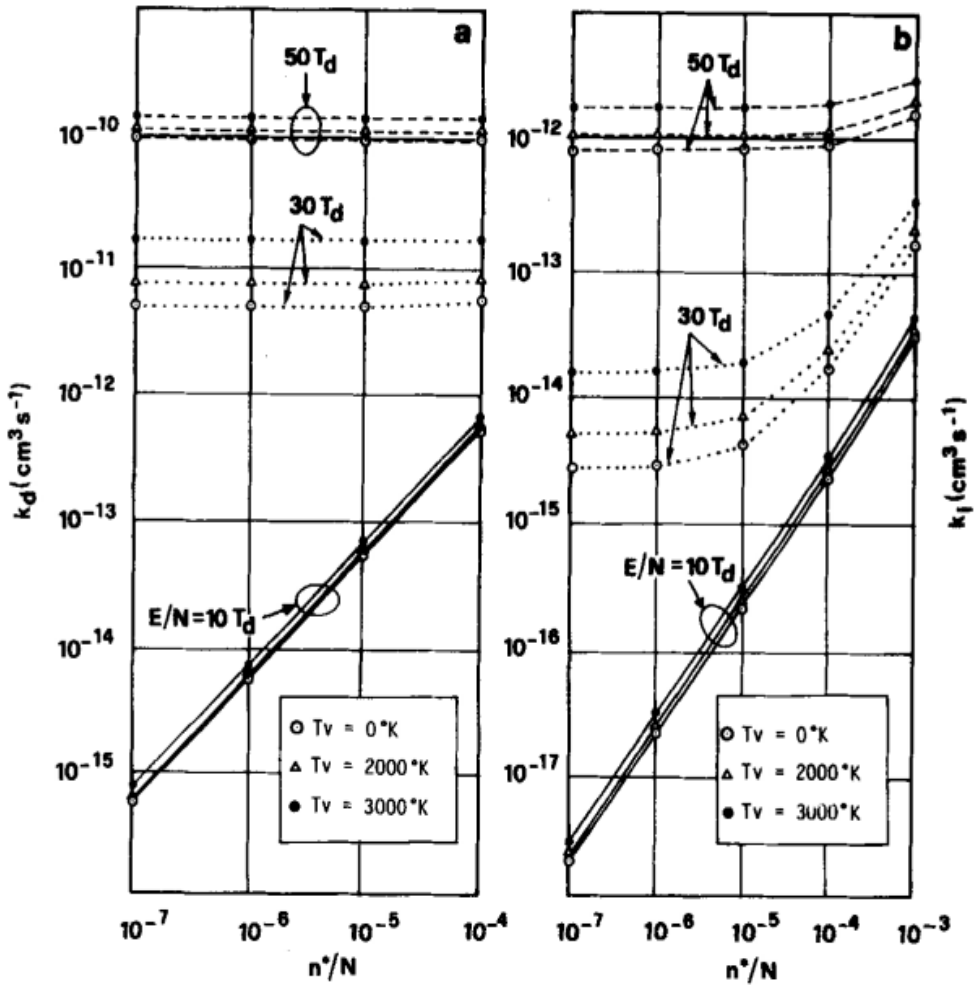

Fig. 3. Dependence of dissociation (a) and ionization (b) rate coefficients for pure H_2 on n^*/N for different E/N and T_v values.

J Loureiro and C M Ferreira 1989 *J. Phys. D: Appl. Phys.* **22** 1680

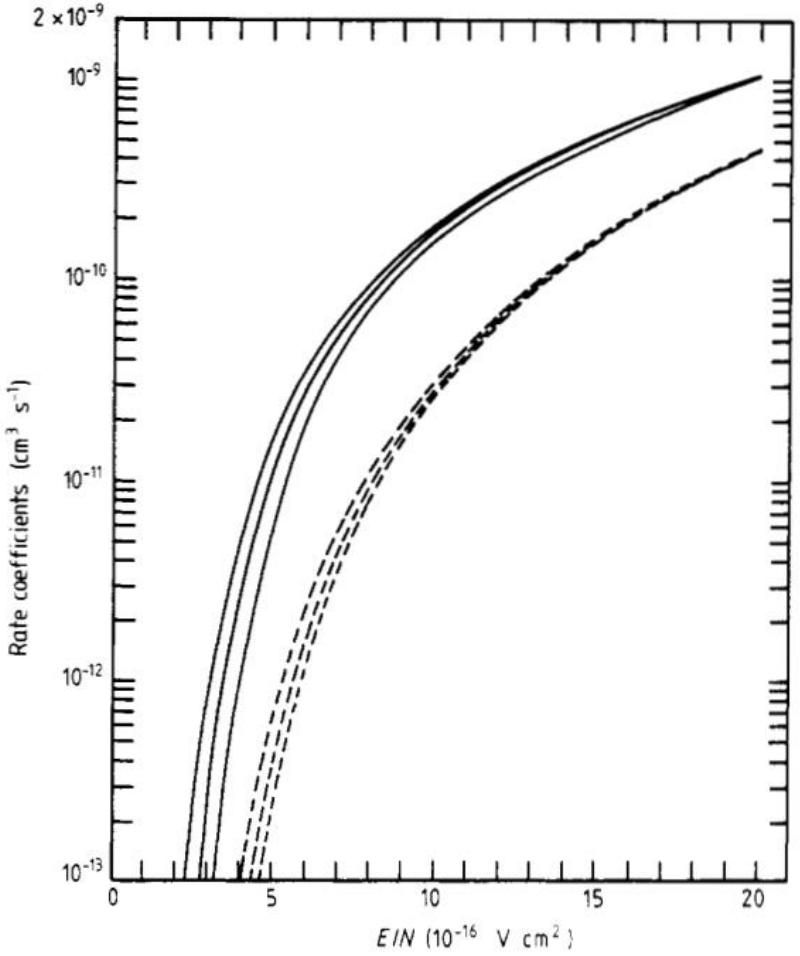

Figure 12. As in figure 10 but for the total rate coefficient for emission of radiation (full curves) and ionisation (broken curves).

H_2

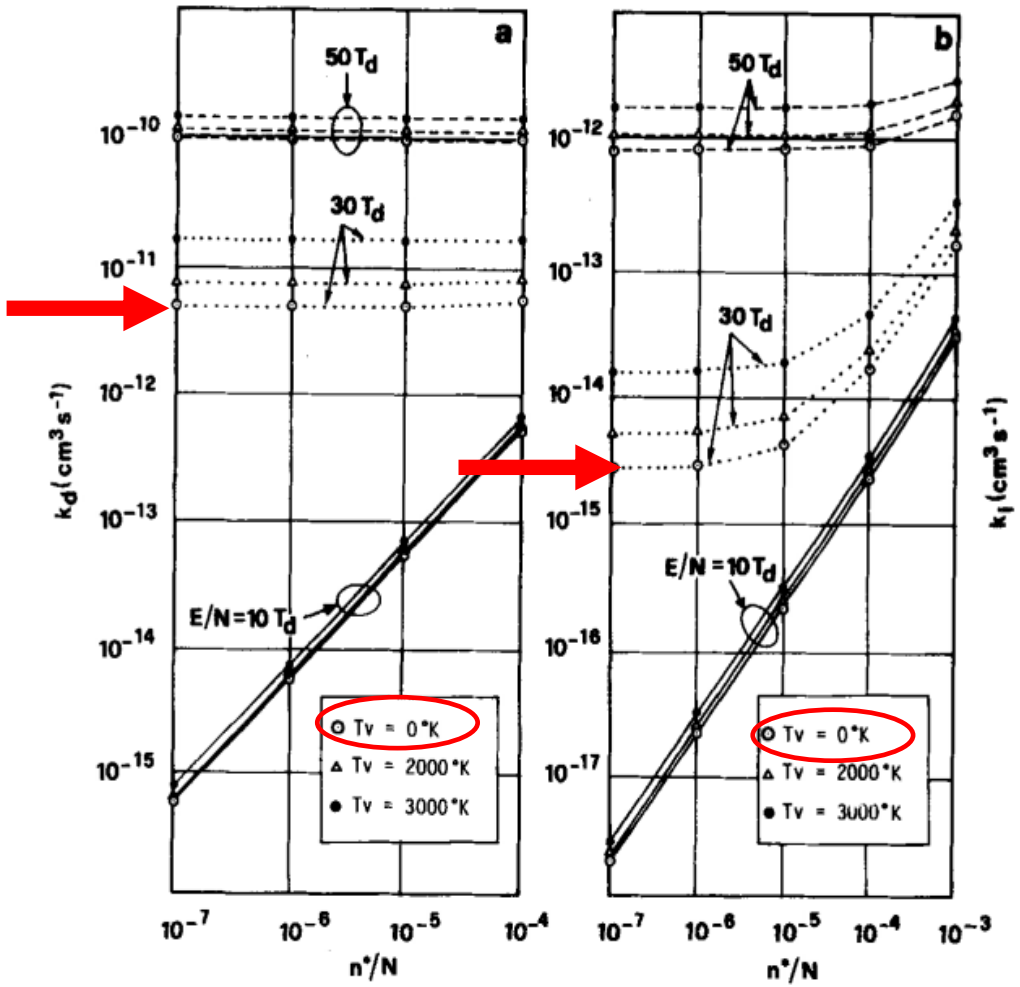

Fig. 3. Dependence of dissociation (a) and ionization (b) rate coefficients for pure H_2 on n^*/N for different E/N and T_v values.

J Loureiro and C M Ferreira 1989 *J. Phys. D: Appl. Phys.* **22** 1680

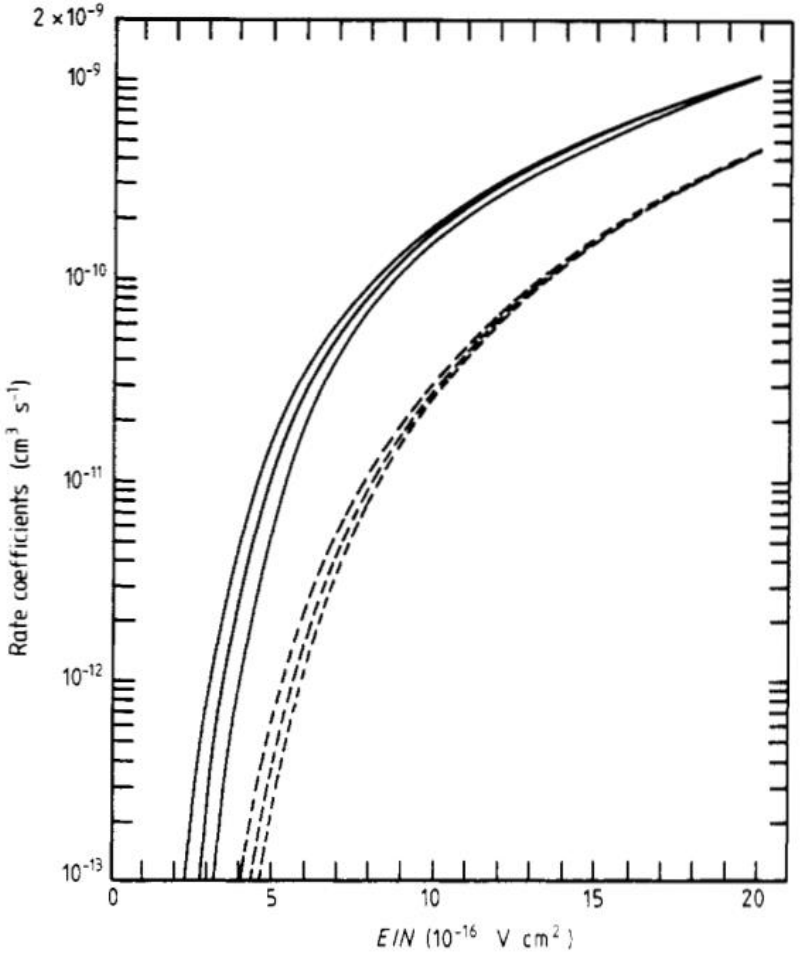

Figure 12. As in figure 10 but for the total rate coefficient for emission of radiation (full curves) and ionisation (broken curves).

H_2

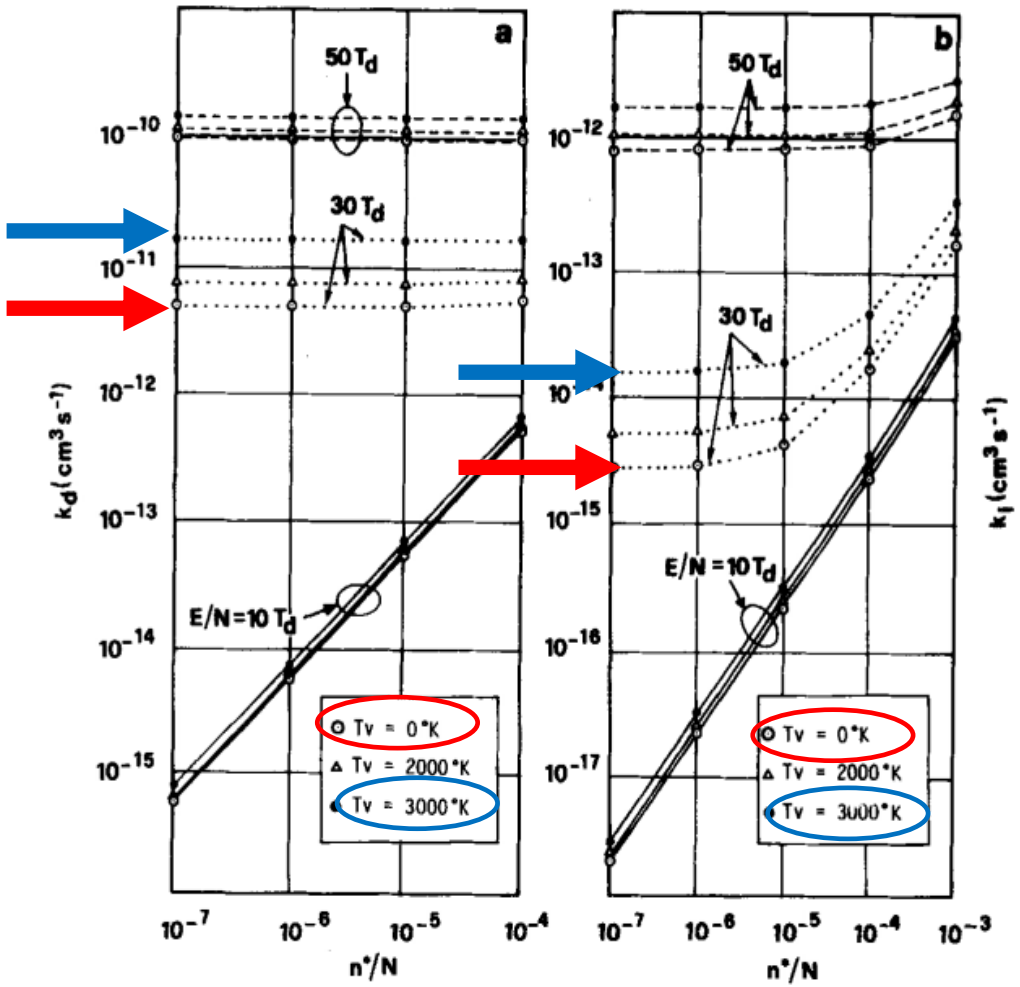

Fig. 3. Dependence of dissociation (a) and ionization (b) rate coefficients for pure H_2 on n^*/N for different E/N and T_v values.

J Loureiro and C M Ferreira 1989 *J. Phys. D: Appl. Phys.* **22** 1680

H_2

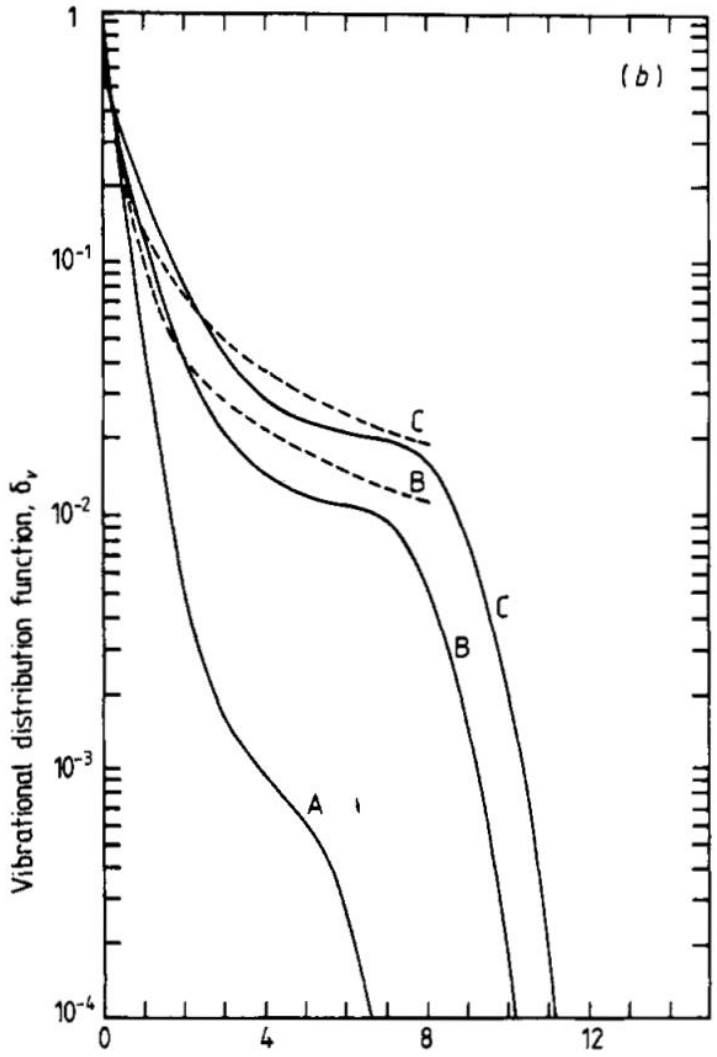

J Loureiro and C M Ferreira 1989 *J. Phys. D: Appl. Phys.* **22** 1680

H_2

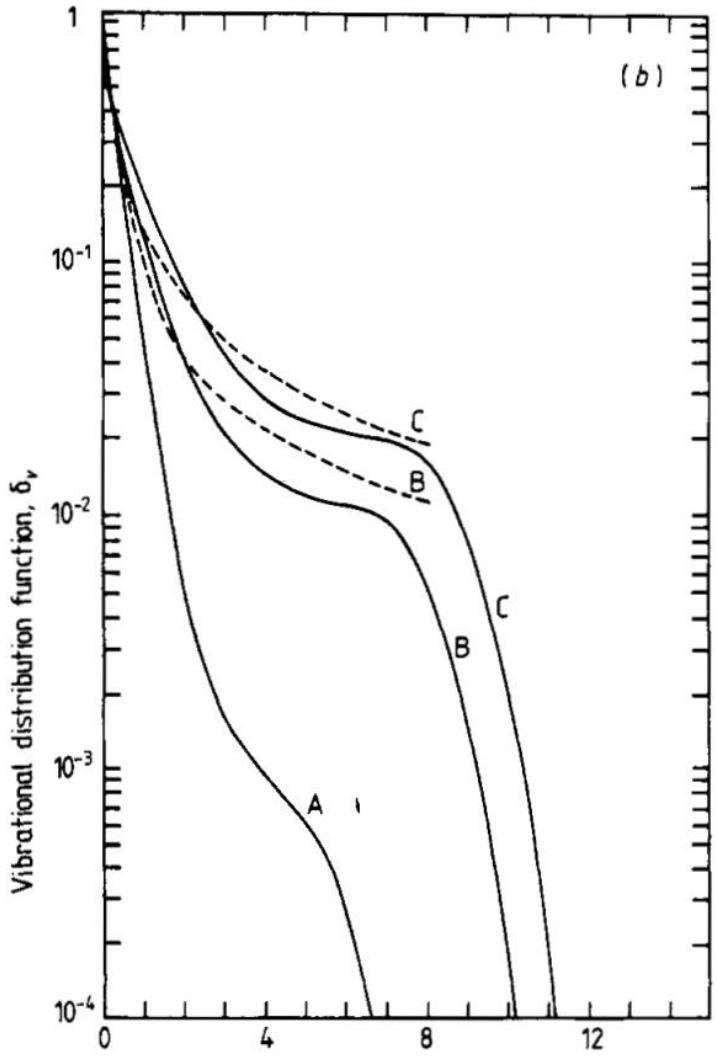

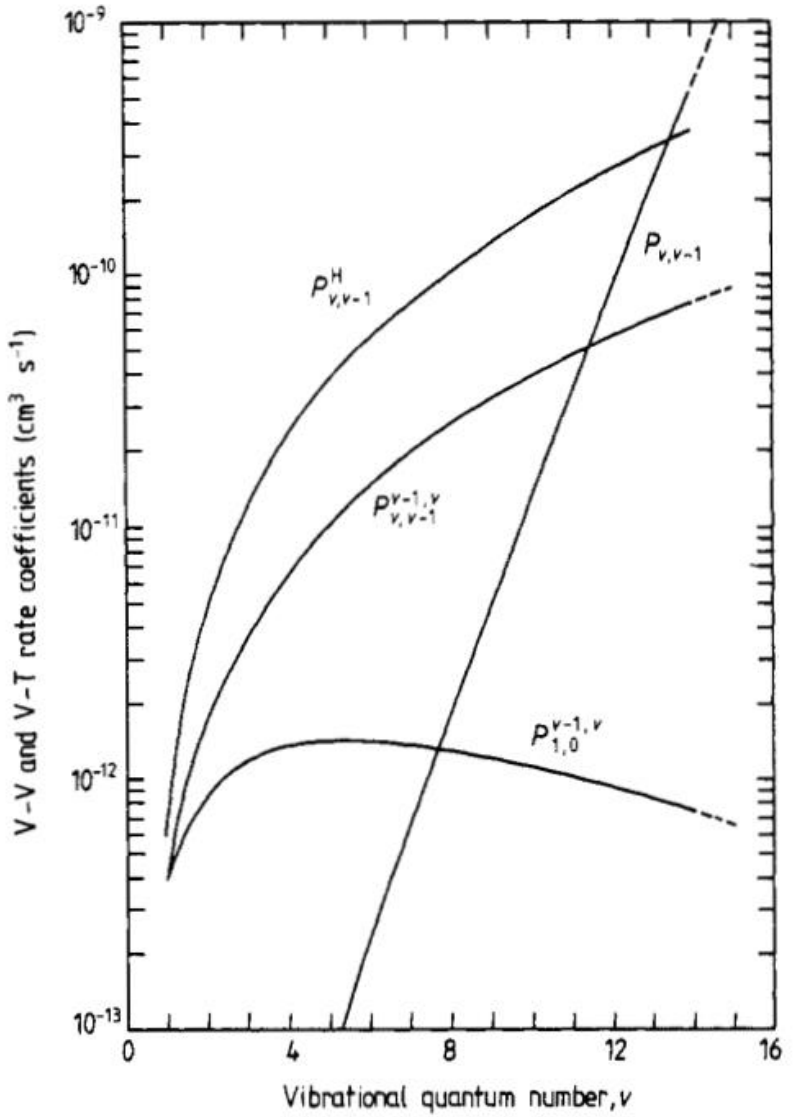

Figure 1. Rate coefficients for V–V and V–T energy exchanges as a function of the vibrational quantum number for T_g = 400 K.

J Loureiro and C M Ferreira 1989 *J. Phys. D: Appl. Phys.* **22** 1680

H_2

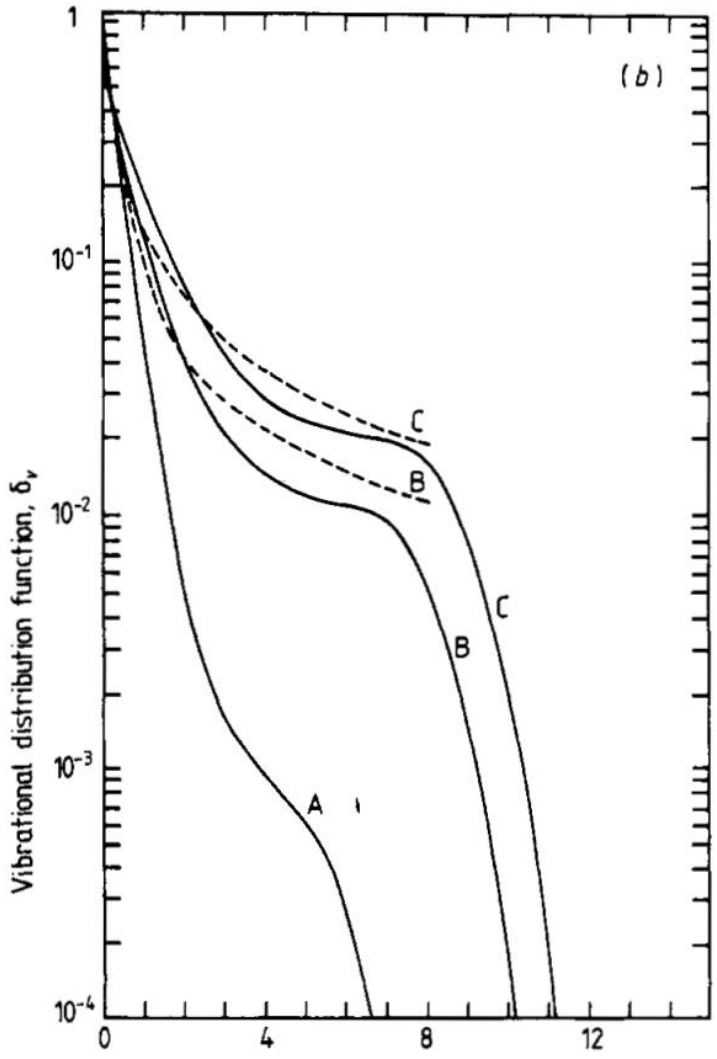

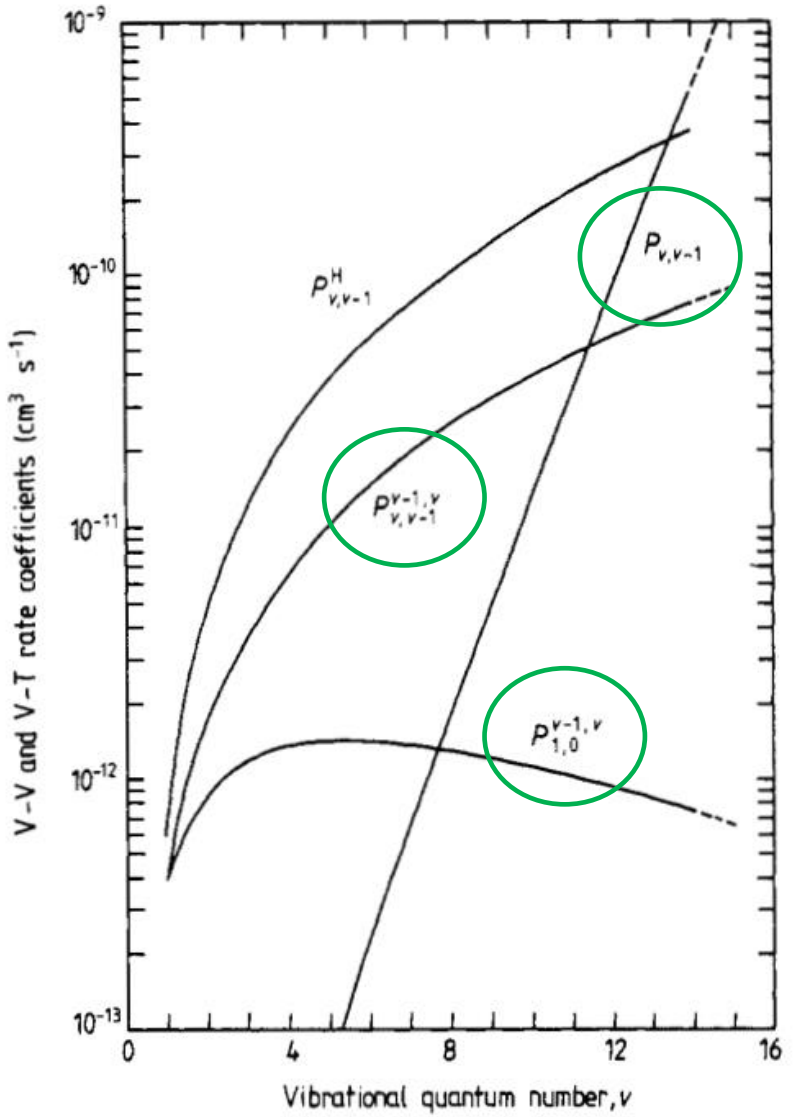

Figure 1. Rate coefficients for V–V and V–T energy exchanges as a function of the vibrational quantum number for T_g = 400 K.

J Loureiro and C M Ferreira 1989 *J. Phys. D: Appl. Phys.* **22** 1680

H_2

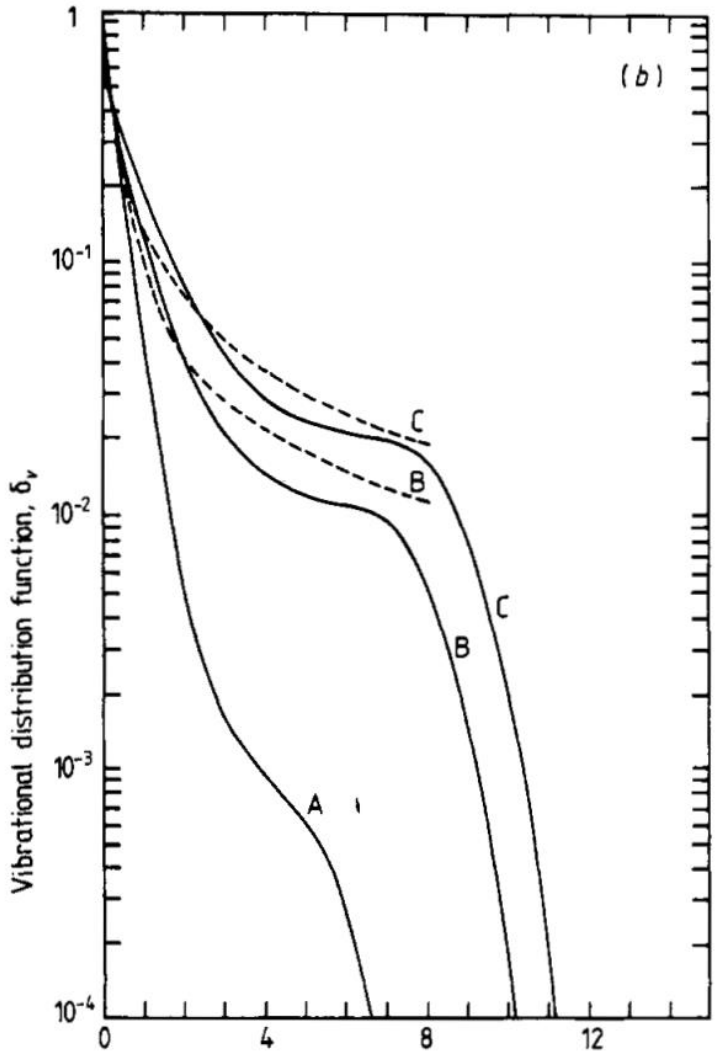

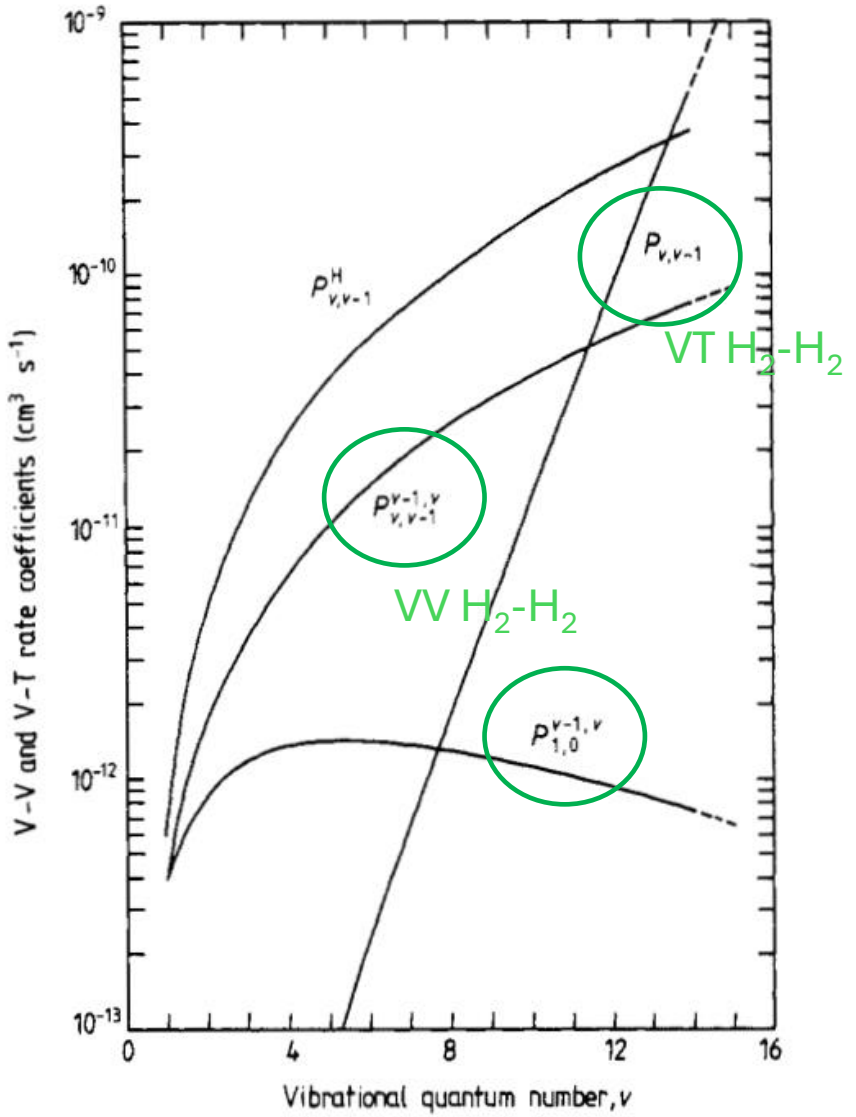

Figure 1. Rate coefficients for V–V and V–T energy exchanges as a function of the vibrational quantum number for T_g = 400 K.

J Loureiro and C M Ferreira 1989 *J. Phys. D: Appl. Phys.* **22** 1680

H_2

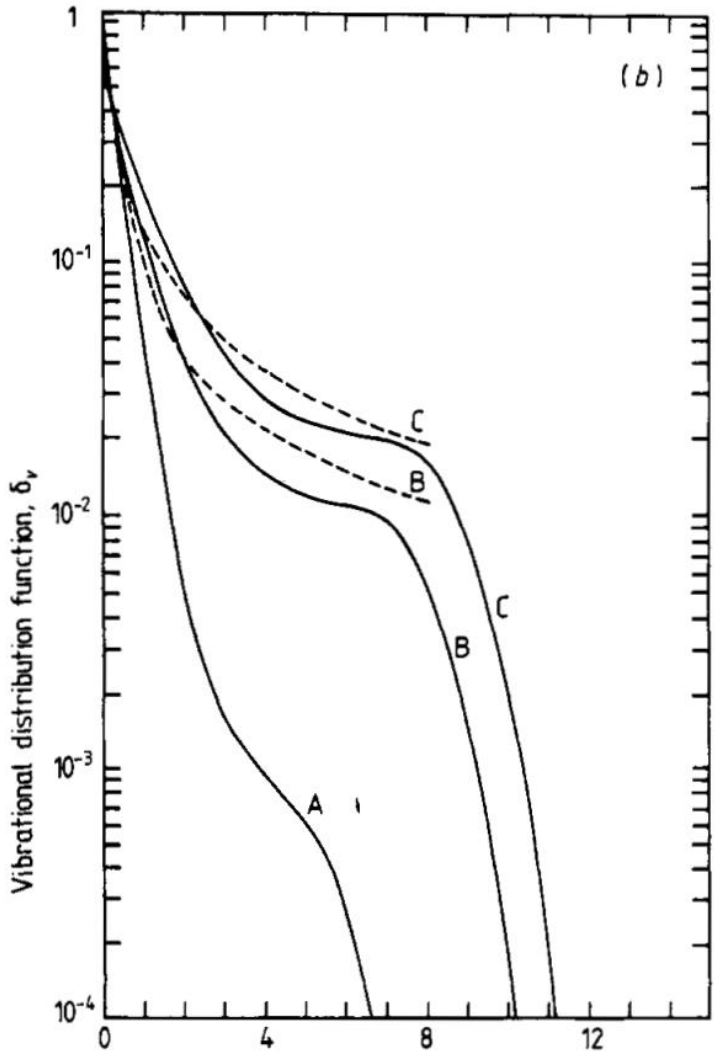

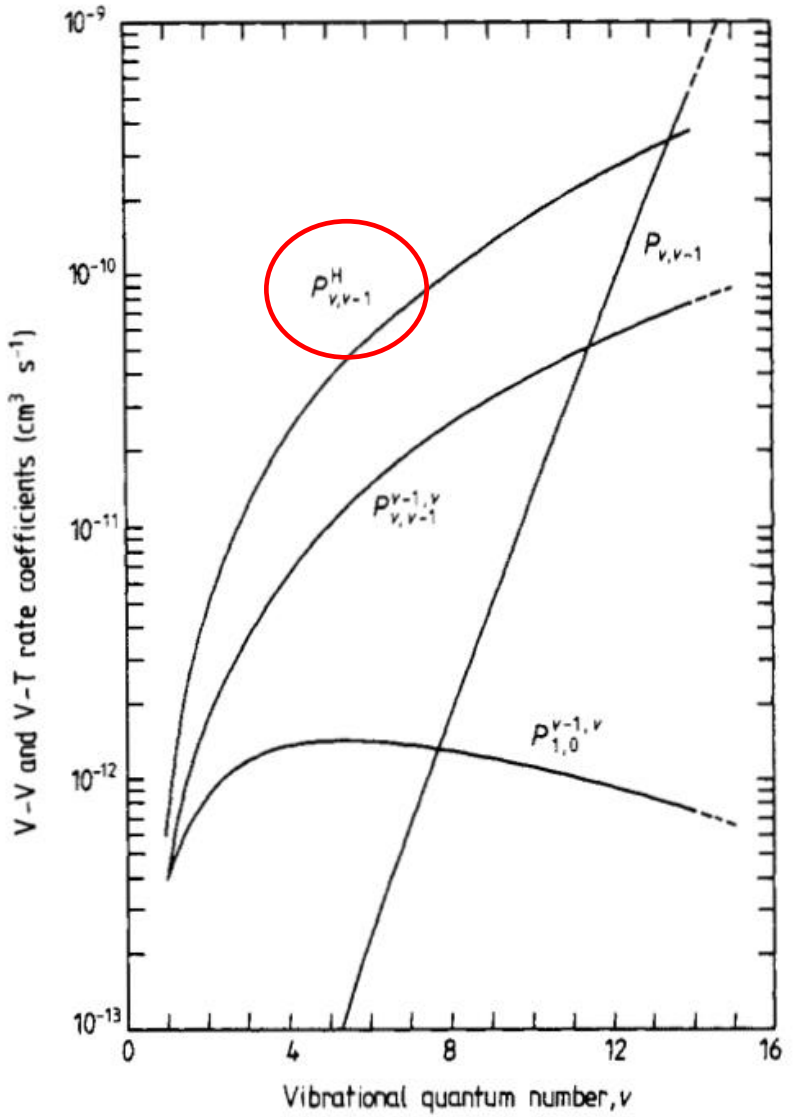

Figure 1. Rate coefficients for V–V and V–T energy exchanges as a function of the vibrational quantum number for T_g = 400 K.

J Loureiro and C M Ferreira 1989 *J. Phys. D: Appl. Phys.* **22** 1680

H_2

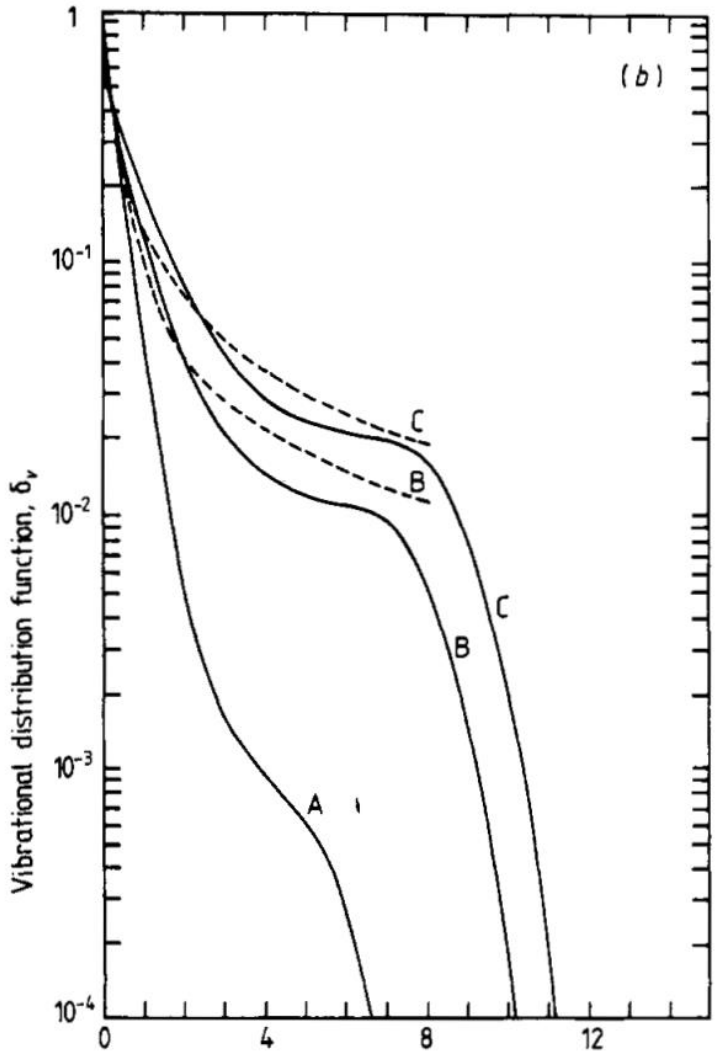

VT H_2-H collisions

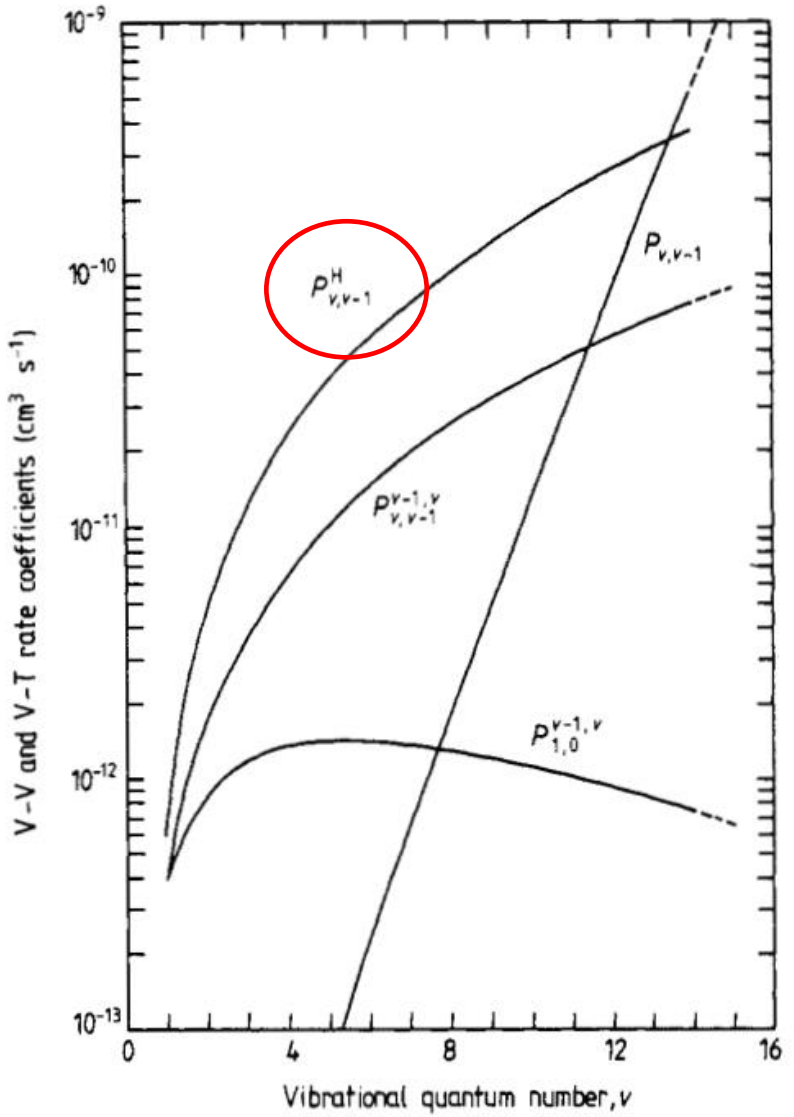

Figure 1. Rate coefficients for V–V and V–T energy exchanges as a function of the vibrational quantum number for T_g = 400 K.

V Guerra and J Loureiro

J. Phys. D: Appl. Phys. **28** (1995) 1903–1918

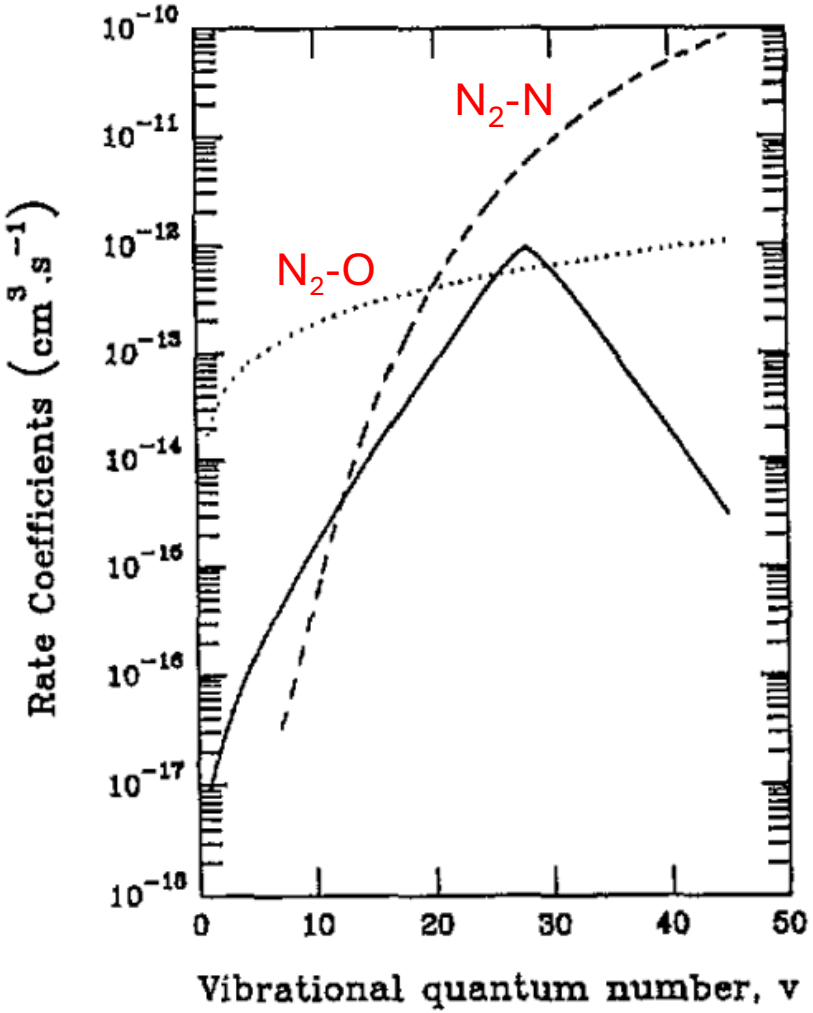

C D Pintassilgo and V Guerra

N_2-N

Plasma Sources Sci. Technol. **26** (2017) 055001

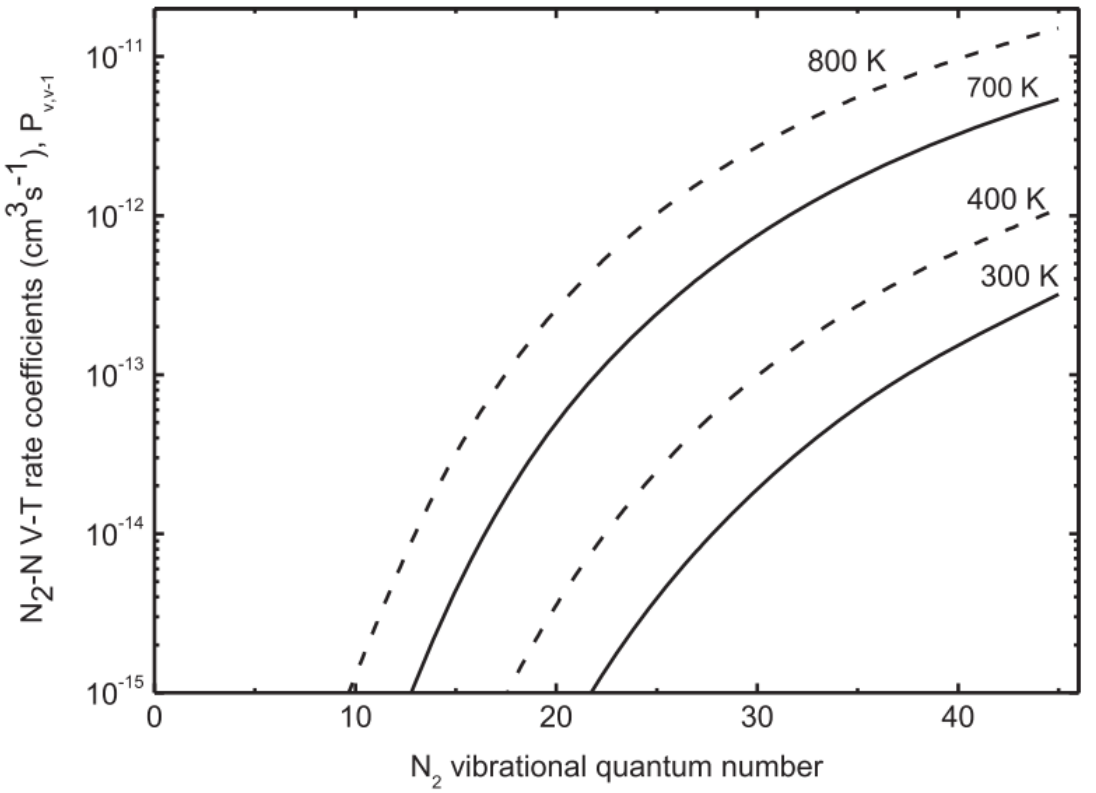

Figure 2. Rate coefficients for V–T energy exchanges in N_2–N collisions, $N_2(v) + N \rightarrow N_2(v\text{-}1) + N$, for different values of the gas temperature, $T_g = 300$, 400, 700, and 800 K.

V Guerra and J Loureiro

J. Phys. D: Appl. Phys. **28** (1995) 1903–1918

95%N_2-5%O_2

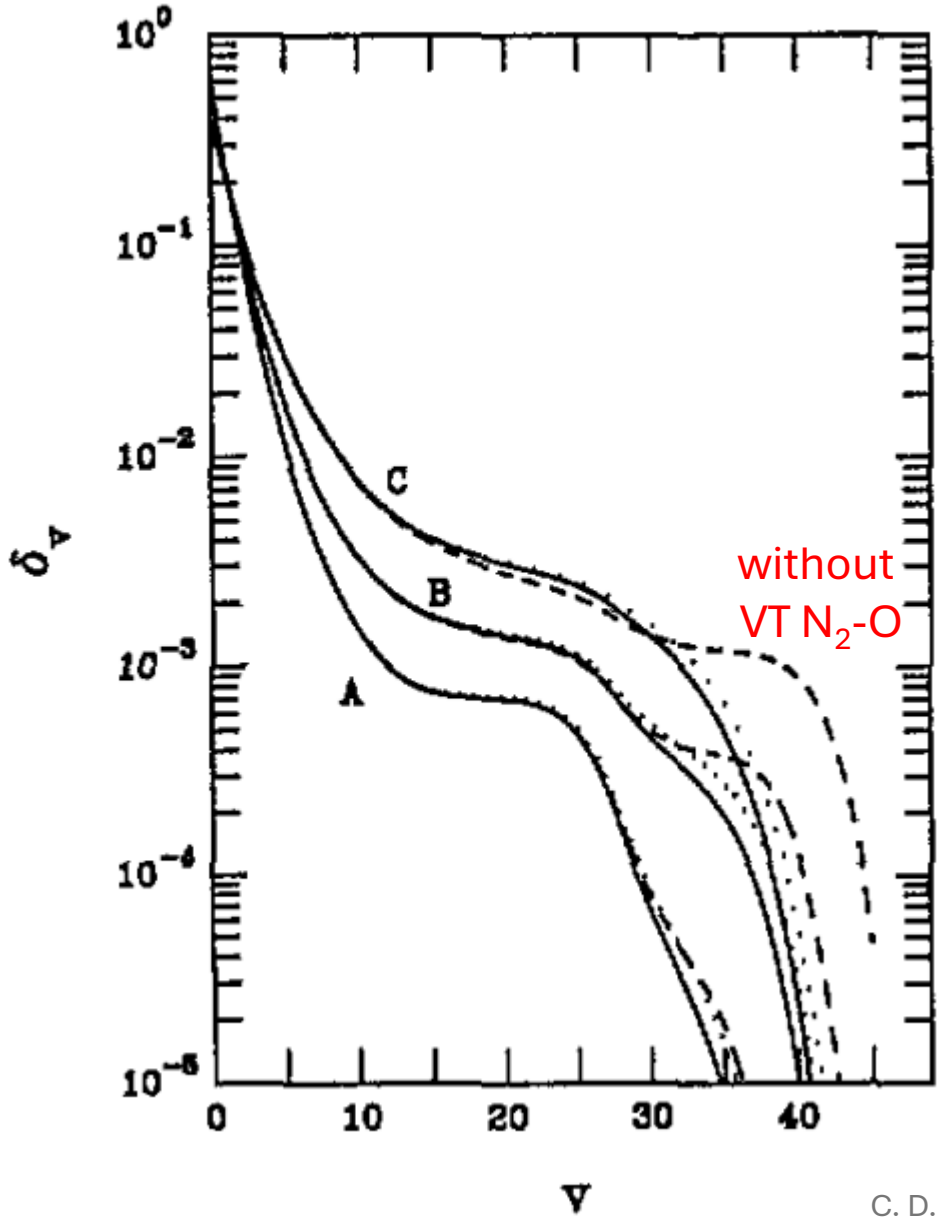

V Guerra and J Loureiro

Plasma Sources Sci. Technol. **6** (1997) 373–385

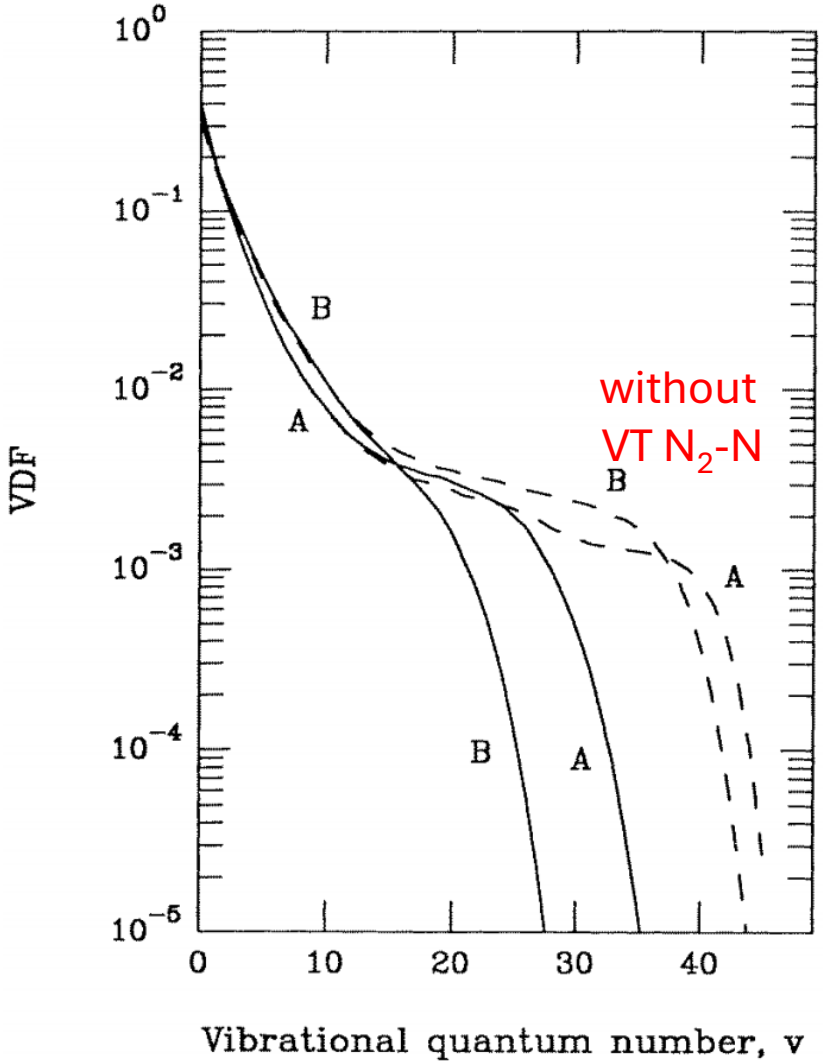

Vibrational kinetics (and consequently electron kinetics) requires a reliable description of the main atomic species produced in the discharge

e-V	$e + N_2(X, v) \rightleftharpoons e + N_2(X, w)$
V-V	$N_2(X, v) + N_2(X, w) \rightleftharpoons N_2(X, v-1) + N_2(X, w+1)$
V-T N_2-N_2	$N_2(X, v) + N_2 \rightleftharpoons N_2(X, v-1) + N_2$

e-V	$e + N_2(X, v) \rightleftharpoons e + N_2(X, w)$
V-V	$N_2(X, v) + N_2(X, w) \rightleftharpoons N_2(X, v-1) + N_2(X, w+1)$
V-T N_2-N_2	$N_2(X, v) + N_2 \rightleftharpoons N_2(X, v-1) + N_2$
V-T N_2-N	$N_2(X, v) + N \rightleftharpoons N_2(X, w) + N$
	$N_2(X, v) + N \rightleftharpoons N + N_2(X, w)$
Chemistry	See Table 5

e-V	$e + N_2(X, v) \rightleftharpoons e + N_2(X, w)$
V-V	$N_2(X, v) + N_2(X, w) \rightleftharpoons N_2(X, v-1) + N_2(X, w+1)$
V-T N_2-N_2	$N_2(X, v) + N_2 \rightleftharpoons N_2(X, v-1) + N_2$
V-T N_2-N	$N_2(X, v) + N \rightleftharpoons N_2(X, w) + N$
	$N_2(X, v) + N \rightleftharpoons N + N_2(X, w)$

Chemistry	See Table 5

Eur. Phys. J. Appl. Phys. **28**, 125-152 (2004)

Table 5. Nitrogen chemistry set.

	Process	Rate coefficient	Reference
C2	$N_2(A)+N_2(A) \rightarrow N_2(B)+N_2(X, v=8)$	$k = 7.7 \times 10^{-11}$ cm^{3}s^{-1}	[45,46]
C3	$N_2(A)+N_2(A) \rightarrow N_2(C)+N_2(X, v=2)$	$k = 1.5 \times 10^{-10}$ cm^{3}s^{-1}	[47,46]
C4	$N_2(A)+N_2(X, 5 \leq v \leq 14) \rightarrow N_2(B)+N_2(X, v=0)$	$k = 2 \times 10^{-11}$ cm^{3}s^{-1}	[48]
C5	$N_2(A)+N_2(X, 14 \leq v \leq 19) \rightarrow N_2(X, v=0)+N+N$	$k = 4.5 \times 10^{-11} \exp(-1765/T_g)$ cm^{3}s^{-1}	[49,50]
C6	$N_2(A)+N(^4S) \rightarrow N_2(X, 6 \leq v \leq 9)+N(^2P)$	$k = 4 \times 10^{-11}$ cm^{3}s^{-1}	[51]

Eur. Phys. J. Appl. Phys. **28**, 125-152 (2004)

Table 5. Nitrogen chemistry set.

	Process	Rate coefficient	Reference
C2	$N_2(A)+N_2(A) \rightarrow N_2(B)+N_2(X, v=8)$	$k = 7.7 \times 10^{-11}$ cm^{3}s^{-1}	[45,46]
C3	$N_2(A)+N_2(A) \rightarrow N_2(C)+N_2(X, v=2)$	$k = 1.5 \times 10^{-10}$ cm^{3}s^{-1}	[47,46]
C4	$N_2(A)+N_2(X, 5 \leq v \leq 14) \rightarrow N_2(B)+N_2(X, v=0)$	$k = 2 \times 10^{-11}$ cm^{3}s^{-1}	[48]
C5	$N_2(A)+N_2(X, 14 \leq v \leq 19) \rightarrow N_2(X, v=0)+N+N$	$k = 4.5 \times 10^{-11} \exp(-1765/T_g)$ cm^{3}s^{-1}	[49,50]
C6	$N_2(A)+N(^4S) \rightarrow N_2(X, 6 \leq v \leq 9)+N(^2P)$	$k = 4 \times 10^{-11}$ cm^{3}s^{-1}	[51]

Eur. Phys. J. Appl. Phys. **28**, 125-152 (2004)

Table 5. Nitrogen chemistry set.

	Process	Rate coefficient	Reference
C2	$N_2(A)+N_2(A) \rightarrow N_2(B)+N_2(X, v=8)$	$k = 7.7 \times 10^{-11}$ cm^{3}s^{-1}	[45,46]
C3	$N_2(A)+N_2(A) \rightarrow N_2(C)+N_2(X, v=2)$	$k = 1.5 \times 10^{-10}$ cm^{3}s^{-1}	[47,46]
C4	$N_2(A)+N_2(X, 5 \leq v \leq 14) \rightarrow N_2(B)+N_2(X, v=0)$	$k = 2 \times 10^{-11}$ cm^{3}s^{-1}	[48]
C5	$N_2(A)+N_2(X, 14 \leq v \leq 19) \rightarrow N_2(X, v=0)+N+N$	$k = 4.5 \times 10^{-11} \exp(-1765/T_g)$ cm^{3}s^{-1}	[49,50]
C6	$N_2(A)+N(^4S) \rightarrow N_2(X, 6 \leq v \leq 9)+N(^2P)$	$k = 4 \times 10^{-11}$ cm^{3}s^{-1}	[51]

Eur. Phys. J. Appl. Phys. **28**, 125-152 (2004)

Table 5. Nitrogen chemistry set.

	Process	Rate coefficient	Reference
C2	$N_2(A)+N_2(A) \rightarrow N_2(B)+N_2(X, v=8)$	$k = 7.7 \times 10^{-11}$ cm^{3}s^{-1}	[45,46]
C3	$N_2(A)+N_2(A) \rightarrow N_2(C)+N_2(X, v=2)$	$k = 1.5 \times 10^{-10}$ cm^{3}s^{-1}	[47,46]
C4	$N_2(A)+N_2(X, 5 \leq v \leq 14) \rightarrow N_2(B)+N_2(X, v=0)$	$k = 2 \times 10^{-11}$ cm^{3}s^{-1}	[48]
C5	$N_2(A)+N_2(X, 14 \leq v \leq 19) \rightarrow N_2(X, v=0)+N+N$	$k = 4.5 \times 10^{-11} \exp(-1765/T_g)$ cm^{3}s^{-1}	[49,50]
C6	$N_2(A)+N(^4S) \rightarrow N_2(X, 6 \leq v \leq 9)+N(^2P)$	$k = 4 \times 10^{-11}$ cm^{3}s^{-1}	[51]

N_2-O_2

N_2-O_2

Table 1. Kinetics of $N_2(X\ ^1\Sigma_g^+, v)$ molecules.

e–V	$e + N_2(X,v) \rightleftharpoons e + N_2(X, v')$
V–T N_2–N_2	$N_2(X,v) + N_2 \rightleftharpoons N_2(X, v-1) + N_2$
V–T N_2–N	$N_2(X,v) + N \rightleftharpoons N_2(X, v' < v) + N$
V–T N_2–O_2	$N_2(X,v) + O_2 \rightleftharpoons N_2(X, v-1) + O_2$
V–T N_2–O	$N_2(X,v) + O \rightleftharpoons N_2(X, v-1) + O$
V–V N_2–N_2	$N_2(X,v) + N_2(X,v') \rightleftharpoons N_2(X,v-1) + N_2(X,v'+1)$
V–V N_2–O_2	$N_2(X,v) + O_2(X,w) \rightleftharpoons N_2(X,v-1) + O_2(X,w+1)$
e–D	$e + N_2(X,v) \rightarrow e + N + N$
V–D	$N_2(X,v_{Max}) + N_2 \rightarrow N + N + N_2$
	$N_2(X,v_{Max}) + N_2(X,v') \rightarrow N + N + N_2(X,v'-1)$
	$N_2(X,v) + N \rightarrow N + N + N$
	$N_2(X,v_{Max}) + O_2 \rightarrow N + N + O_2$
	$N_2(X,v_{Max}) + O_2(X,w) \rightarrow N + N + O_2(X,w-1)$
	$N_2(X,v_{Max}) + O \rightarrow N + N + O$
	$2N_2(X,v = 10{:}25) \rightarrow N + N + N_2$
Z	$N_2(X,v) + O \rightarrow NO + N$
W	$N_2(X,v) + \text{wall} \rightleftharpoons N_2(X,v-1)$

N_2-O_2

Table 1. Kinetics of $N_2(X\ ^1\Sigma_g^+, v)$ molecules.

e–V	$e + N_2(X,v) \rightleftharpoons e + N_2(X, v')$
V–T N_2–N_2	$N_2(X,v) + N_2 \rightleftharpoons N_2(X, v-1) + N_2$
V–T N_2–N	$N_2(X,v) + N \rightleftharpoons N_2(X, v' < v) + N$
V–T N_2–O_2	$N_2(X,v) + O_2 \rightleftharpoons N_2(X, v-1) + O_2$
V–T N_2–O	$N_2(X,v) + O \rightleftharpoons N_2(X, v-1) + O$
V–V N_2–N_2	$N_2(X,v) + N_2(X,v') \rightleftharpoons N_2(X,v-1) + N_2(X,v'+1)$
V–V N_2–O_2	$N_2(X,v) + O_2(X,w) \rightleftharpoons N_2(X,v-1) + O_2(X,w+1)$
e–D	$e + N_2(X,v) \rightarrow e + N + N$
V–D	$N_2(X,v_{Max}) + N_2 \rightarrow N + N + N_2$
	$N_2(X,v_{Max}) + N_2(X,v') \rightarrow N + N + N_2(X,v'-1)$
	$N_2(X,v) + N \rightarrow N + N + N$
	$N_2(X,v_{Max}) + O_2 \rightarrow N + N + O_2$
	$N_2(X,v_{Max}) + O_2(X,w) \rightarrow N + N + O_2(X,w-1)$
	$N_2(X,v_{Max}) + O \rightarrow N + N + O$
	$2N_2(X,v = 10{:}25) \rightarrow N + N + N_2$
Z	$N_2(X,v) + O \rightarrow NO + N$
W	$N_2(X,v) + \text{wall} \rightleftharpoons N_2(X,v-1)$

N_2-O_2

Table 1. Kinetics of $N_2(X\ ^1\Sigma_g^+, v)$ molecules.

e–V	$e + N_2(X,v) \rightleftharpoons e + N_2(X, v')$
V–T N_2–N_2	$N_2(X,v) + N_2 \rightleftharpoons N_2(X, v-1) + N_2$
V–T N_2–N	$N_2(X,v) + N \rightleftharpoons N_2(X, v' < v) + N$
V–T N_2–O_2	$N_2(X,v) + O_2 \rightleftharpoons N_2(X, v-1) + O_2$
V–T N_2–O	$N_2(X,v) + O \rightleftharpoons N_2(X, v-1) + O$
V–V N_2–N_2	$N_2(X,v) + N_2(X,v') \rightleftharpoons N_2(X,v-1) + N_2(X,v'+1)$
V–V N_2–O_2	$N_2(X,v) + O_2(X,w) \rightleftharpoons N_2(X,v-1) + O_2(X,w+1)$
e–D	$e + N_2(X,v) \rightarrow e + N + N$
V–D	$N_2(X,v_{Max}) + N_2 \rightarrow N + N + N_2$
	$N_2(X,v_{Max}) + N_2(X,v') \rightarrow N + N + N_2(X,v'-1)$
	$N_2(X,v) + N \rightarrow N + N + N$
	$N_2(X,v_{Max}) + O_2 \rightarrow N + N + O_2$
	$N_2(X,v_{Max}) + O_2(X,w) \rightarrow N + N + O_2(X,w-1)$
	$N_2(X,v_{Max}) + O \rightarrow N + N + O$
	$2N_2(X,v = 10{:}25) \rightarrow N + N + N_2$
Z	$N_2(X,v) + O \rightarrow NO + N$
W	$N_2(X,v) + \text{wall} \rightleftharpoons N_2(X,v-1)$

N_2-O_2

Table 1. Kinetics of $N_2(X\ ^1\Sigma_g^+, v)$ molecules.

e–V	$e + N_2(X,v) \rightleftharpoons e + N_2(X, v')$
V–T N_2–N_2	$N_2(X,v) + N_2 \rightleftharpoons N_2(X, v-1) + N_2$
V–T N_2–N	$N_2(X,v) + N \rightleftharpoons N_2(X, v' < v) + N$
V–T N_2–O_2	$N_2(X,v) + O_2 \rightleftharpoons N_2(X, v-1) + O_2$
V–T N_2–O	$N_2(X,v) + O \rightleftharpoons N_2(X, v-1) + O$
V–V N_2–N_2	$N_2(X,v) + N_2(X,v') \rightleftharpoons N_2(X,v-1) + N_2(X,v'+1)$
V–V N_2–O_2	$N_2(X,v) + O_2(X,w) \rightleftharpoons N_2(X,v-1) + O_2(X,w+1)$
e–D	$e + N_2(X,v) \rightarrow e + N + N$
V–D	$N_2(X,v_{Max}) + N_2 \rightarrow N + N + N_2$
	$N_2(X,v_{Max}) + N_2(X,v') \rightarrow N + N + N_2(X,v'-1)$
	$N_2(X,v) + N \rightarrow N + N + N$
	$N_2(X,v_{Max}) + O_2 \rightarrow N + N + O_2$
	$N_2(X,v_{Max}) + O_2(X,w) \rightarrow N + N + O_2(X,w-1)$
	$N_2(X,v_{Max}) + O \rightarrow N + N + O$
	$2N_2(X,v = 10{:}25) \rightarrow N + N + N_2$
Z	$N_2(X,v) + O \rightarrow NO + N$
W	$N_2(X,v) + \text{wall} \rightleftharpoons N_2(X,v-1)$

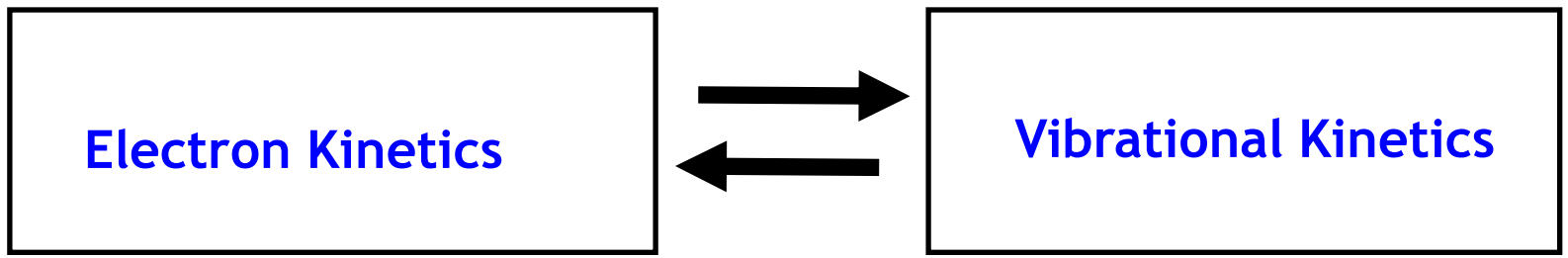
Electron Kinetics
Vibrational Kinetics

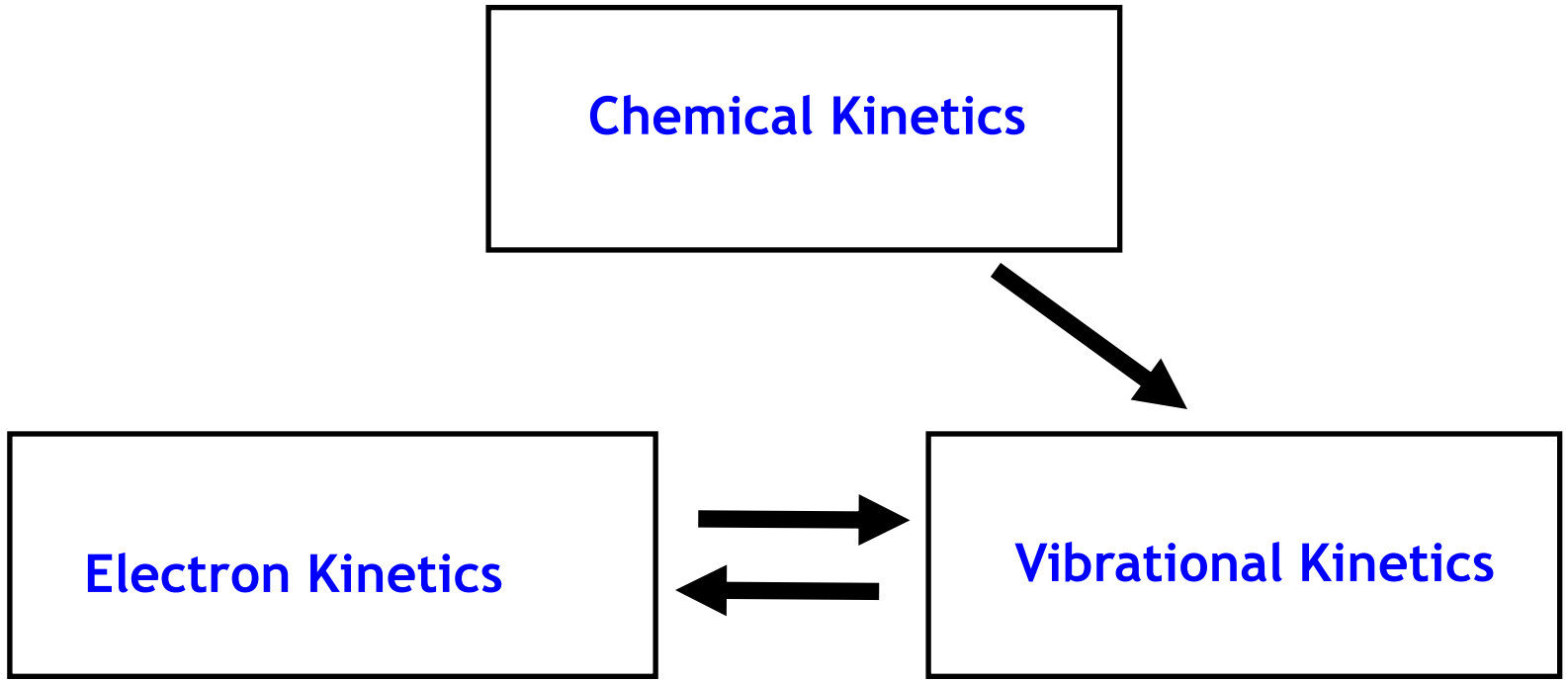
Chemical Kinetics
Electron Kinetics
Vibrational Kinetics

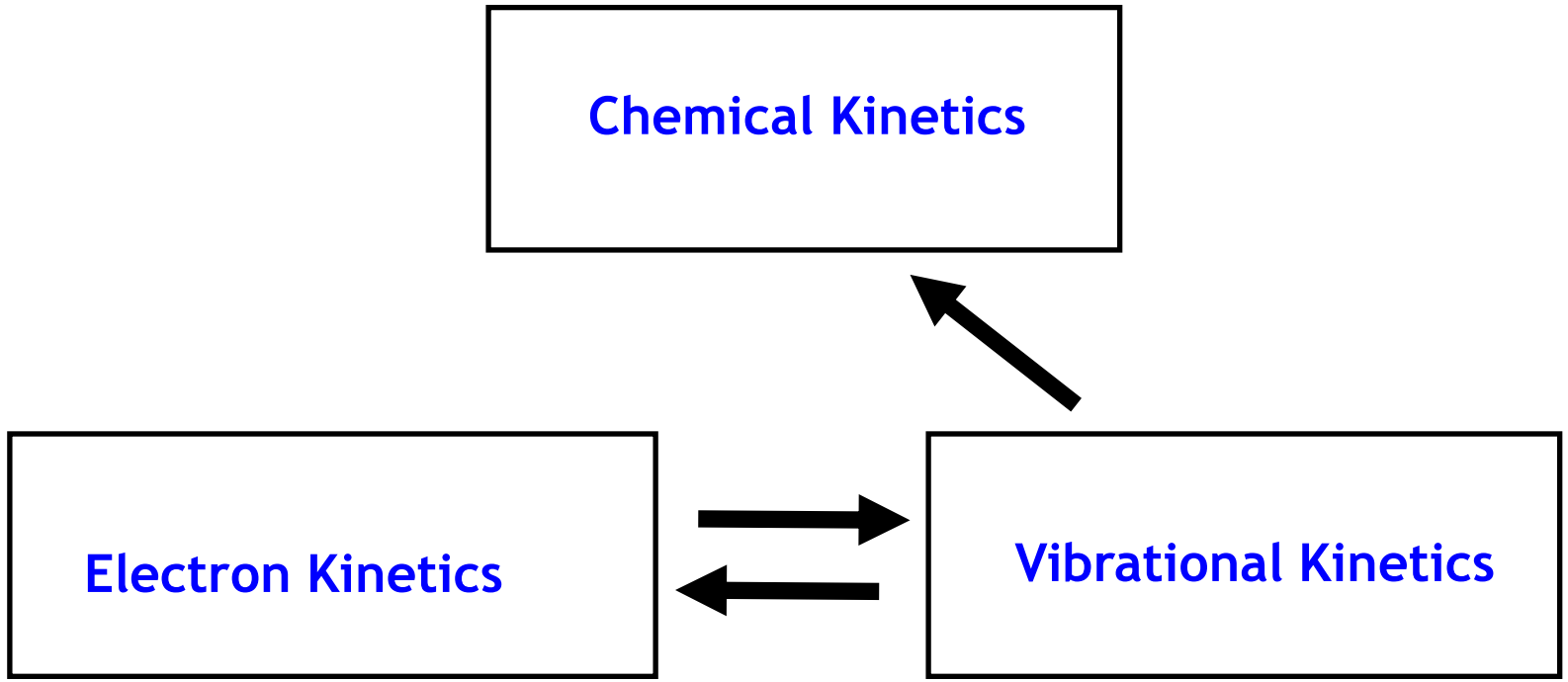
Chemical Kinetics
Electron Kinetics
Vibrational Kinetics

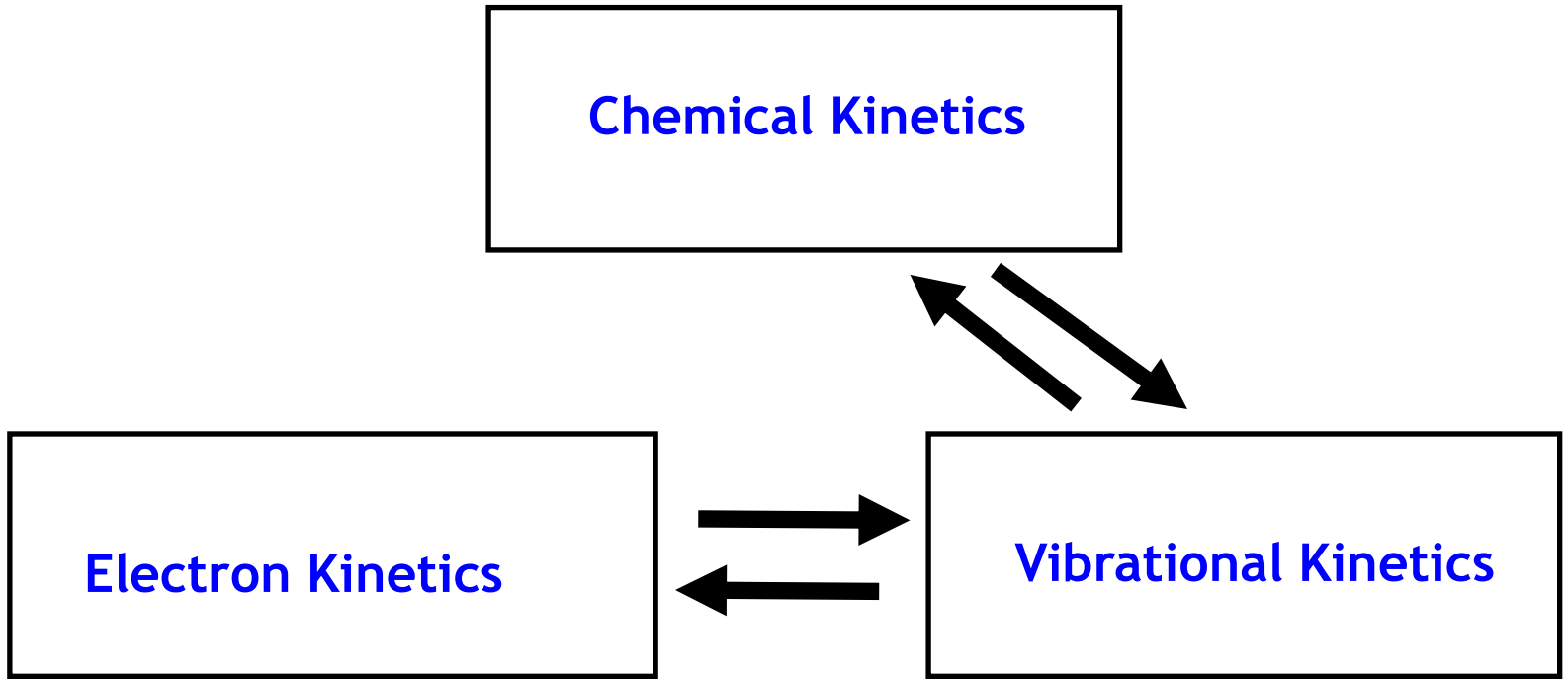
Chemical Kinetics
Electron Kinetics
Vibrational Kinetics

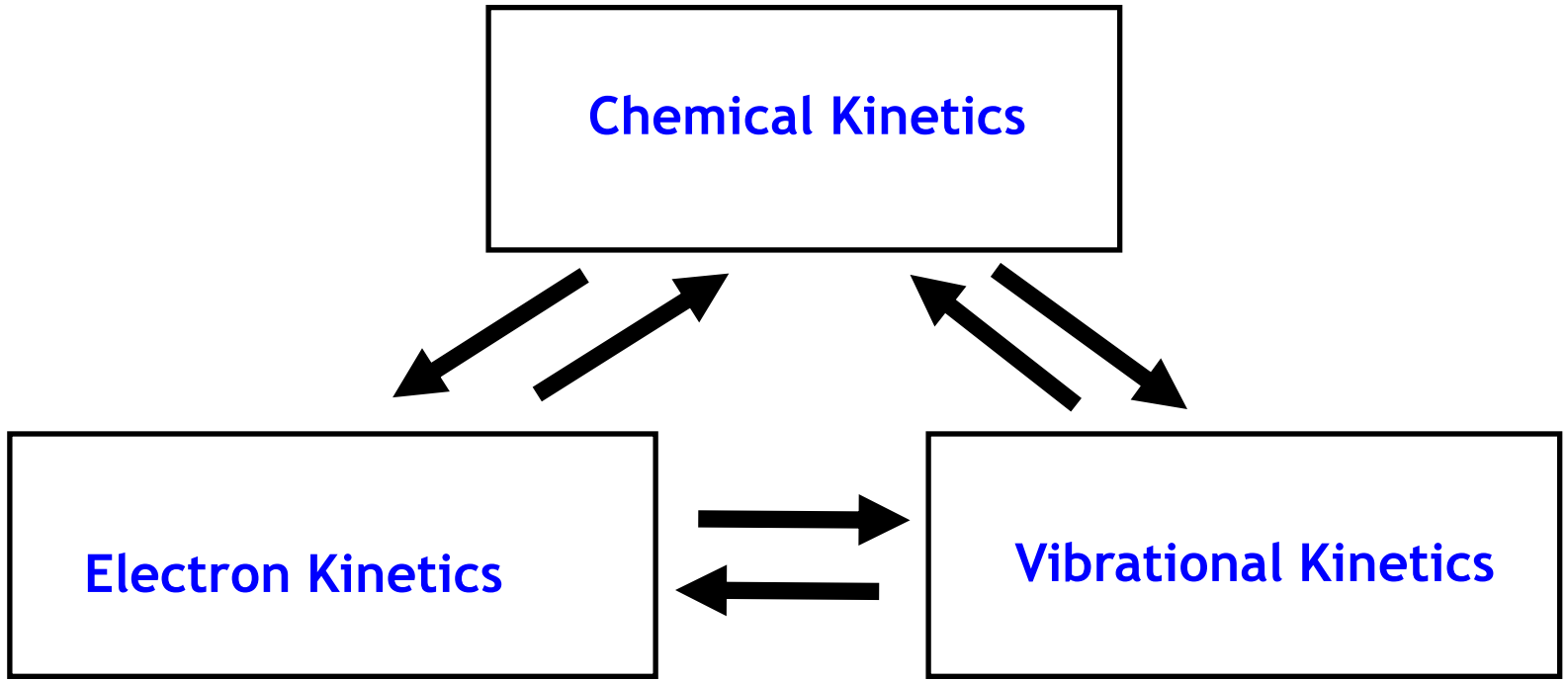
Chemical Kinetics
Electron Kinetics
Vibrational Kinetics

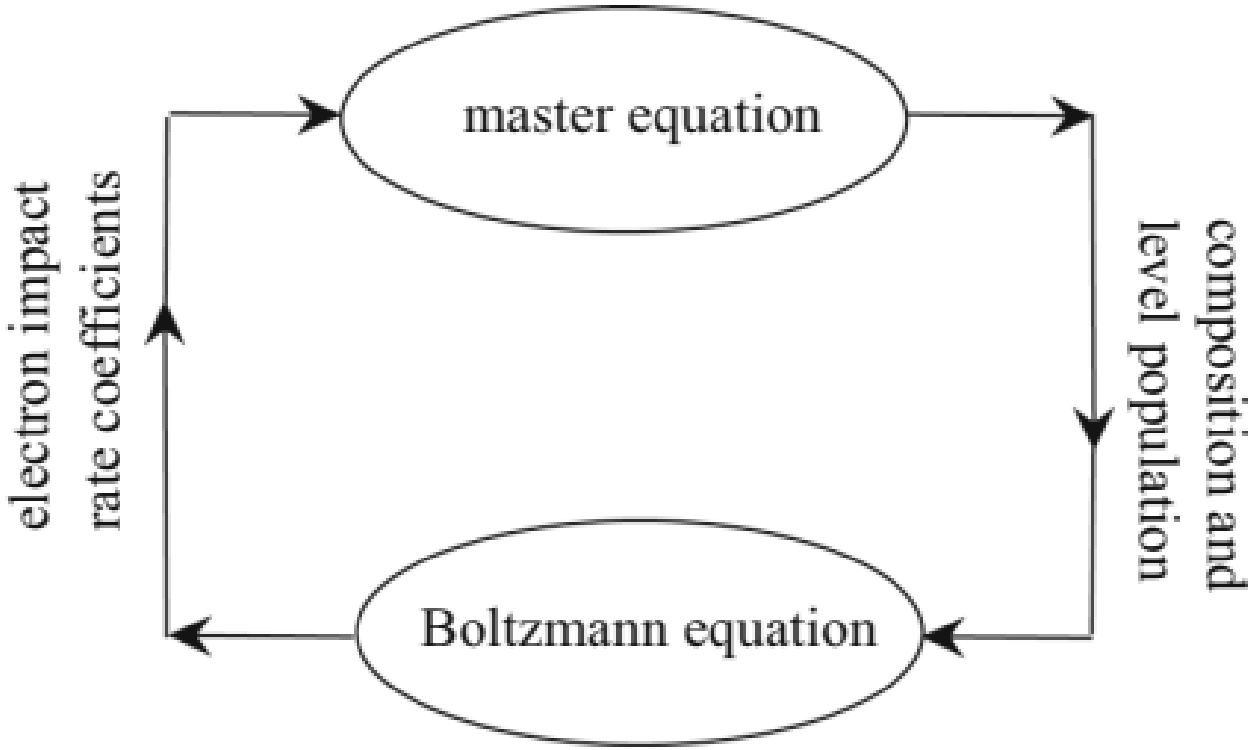
master equation
composition and
level population
Boltzmann equation
electron impact
rate coefficients

By the way…

The LisbOn KInetics (LoKI-GM) simulation tool

(developed under MATLAB®)

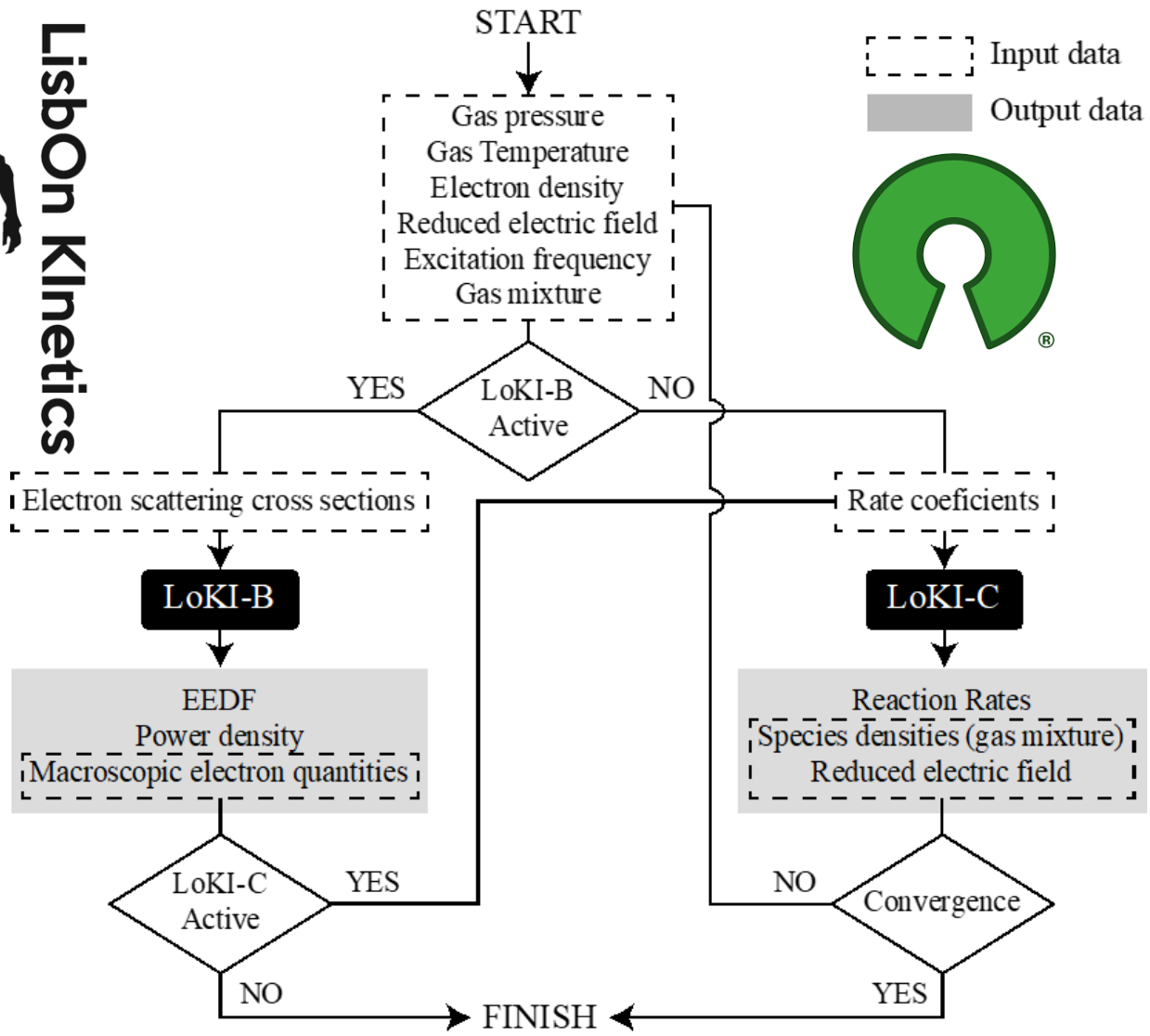

LoKI-B

- solves the space independent form of the two-term electron Boltzmann equation, for DC/HF or time-dependent (non-oscillatory) electric fields.
- includes e-e collisions, CAR operator, and growth models for the electron density.

LoKI-C

- solves the system of 0D rate balance equations for the heavy particles of pure gases or gaseous mixtures.
- includes modules to describe

(i) the collisional, radiative and transport mechanisms controlling the creation / destruction of volume and surface species

(ii) the thermal heating of the neutral gas

loki@tecnico.ulisboa.pt

https://github.com/LoKI-suite

Let me mention **the numerical tool LoKI-GM**, available as open-source.

Release this evening 19h-20 h.

Poster session 2 LoKI-GM: a global model tool for plasma chemistry studies

OUTLINE

Fundamentals

coupling between electron, chemical and vibrational kinetics

Typical examples

pulsed discharges (N_2-O_2, N_2)

Application to DBD discharges

N_2-O_2-H_20 plasmas (humid air)

OUTLINE

Fundamentals

coupling between electron, chemical and vibrational kinetics

Typical examples

pulsed discharges (N_2-O_2, N_2)

Application to DBD discharges

N_2-O_2-H_2O plasmas (humid air)

N_2-O_2

Table 1. Kinetics of $N_2(X\ ^1\Sigma_g^+, v)$ molecules.

e–V	$e + N_2(X,v) \rightleftharpoons e + N_2(X, v')$
V–T N_2–N_2	$N_2(X,v) + N_2 \rightleftharpoons N_2(X, v-1) + N_2$
V–T N_2–N	$N_2(X,v) + N \rightleftharpoons N_2(X, v' < v) + N$
V–T N_2–O_2	$N_2(X,v) + O_2 \rightleftharpoons N_2(X, v-1) + O_2$
V–T N_2–O	$N_2(X,v) + O \rightleftharpoons N_2(X, v-1) + O$
V–V N_2–N_2	$N_2(X,v) + N_2(X,v') \rightleftharpoons N_2(X,v-1) + N_2(X,v'+1)$
V–V N_2–O_2	$N_2(X,v) + O_2(X,w) \rightleftharpoons N_2(X,v-1) + O_2(X,w+1)$
e–D	$e + N_2(X,v) \rightarrow e + N + N$
V–D	$N_2(X,v_{Max}) + N_2 \rightarrow N + N + N_2$
	$N_2(X,v_{Max}) + N_2(X,v') \rightarrow N + N + N_2(X,v'-1)$
	$N_2(X,v) + N \rightarrow N + N + N$
	$N_2(X,v_{Max}) + O_2 \rightarrow N + N + O_2$
	$N_2(X,v_{Max}) + O_2(X,w) \rightarrow N + N + O_2(X,w-1)$
	$N_2(X,v_{Max}) + O \rightarrow N + N + O$
	$2N_2(X,v = 10{:}25) \rightarrow N + N + N_2$
Z	$N_2(X,v) + O \rightarrow NO + N$
W	$N_2(X,v) + \text{wall} \rightleftharpoons N_2(X,v-1)$

Table 1. Kinetics of $N_2(X\ ^1\Sigma_g^+, v)$ molecules.

e–V	$e + N_2(X,v) \rightleftharpoons e + N_2(X, v')$
V–T N_2–N_2	$N_2(X,v) + N_2 \rightleftharpoons N_2(X, v-1) + N_2$
V–T N_2–N	$N_2(X,v) + N \rightleftharpoons N_2(X, v' < v) + N$
V–T N_2–O_2	$N_2(X,v) + O_2 \rightleftharpoons N_2(X, v-1) + O_2$
V–T N_2–O	$N_2(X,v) + O \rightleftharpoons N_2(X, v-1) + O$
V–V N_2–N_2	$N_2(X,v) + N_2(X,v') \rightleftharpoons N_2(X,v-1) + N_2(X,v'+1)$
V–V N_2–O_2	$N_2(X,v) + O_2(X,w) \rightleftharpoons N_2(X,v-1) + O_2(X,w+1)$
e–D	$e + N_2(X,v) \rightarrow e + N + N$
V–D	$N_2(X,v_{Max}) + N_2 \rightarrow N + N + N_2$
	$N_2(X,v_{Max}) + N_2(X,v') \rightarrow N + N + N_2(X,v'-1)$
	$N_2(X,v) + N \rightarrow N + N + N$
	$N_2(X,v_{Max}) + O_2 \rightarrow N + N + O_2$
	$N_2(X,v_{Max}) + O_2(X,w) \rightarrow N + N + O_2(X,w-1)$
	$N_2(X,v_{Max}) + O \rightarrow N + N + O$
	$2N_2(X,v = 10{:}25) \rightarrow N + N + N_2$
Z	$N_2(X,v) + O \rightarrow NO + N$
W	$N_2(X,v) + \text{wall} \rightleftharpoons N_2(X,v-1)$

$$N_2(X, v \geqslant 13) + O(^3P) \rightarrow NO(X) + N(^4S)$$

C D Pintassilgo *et al* Plasma Sources Sci. Technol. **18** (2009)

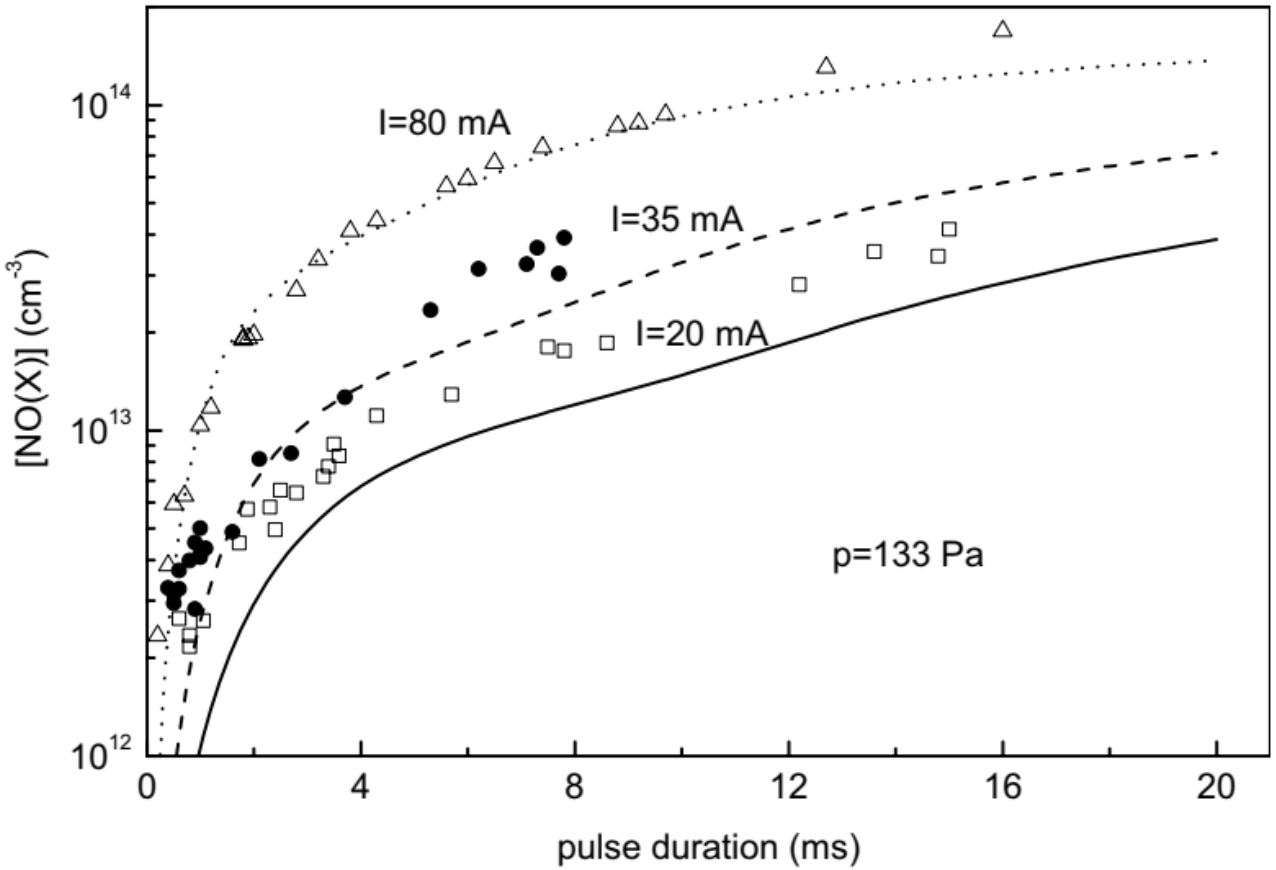

80%N_2-20%O_2

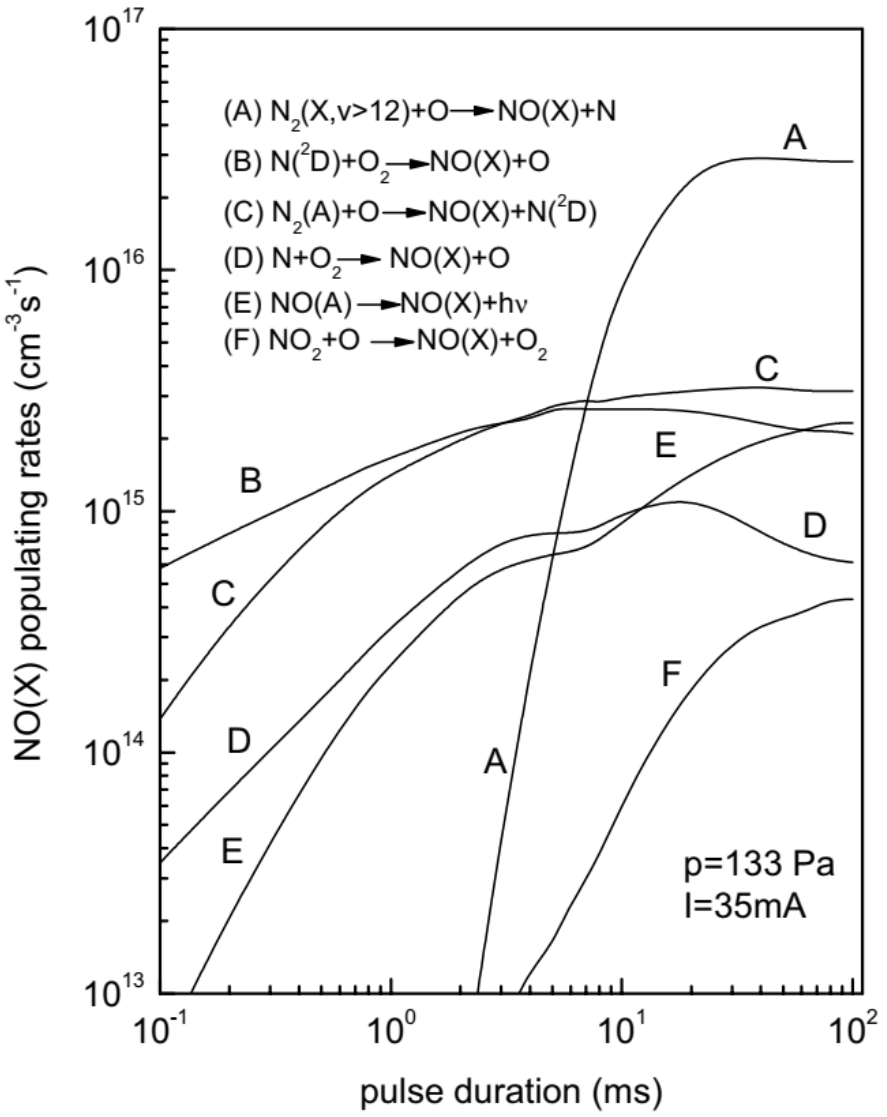
(A) $N_2(X,v>12)+O \rightarrow NO(X)+N$
(B) $N(^2D)+O_2 \rightarrow NO(X)+O$
(C) $N_2(A)+O \rightarrow NO(X)+N(^2D)$
(D) $N+O_2 \rightarrow NO(X)+O$
(E) $NO(A) \rightarrow NO(X)+h\nu$
(F) $NO_2+O \rightarrow NO(X)+O_2$
A
B
C
D
E
F
p=133 Pa
I=35mA
NO(X) populating rates ($cm^{-3}s^{-1}$)
pulse duration (ms)

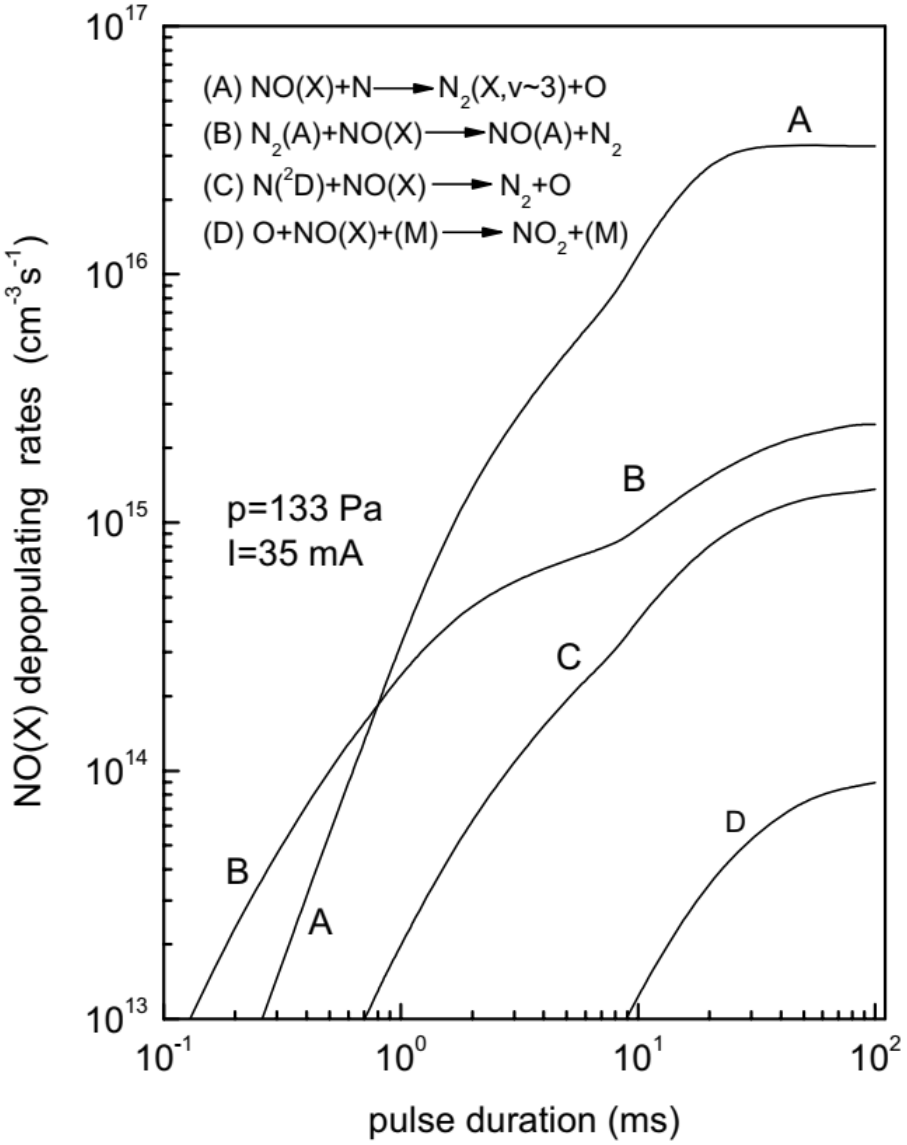
(A) $NO(X)+N \rightarrow N_2(X,v\sim3)+O$
(B) $N_2(A)+NO(X) \rightarrow NO(A)+N_2$
(C) $N(^2D)+NO(X) \rightarrow N_2+O$
(D) $O+NO(X)+(M) \rightarrow NO_2+(M)$
A
B
C
D
p=133 Pa
I=35 mA
NO(X) depopulating rates ($cm^{-3}s^{-1}$)
pulse duration (ms)

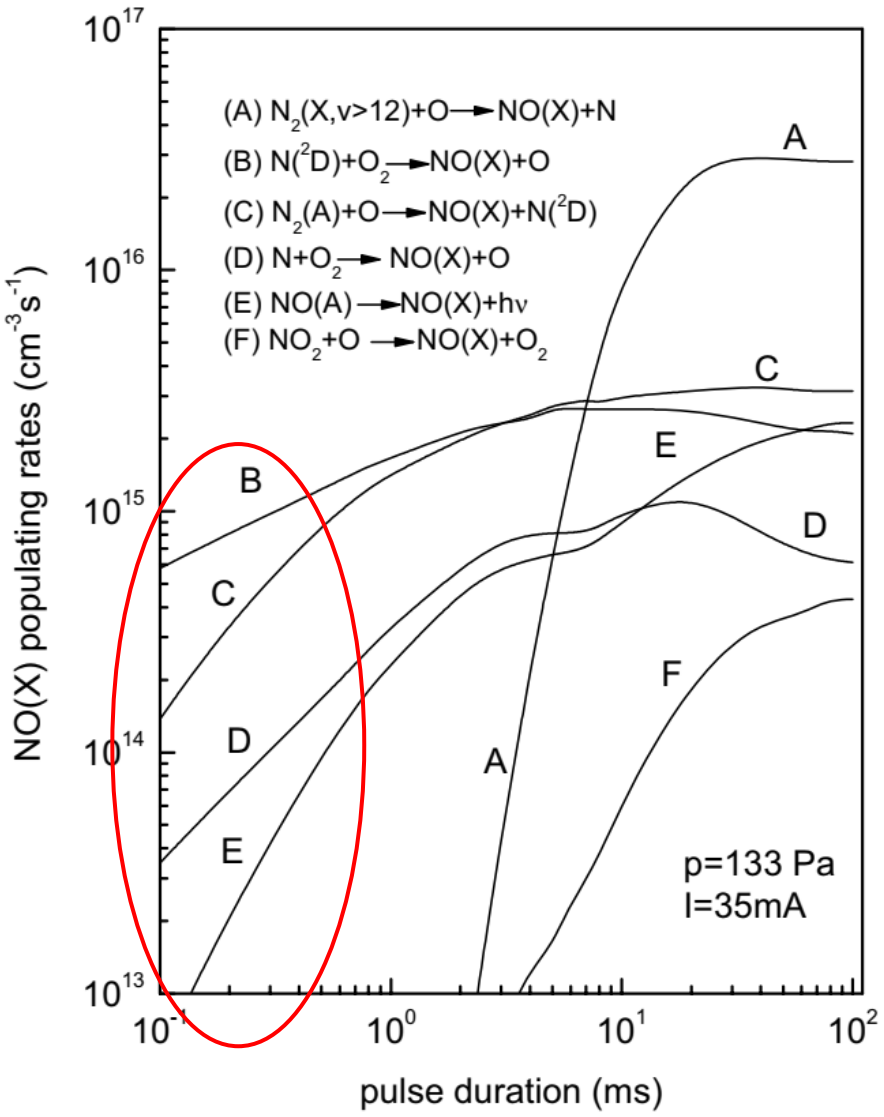
(A) $N_2(X,v>12)+O \rightarrow NO(X)+N$
(B) $N(^2D)+O_2 \rightarrow NO(X)+O$
(C) $N_2(A)+O \rightarrow NO(X)+N(^2D)$
(D) $N+O_2 \rightarrow NO(X)+O$
(E) $NO(A) \rightarrow NO(X)+h\nu$
(F) $NO_2+O \rightarrow NO(X)+O_2$
A
B
C
D
E
F
p=133 Pa
I=35mA
NO(X) populating rates ($cm^{-3}s^{-1}$)
pulse duration (ms)

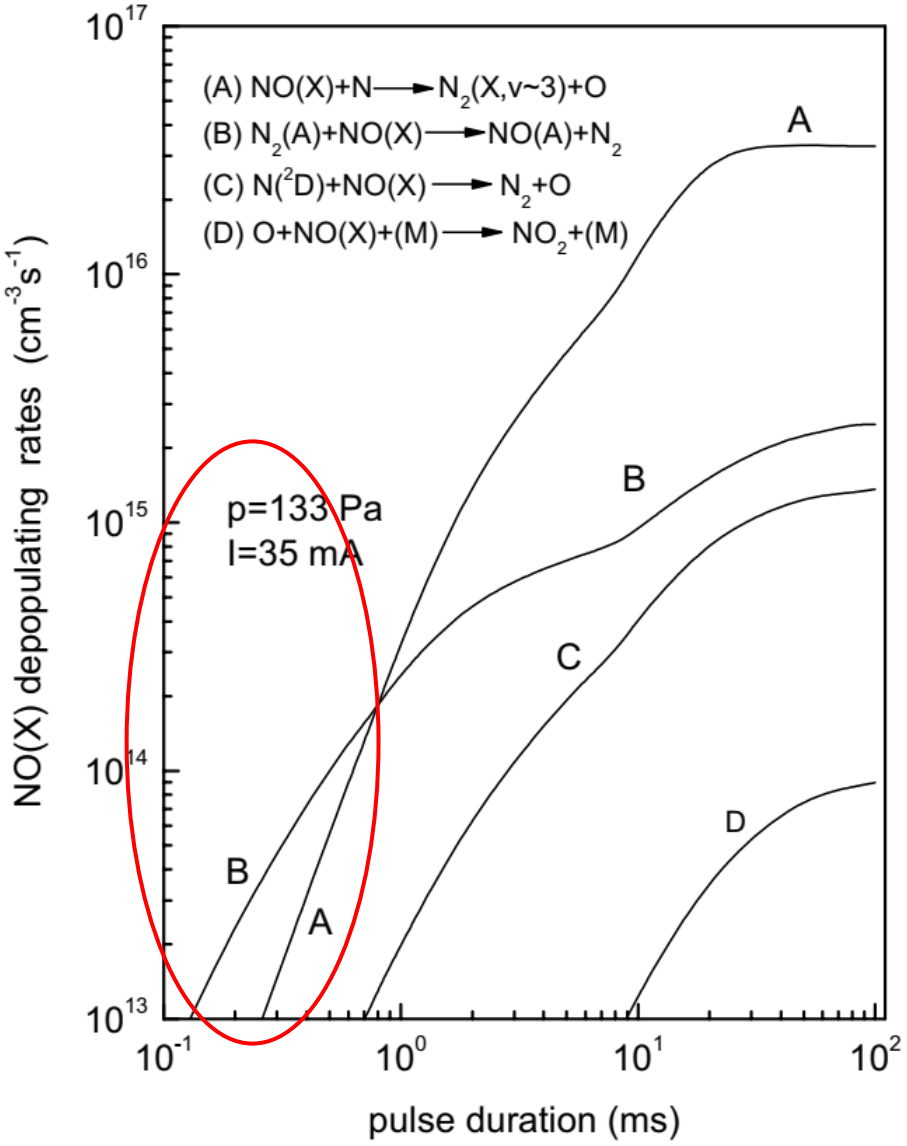
(A) $NO(X)+N \rightarrow N_2(X,v\sim3)+O$
(B) $N_2(A)+NO(X) \rightarrow NO(A)+N_2$
(C) $N(^2D)+NO(X) \rightarrow N_2+O$
(D) $O+NO(X)+(M) \rightarrow NO_2+(M)$
A
B
C
D
p=133 Pa
I=35 mA
NO(X) depopulating rates ($cm^{-3}s^{-1}$)
pulse duration (ms)

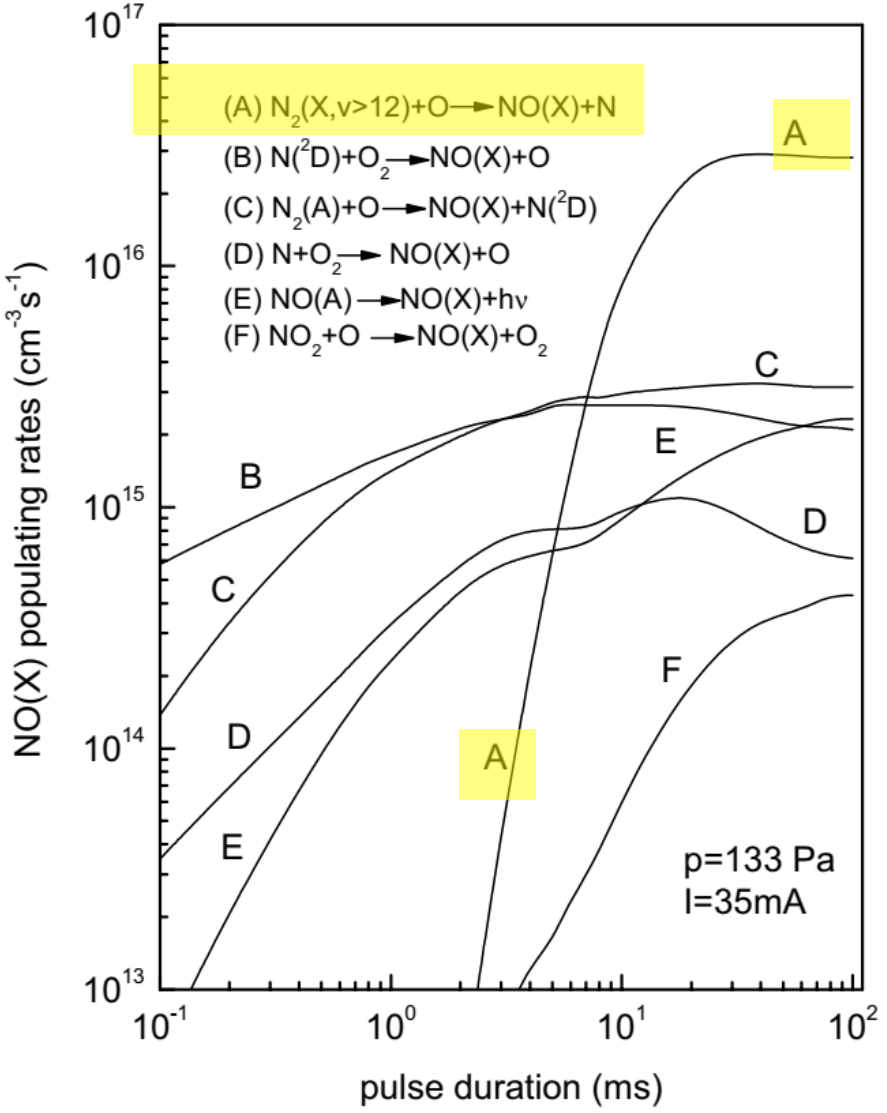
(A) N2(X,v>12)+O→NO(X)+N
(B) N(2D)+O2→NO(X)+O
(C) N2(A)+O→NO(X)+N(2D)
(D) N+O2→ NO(X)+O
(E) NO(A)→NO(X)+hν
(F) NO2+O →NO(X)+O2
A
B
C
D
E
F
p=133 Pa
I=35mA
NO(X) populating rates (cm-3s-1)
pulse duration (ms)
10^17
10^16
10^15
10^14
10^13
10^-1
10^0
10^1
10^2

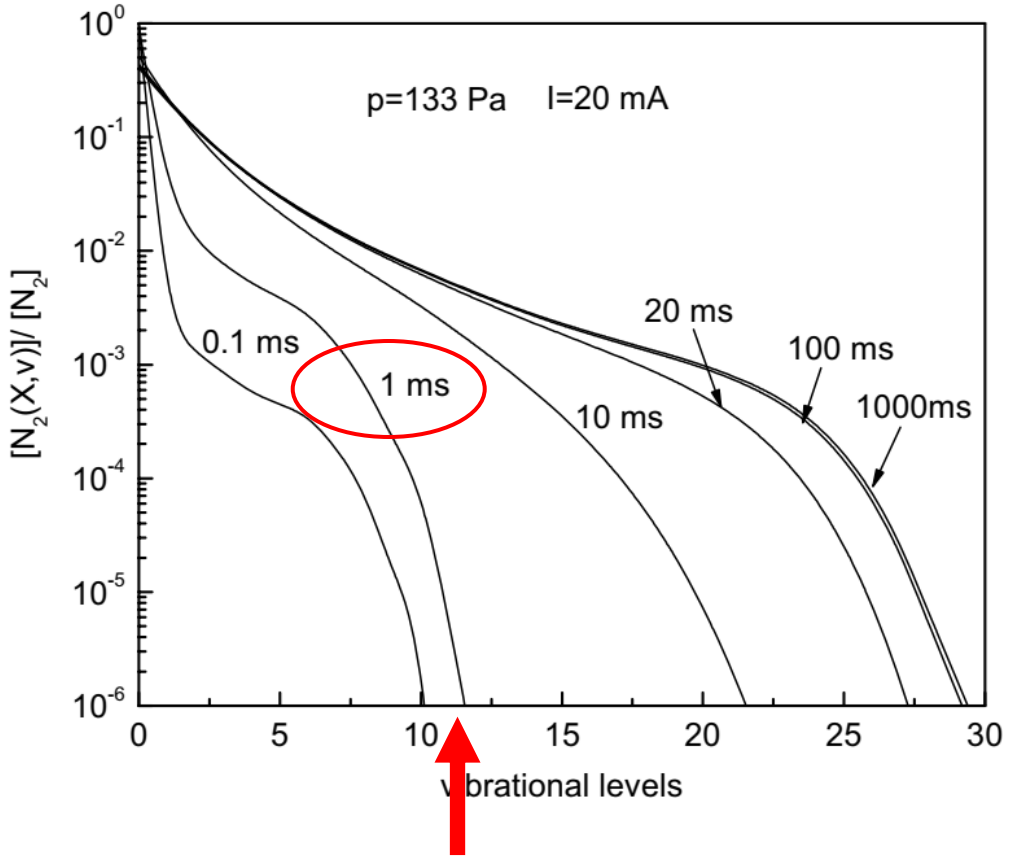
p=133 Pa I=20 mA
0.1 ms
1 ms
10 ms
20 ms
100 ms
1000ms
[N2(X,v)]/ [N2]
vibrational levels

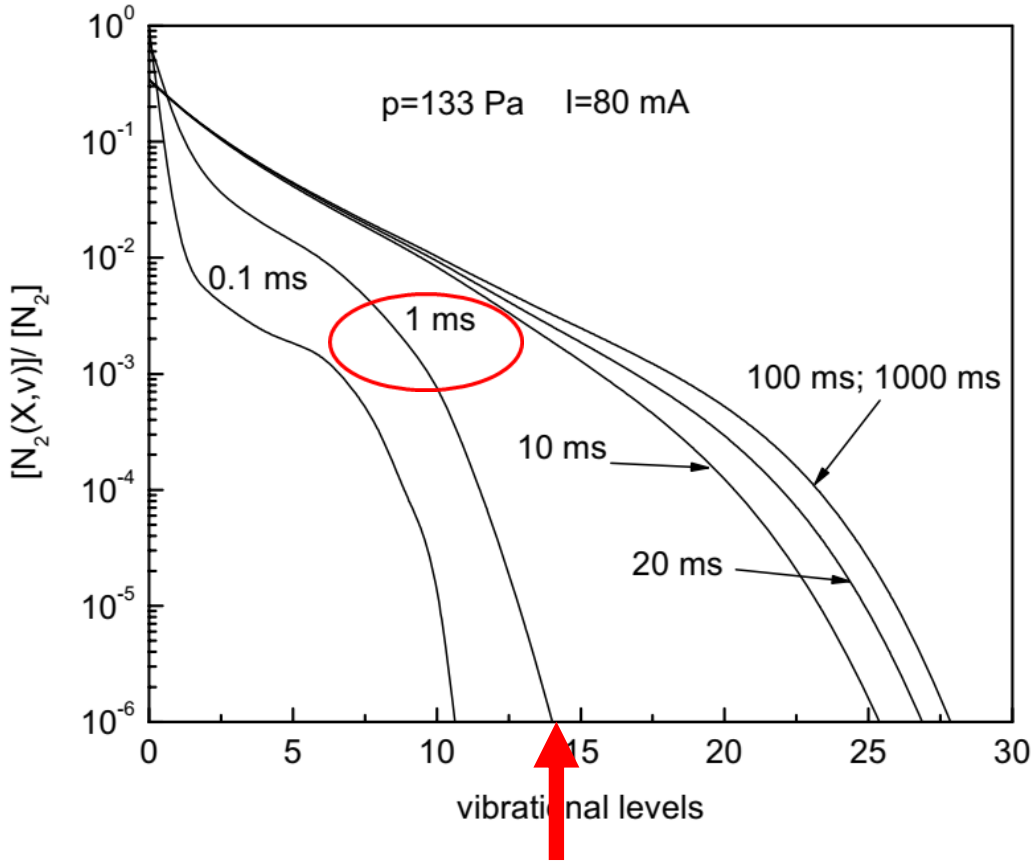
p=133 Pa I=80 mA
0.1 ms
1 ms
10 ms
20 ms
100 ms; 1000 ms
[N2(X,v)]/ [N2]
vibrational levels

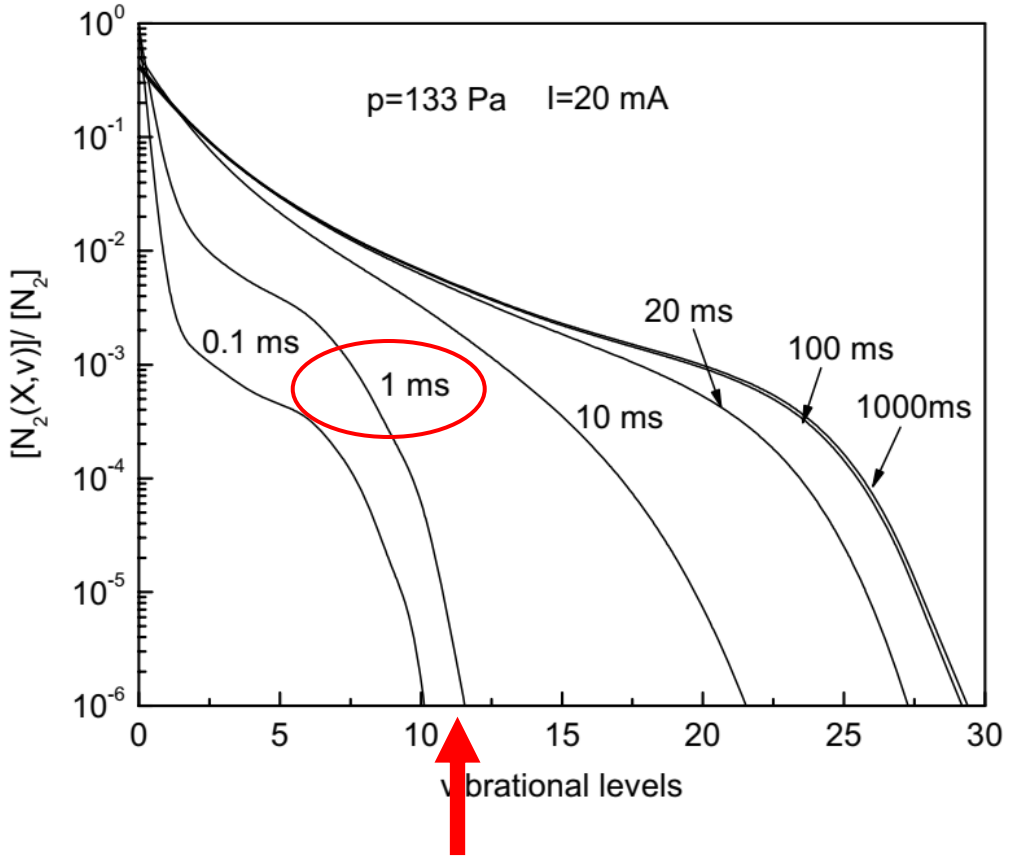

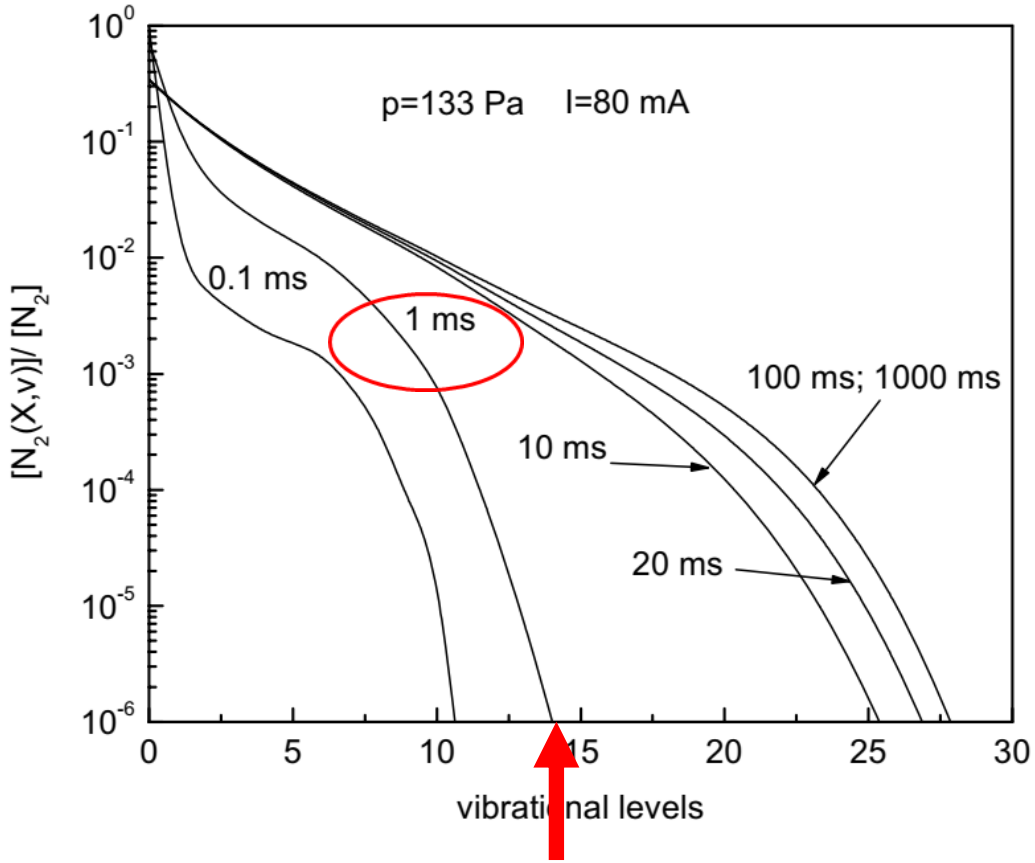

$$N_2(X, v \geqslant 13) + O(^3P) \rightarrow NO(X) + N(^4S)$$

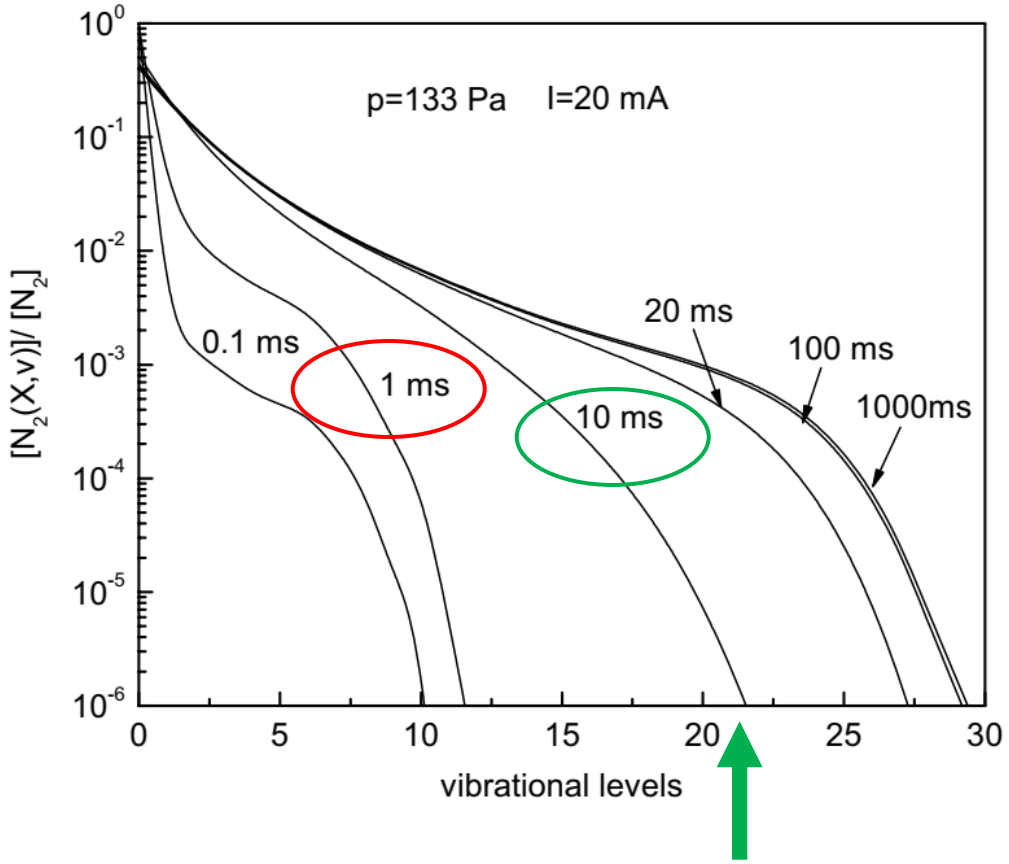

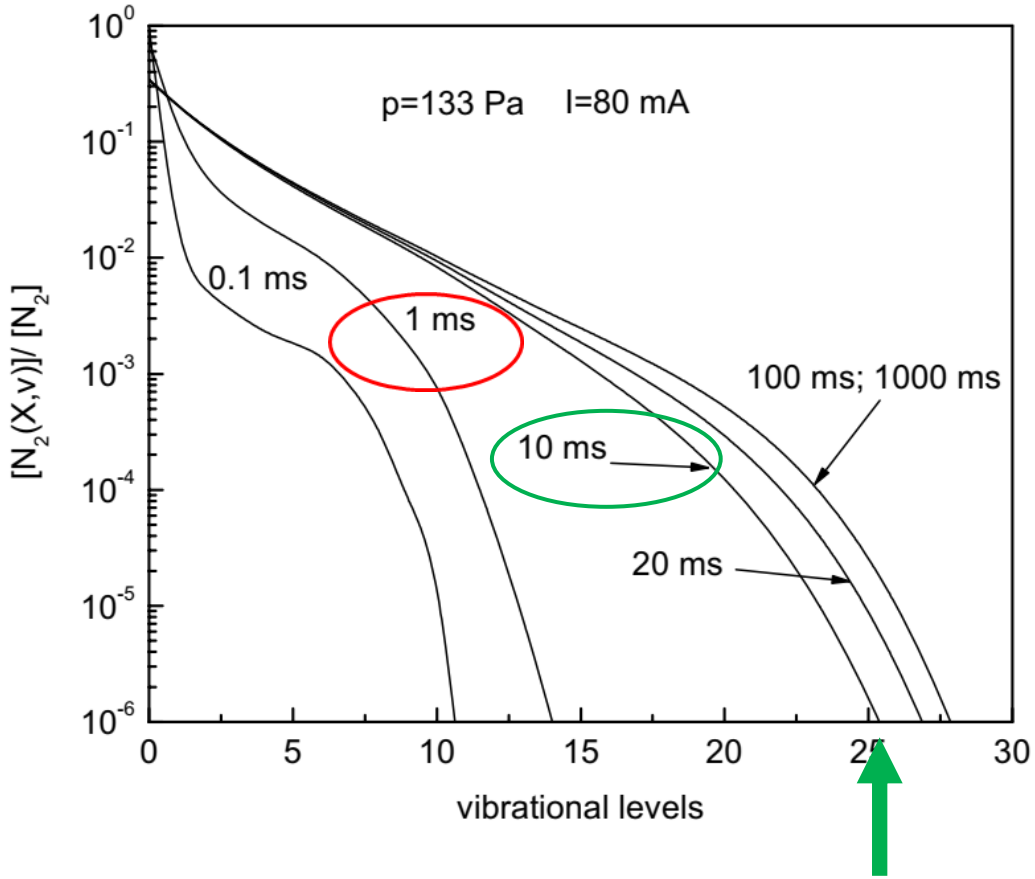

$$N_2(X, v \geqslant 13) + O(^3P) \rightarrow NO(X) + N(^4S)$$

C D Pintassilgo *et al* Plasma Sources Sci. Technol. **18** (2009)

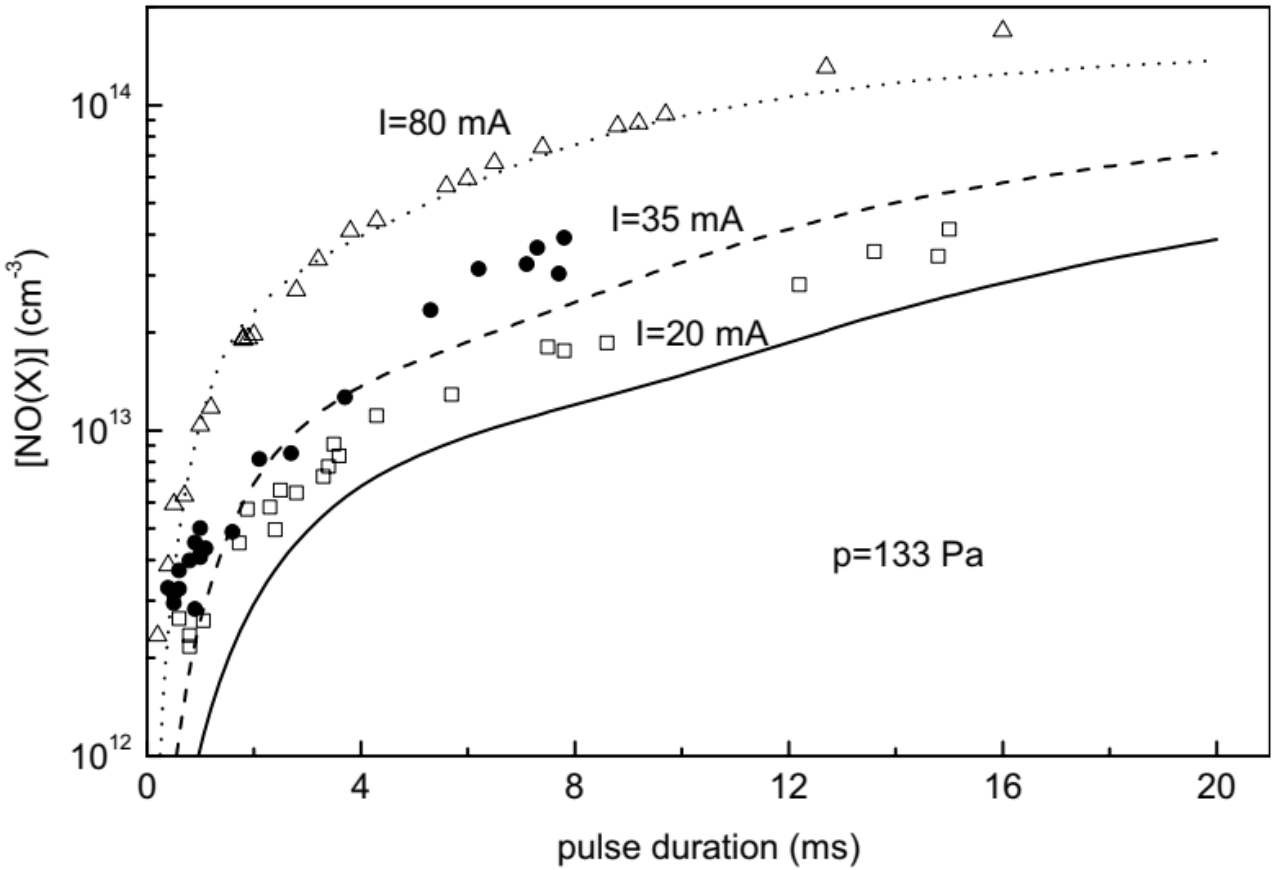

80%N_2-20%O_2

More about chemical kinetics

Table 6. List of reactions describing the oxygen chemical kinetics. Rate coefficients are expressed in $m^3\ s^{-1}$ and $m^6\ s^{-1}$ for two-body and three-body reactions, respectively. Gas temperature, T_g, is expressed in K.

(O10)	$2O(^3P) + O_2(X) \rightarrow O_2(X,v=0) + O_2(X)$	$0.50*3.81 \times 10^{-42} \exp(-170/T_g)/T_g$	[212, 213]
(O11)	$2O(^3P) + O_2(X) \rightarrow O_2(a) + O_2(X)$	$0.33*3.81 \times 10^{-42} \exp(-170/T_g)/T_g$	[212, 213]
(O12)	$2O(^3P) + O_2(X) \rightarrow O_2(b) + O_2(X)$	$0.17*3.81 \times 10^{-42} \exp(-170/T_g)/T_g$	[212, 213]
(O13)	$2O(^3P) + O(^3P) \rightarrow O_2(X,v=0) + O(^3P)$	$3.6 \times 10^{-44}(1/T_g)^{0.63}$	[171]
(O14)	$O_2(X,v=0) + O(^3P) + O(^3P) \rightarrow O_3(X) + O(^3P)$	$2.1 \times 10^{-46} \exp(345/T_g)$	[21, 212]
(O15)	$O_2(X,v=0) + O(^3P) + O_2(X) \rightarrow O_3(X) + O_2(X)$	$0.33*6.4 \times 10^{-47} \exp(663/T_g)$	[21, 212]
(O16)	$O_2(X,v=0) + O(^3P) + O_2(X) \rightarrow O_3^* + O_2(X)$	$0.67*6.4 \times 10^{-47} \exp(663/T_g)$	[212, 214]
(O17)	$O_2(X,v=0) + O(^3P) + O_3(X) \rightarrow O_3(X) + O_3(X)$	$1.66 \times 10^{-46} \exp(T_g/300)$	[215]
(O18)	$O_3(X) + O_2(b) \rightarrow 2O_2(X,v=0) + O(^3P)$	1.5×10^{-17}	[21, 212]
(O19)	$O_3(X) + O_2(a) \rightarrow 2O_2(X,v=0) + O(^3P)$	$5.2 \times 10^{-17} \exp(-2840/T_g)$	[21, 212]
(O20)	$O_3(X) + O(^3P) \rightarrow 2O_2(X,v=0)$	$0.50*1.8 \times 10^{-17} \exp(-2300/T_g)$	[212, 213]
(O21)	$O_3(X) + O(^3P) \rightarrow O_2(a) + O_2(X,v=0)$	$0.33*1.8 \times 10^{-17} \exp(-2300/T_g)$	[212, 213]
(O22)	$O_3(X) + O(^3P) \rightarrow O_2(b) + O_2(X,v=0)$	$0.17*1.8 \times 10^{-17} \exp(-2300/T_g)$	[212, 213]

Table 6. List of reactions describing the oxygen chemical kinetics. Rate coefficients are expressed in $m^3\ s^{-1}$ and $m^6\ s^{-1}$ for two-body and three-body reactions, respectively. Gas temperature, T_g, is expressed in K.

O_2

(O10)	$2O(^3P) + O_2(X) \rightarrow O_2(X,v=0) + O_2(X)$	$0.50*3.81 \times 10^{-42} \exp(-170/T_g)/T_g$	[212, 213]
(O11)	$2O(^3P) + O_2(X) \rightarrow O_2(a) + O_2(X)$	$0.33*3.81 \times 10^{-42} \exp(-170/T_g)/T_g$	[212, 213]
(O12)	$2O(^3P) + O_2(X) \rightarrow O_2(b) + O_2(X)$	$0.17*3.81 \times 10^{-42} \exp(-170/T_g)/T_g$	[212, 213]
(O13)	$2O(^3P) + O(^3P) \rightarrow O_2(X,v=0) + O(^3P)$	$3.6 \times 10^{-44}(1/T_g)^{0.63}$	[171]
(O14)	$O_2(X,v=0) + O(^3P) + O(^3P) \rightarrow O_3(X) + O(^3P)$	$2.1 \times 10^{-46} \exp(345/T_g)$	[21, 212]
(O15)	$O_2(X,v=0) + O(^3P) + O_2(X) \rightarrow O_3(X) + O_2(X)$	$0.33*6.4 \times 10^{-47} \exp(663/T_g)$	[21, 212]
(O16)	$O_2(X,v=0) + O(^3P) + O_2(X) \rightarrow O_3^* + O_2(X)$	$0.67*6.4 \times 10^{-47} \exp(663/T_g)$	[212, 214]
(O17)	$O_2(X,v=0) + O(^3P) + O_3(X) \rightarrow O_3(X) + O_3(X)$	$1.66 \times 10^{-46} \exp(T_g/300)$	[215]
(O18)	$O_3(X) + O_2(b) \rightarrow 2O_2(X,v=0) + O(^3P)$	1.5×10^{-17}	[21, 212]
(O19)	$O_3(X) + O_2(a) \rightarrow 2O_2(X,v=0) + O(^3P)$	$5.2 \times 10^{-17} \exp(-2840/T_g)$	[21, 212]
(O20)	$O_3(X) + O(^3P) \rightarrow 2O_2(X,v=0)$	$0.50*1.8 \times 10^{-17} \exp(-2300/T_g)$	[212, 213]
(O21)	$O_3(X) + O(^3P) \rightarrow O_2(a) + O_2(X,v=0)$	$0.33*1.8 \times 10^{-17} \exp(-2300/T_g)$	[212, 213]
(O22)	$O_3(X) + O(^3P) \rightarrow O_2(b) + O_2(X,v=0)$	$0.17*1.8 \times 10^{-17} \exp(-2300/T_g)$	[212, 213]

Table 6. List of reactions describing the oxygen chemical kinetics. Rate coefficients are expressed in $m^3\ s^{-1}$ and $m^6\ s^{-1}$ for two-body and three-body reactions, respectively. Gas temperature, T_g, is expressed in K.

O_2

(O10)	$2O(^3P) + O_2(X) \rightarrow O_2(X,v=0) + O_2(X)$	$0.50*3.81 \times 10^{-42} \exp(-170/T_g)/T_g$	[212, 213]
(O11)	$2O(^3P) + O_2(X) \rightarrow O_2(a) + O_2(X)$	$0.33*3.81 \times 10^{-42} \exp(-170/T_g)/T_g$	[212, 213]
(O12)	$2O(^3P) + O_2(X) \rightarrow O_2(b) + O_2(X)$	$0.17*3.81 \times 10^{-42} \exp(-170/T_g)/T_g$	[212, 213]
(O13)	$2O(^3P) + O(^3P) \rightarrow O_2(X,v=0) + O(^3P)$	$3.6 \times 10^{-44}(1/T_g)^{0.63}$	[171]
(O14)	$O_2(X,v=0) + O(^3P) + O(^3P) \rightarrow O_3(X) + O(^3P)$	$2.1 \times 10^{-46} \exp(345/T_g)$	[21, 212]
(O15)	$O_2(X,v=0) + O(^3P) + O_2(X) \rightarrow O_3(X) + O_2(X)$	$0.33*6.4 \times 10^{-47} \exp(663/T_g)$	[21, 212]
(O16)	$O_2(X,v=0) + O(^3P) + O_2(X) \rightarrow O_3^* + O_2(X)$	$0.67*6.4 \times 10^{-47} \exp(663/T_g)$	[212, 214]
(O17)	$O_2(X,v=0) + O(^3P) + O_3(X) \rightarrow O_3(X) + O_3(X)$	$1.66 \times 10^{-46} \exp(T_g/300)$	[215]
(O18)	$O_3(X) + O_2(b) \rightarrow 2O_2(X,v=0) + O(^3P)$	1.5×10^{-17}	[21, 212]
(O19)	$O_3(X) + O_2(a) \rightarrow 2O_2(X,v=0) + O(^3P)$	$5.2 \times 10^{-17} \exp(-2840/T_g)$	[21, 212]
(O20)	$O_3(X) + O(^3P) \rightarrow 2O_2(X,v=0)$	$0.50*1.8 \times 10^{-17} \exp(-2300/T_g)$	[212, 213]
(O21)	$O_3(X) + O(^3P) \rightarrow O_2(a) + O_2(X,v=0)$	$0.33*1.8 \times 10^{-17} \exp(-2300/T_g)$	[212, 213]
(O22)	$O_3(X) + O(^3P) \rightarrow O_2(b) + O_2(X,v=0)$	$0.17*1.8 \times 10^{-17} \exp(-2300/T_g)$	[212, 213]

Table 7. List of reactions describing the nitrogen and oxygen mixture chemical kinetics. Rate coefficients are expressed in m^3s^{-1} and m^6s^{-1} for two-body and three-body reactions, respectively. Transition probabilities are expressed in s^{-1} for radiative transitions. Gas temperature, T_g, is expressed in K.

(NO10)	$N(^4S) + N(^4S) + O_2(X) \rightarrow N_2(X) + O_2(X)$	$8.27 \times 10^{-46} \exp(500/T_g)$	[192]
(NO11)	$O(^3P) + O(^3P) + N_2(X) \rightarrow O_2(X) + N_2(X)$	$2.76 \times 10^{-46} \exp(720/T_g)$	[192]
(NO12)	$O(^3P) + O_2(X,v = 0) + N_2(X) \rightarrow O_3 + N_2(X)$	$5.7 \times 10^{-46}(300/T_g)^{2.8}$	[131]
(NO13)	$N_2(X,v \geqslant 13) + O(^3P) \rightarrow NO(X) + N(^4S)$	10^{-19}	[79]
(NO14)	$N_2(A) + O(^3P) \rightarrow NO(X) + N(^2D)$	7×10^{-18}	[79]
(NO15)	$O_2(X,v = 0) + N(^4S) \rightarrow NO(X) + O(^3P)$	$1.1 \times 10^{-20} T_g \exp(-3150/T_g)$	[192]
(NO16)	$O_2(X,v = 0) + N(^2D) \rightarrow NO(X) + O(^3P)$	$1.5 \times 10^{-18}\sqrt{T_g/300}$	[192]
(NO17)	$O_2(X,v = 0) + N(^2D) \rightarrow NO(X) + O(^1D)$	$6 \times 10^{-18}\sqrt{T_g/300}$	[192]
(NO18)	$O_2(X,v = 0) + N(^2P) \rightarrow NO(X) + O(^3P)$	2.6×10^{-18}	[192]
(NO19)	$O_2(a) + N(^4S) \rightarrow NO(X) + O(^3P)$	$2 \times 10^{-20} \exp(-600/T_g)$	[192]
(NO20)	$N(^4S) + O(^3P) \rightarrow NO(A)$	$1.18 \times 10^{-23}(300/T_g)^{0.35}$	[218]
(NO21)	$N(^4S) + O(^3P) + N_2(X) \rightarrow NO(X) + N_2(X)$	$1.76 \times 10^{-43}\sqrt{1/T_g}$	[192]
(NO22)	$N(^4S) + O(^3P) + N_2(X) \rightarrow NO(A) + N_2(X)$	$2.12 \times 10^{-46}(300/T_g)^{1.24}$	[218]
(NO23)	$N(^4S) + O(^3P) + N_2(X) \rightarrow NO(B) + N_2(X)$	$3.09 \times 10^{-46}(300/T_g)^{1.4}$	[218]
(NO24)	$N(^4S) + O(^3P) + O_2(X) \rightarrow NO(X) + O_2(X)$	$1.76 \times 10^{-43}\sqrt{1/T_g}$	[192]
(NO25)	$N(^4S) + O(^3P) + O_2(X) \rightarrow NO(B) + O_2(X)$	$3.09 \times 10^{-46}(300/T_g)^{1.4}$	[218]

Table 7. List of reactions describing the nitrogen and oxygen mixture chemical kinetics. Rate coefficients are expressed in m^3s^{-1} and m^6s^{-1} for two-body and three-body reactions, respectively. Transition probabilities are expressed in s^{-1} for radiative transitions. Gas temperature, T_g, is expressed in K.

N_2-O_2

(NO10)	$N(^4S) + N(^4S) + O_2(X) \rightarrow N_2(X) + O_2(X)$	$8.27 \times 10^{-46} \exp(500/T_g)$	[192]
(NO11)	$O(^3P) + O(^3P) + N_2(X) \rightarrow O_2(X) + N_2(X)$	$2.76 \times 10^{-46} \exp(720/T_g)$	[192]
(NO12)	$O(^3P) + O_2(X,v = 0) + N_2(X) \rightarrow O_3 + N_2(X)$	$5.7 \times 10^{-46}(300/T_g)^{2.8}$	[131]
(NO13)	$N_2(X,v \geqslant 13) + O(^3P) \rightarrow NO(X) + N(^4S)$	10^{-19}	[79]
(NO14)	$N_2(A) + O(^3P) \rightarrow NO(X) + N(^2D)$	7×10^{-18}	[79]
(NO15)	$O_2(X,v = 0) + N(^4S) \rightarrow NO(X) + O(^3P)$	$1.1 \times 10^{-20} T_g \exp(-3150/T_g)$	[192]
(NO16)	$O_2(X,v = 0) + N(^2D) \rightarrow NO(X) + O(^3P)$	$1.5 \times 10^{-18}\sqrt{T_g/300}$	[192]
(NO17)	$O_2(X,v = 0) + N(^2D) \rightarrow NO(X) + O(^1D)$	$6 \times 10^{-18}\sqrt{T_g/300}$	[192]
(NO18)	$O_2(X,v = 0) + N(^2P) \rightarrow NO(X) + O(^3P)$	2.6×10^{-18}	[192]
(NO19)	$O_2(a) + N(^4S) \rightarrow NO(X) + O(^3P)$	$2 \times 10^{-20} \exp(-600/T_g)$	[192]
(NO20)	$N(^4S) + O(^3P) \rightarrow NO(A)$	$1.18 \times 10^{-23}(300/T_g)^{0.35}$	[218]
(NO21)	$N(^4S) + O(^3P) + N_2(X) \rightarrow NO(X) + N_2(X)$	$1.76 \times 10^{-43}\sqrt{1/T_g}$	[192]
(NO22)	$N(^4S) + O(^3P) + N_2(X) \rightarrow NO(A) + N_2(X)$	$2.12 \times 10^{-46}(300/T_g)^{1.24}$	[218]
(NO23)	$N(^4S) + O(^3P) + N_2(X) \rightarrow NO(B) + N_2(X)$	$3.09 \times 10^{-46}(300/T_g)^{1.4}$	[218]
(NO24)	$N(^4S) + O(^3P) + O_2(X) \rightarrow NO(X) + O_2(X)$	$1.76 \times 10^{-43}\sqrt{1/T_g}$	[192]
(NO25)	$N(^4S) + O(^3P) + O_2(X) \rightarrow NO(B) + O_2(X)$	$3.09 \times 10^{-46}(300/T_g)^{1.4}$	[218]

Table 7. List of reactions describing the nitrogen and oxygen mixture chemical kinetics. Rate coefficients are expressed in m^3s^{-1} and m^6s^{-1} for two-body and three-body reactions, respectively. Transition probabilities are expressed in s^{-1} for radiative transitions. Gas temperature, T_g, is expressed in K.

N_2-O_2

(NO10)	$N(^4S) + N(^4S) + O_2(X) \rightarrow N_2(X) + O_2(X)$	$8.27 \times 10^{-46} \exp(500/T_g)$	[192]
(NO11)	$O(^3P) + O(^3P) + N_2(X) \rightarrow O_2(X) + N_2(X)$	$2.76 \times 10^{-46} \exp(720/T_g)$	[192]
(NO12)	$O(^3P) + O_2(X,v = 0) + N_2(X) \rightarrow O_3 + N_2(X)$	$5.7 \times 10^{-46}(300/T_g)^{2.8}$	[131]
(NO13)	$N_2(X,v \geqslant 13) + O(^3P) \rightarrow NO(X) + N(^4S)$	10^{-19}	[79]
(NO14)	$N_2(A) + O(^3P) \rightarrow NO(X) + N(^2D)$	7×10^{-18}	[79]
(NO15)	$O_2(X,v = 0) + N(^4S) \rightarrow NO(X) + O(^3P)$	$1.1 \times 10^{-20} T_g \exp(-3150/T_g)$	[192]
(NO16)	$O_2(X,v = 0) + N(^2D) \rightarrow NO(X) + O(^3P)$	$1.5 \times 10^{-18}\sqrt{T_g/300}$	[192]
(NO17)	$O_2(X,v = 0) + N(^2D) \rightarrow NO(X) + O(^1D)$	$6 \times 10^{-18}\sqrt{T_g/300}$	[192]
(NO18)	$O_2(X,v = 0) + N(^2P) \rightarrow NO(X) + O(^3P)$	2.6×10^{-18}	[192]
(NO19)	$O_2(a) + N(^4S) \rightarrow NO(X) + O(^3P)$	$2 \times 10^{-20} \exp(-600/T_g)$	[192]
(NO20)	$N(^4S) + O(^3P) \rightarrow NO(A)$	$1.18 \times 10^{-23}(300/T_g)^{0.35}$	[218]
(NO21)	$N(^4S) + O(^3P) + N_2(X) \rightarrow NO(X) + N_2(X)$	$1.76 \times 10^{-43}\sqrt{1/T_g}$	[192]
(NO22)	$N(^4S) + O(^3P) + N_2(X) \rightarrow NO(A) + N_2(X)$	$2.12 \times 10^{-46}(300/T_g)^{1.24}$	[218]
(NO23)	$N(^4S) + O(^3P) + N_2(X) \rightarrow NO(B) + N_2(X)$	$3.09 \times 10^{-46}(300/T_g)^{1.4}$	[218]
(NO24)	$N(^4S) + O(^3P) + O_2(X) \rightarrow NO(X) + O_2(X)$	$1.76 \times 10^{-43}\sqrt{1/T_g}$	[192]
(NO25)	$N(^4S) + O(^3P) + O_2(X) \rightarrow NO(B) + O_2(X)$	$3.09 \times 10^{-46}(300/T_g)^{1.4}$	[218]

IOP Publishing
Plasma Sources Science and Technology
Plasma Sources Sci. Technol. 31 (2022) 094010 (11pp)
https://doi.org/10.1088/1361-6595/ac9082

On the relevance of accurate input data for vibrational kinetics in air cold plasmas: the case of nitrogen fixation

Fabrizio Esposito*

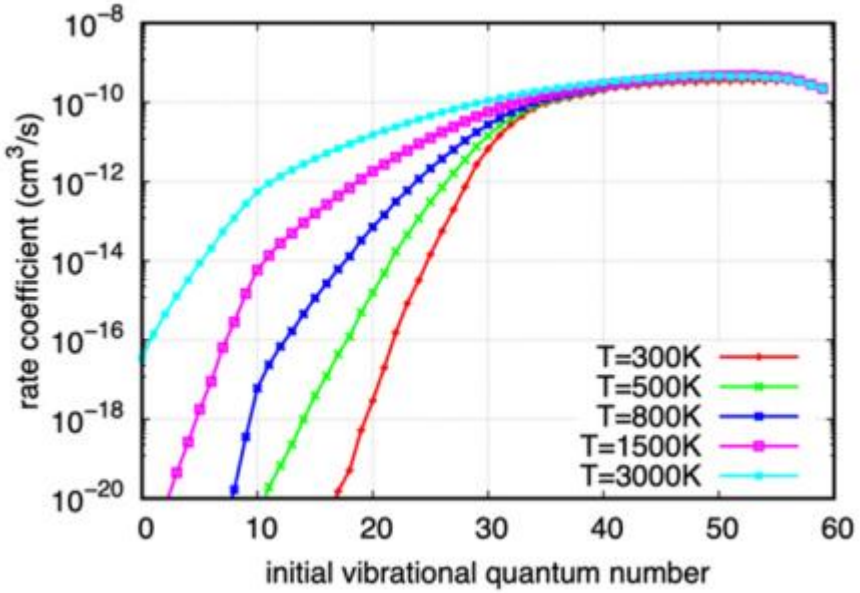

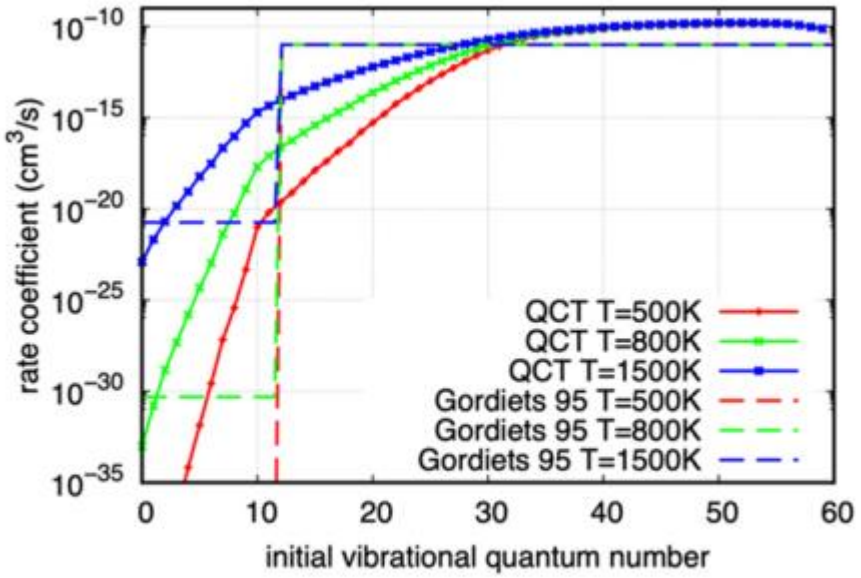

Figure 2. Comparison of QCT results (lines with markers) with Gordiets model [24] (broken lines) of the first Zeldovich reaction.

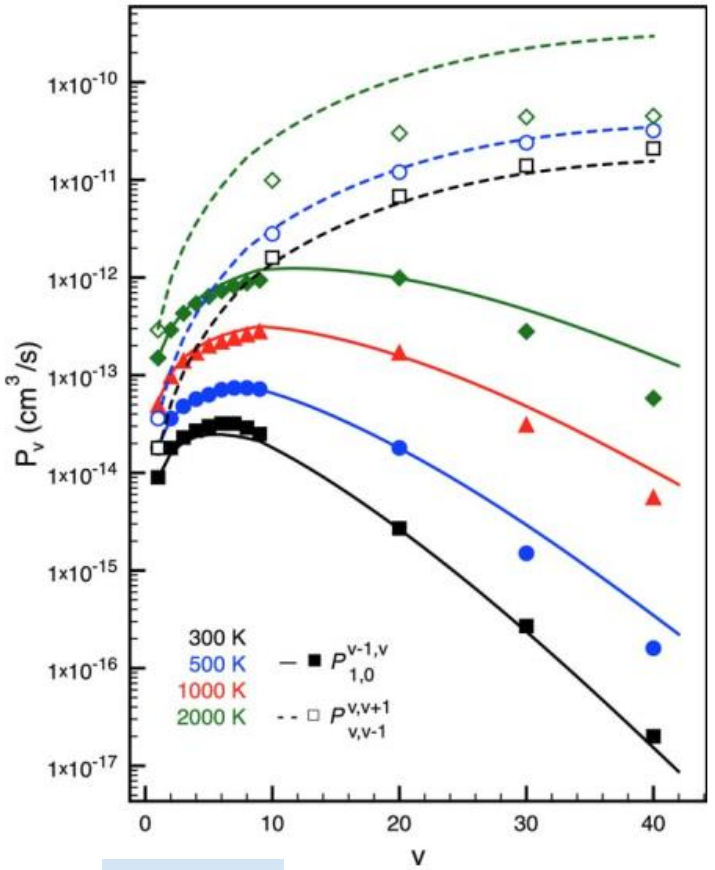

Figure 6. V–V N_2–N_2 rate coefficients $P_{1,0}^{v-1,v}$ (full lines and closed symbols) and $P_{v,v-1}^{v,v+1}$ (dashed lines and open symbols), for different values of the gas temperature; the lines are the calculations according equations (14), (22) and (23), the symbols are the semi-classical calculations from [117, 124].

Plasma Sources Sci. Technol. **26** (2017) 055001

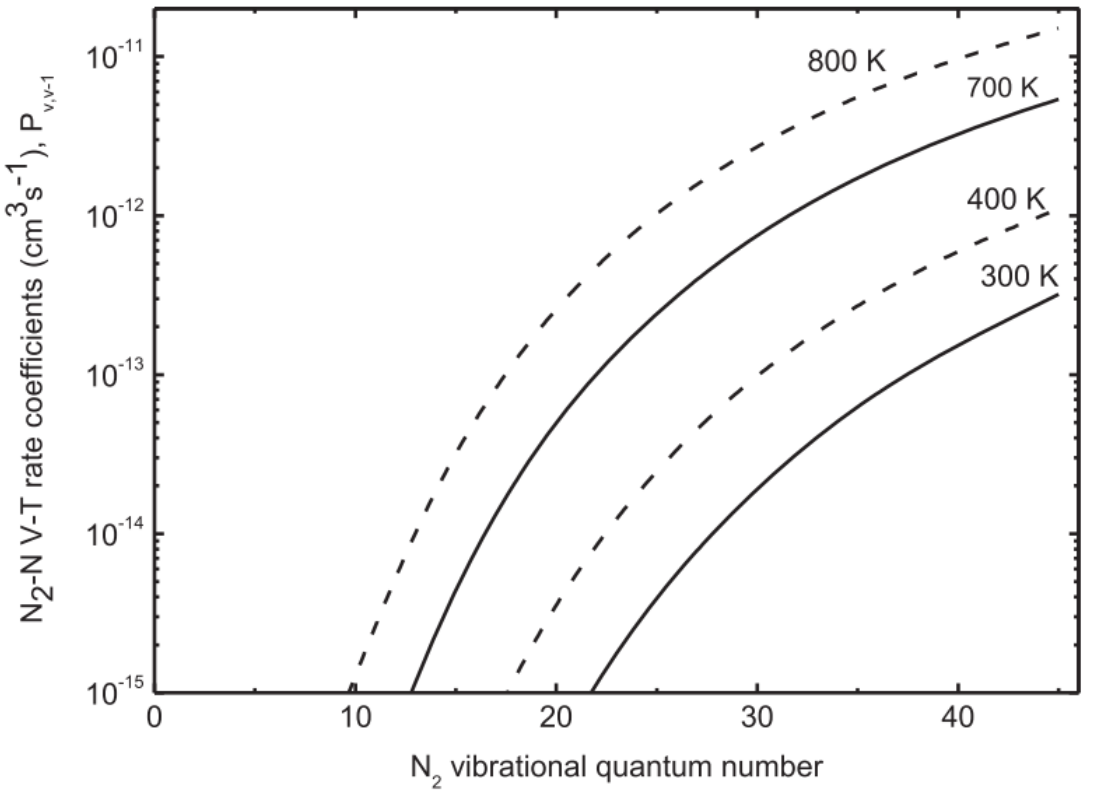

Figure 2. Rate coefficients for V–T energy exchanges in N_2–N collisions, $N_2(v) + N \rightarrow N_2(v\text{-}1) + N$, for different values of the gas temperature, $T_g = 300$, 400, 700, and 800 K.

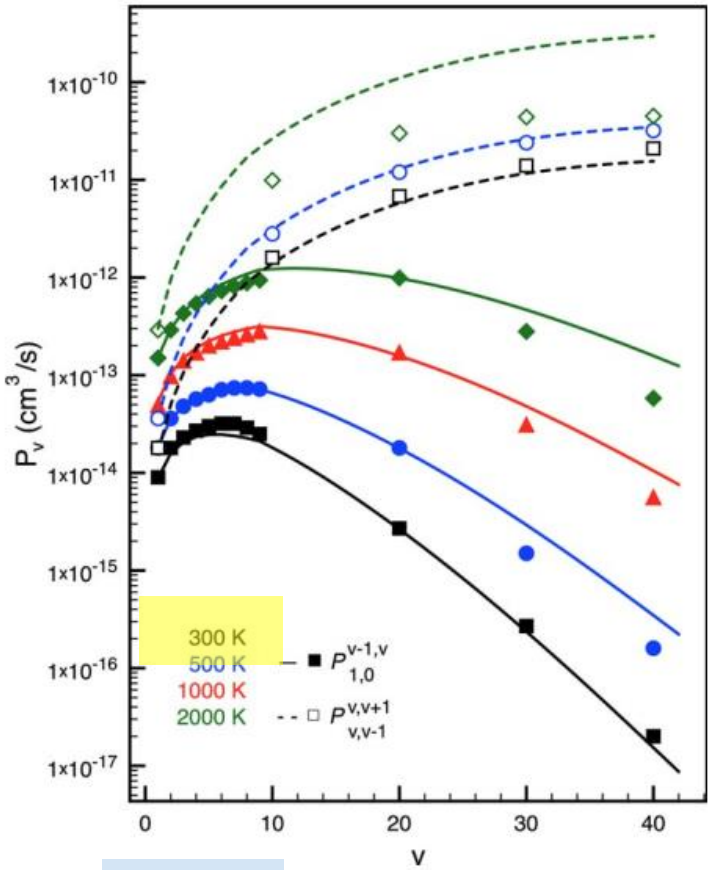

Figure 6. V–V N_2–N_2 rate coefficients $P_{1,0}^{v-1,v}$ (full lines and closed symbols) and $P_{v,v-1}^{v,v+1}$ (dashed lines and open symbols), for different values of the gas temperature; the lines are the calculations according equations (14), (22) and (23), the symbols are the semi-classical calculations from [117, 124].

Plasma Sources Sci. Technol. **26** (2017) 055001

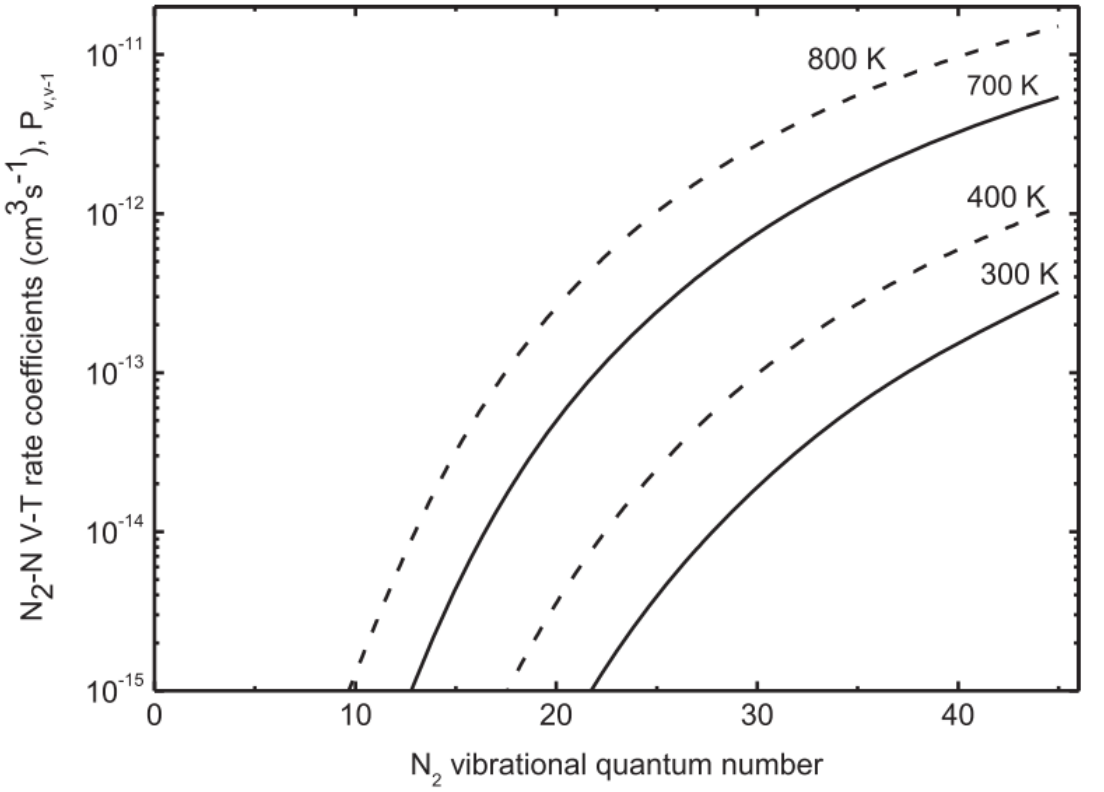

Figure 2. Rate coefficients for V–T energy exchanges in N_2–N collisions, $N_2(v) + N \rightarrow N_2(v\text{-}1) + N$, for different values of the gas temperature, $T_g = 300$, 400, 700, and 800 K.

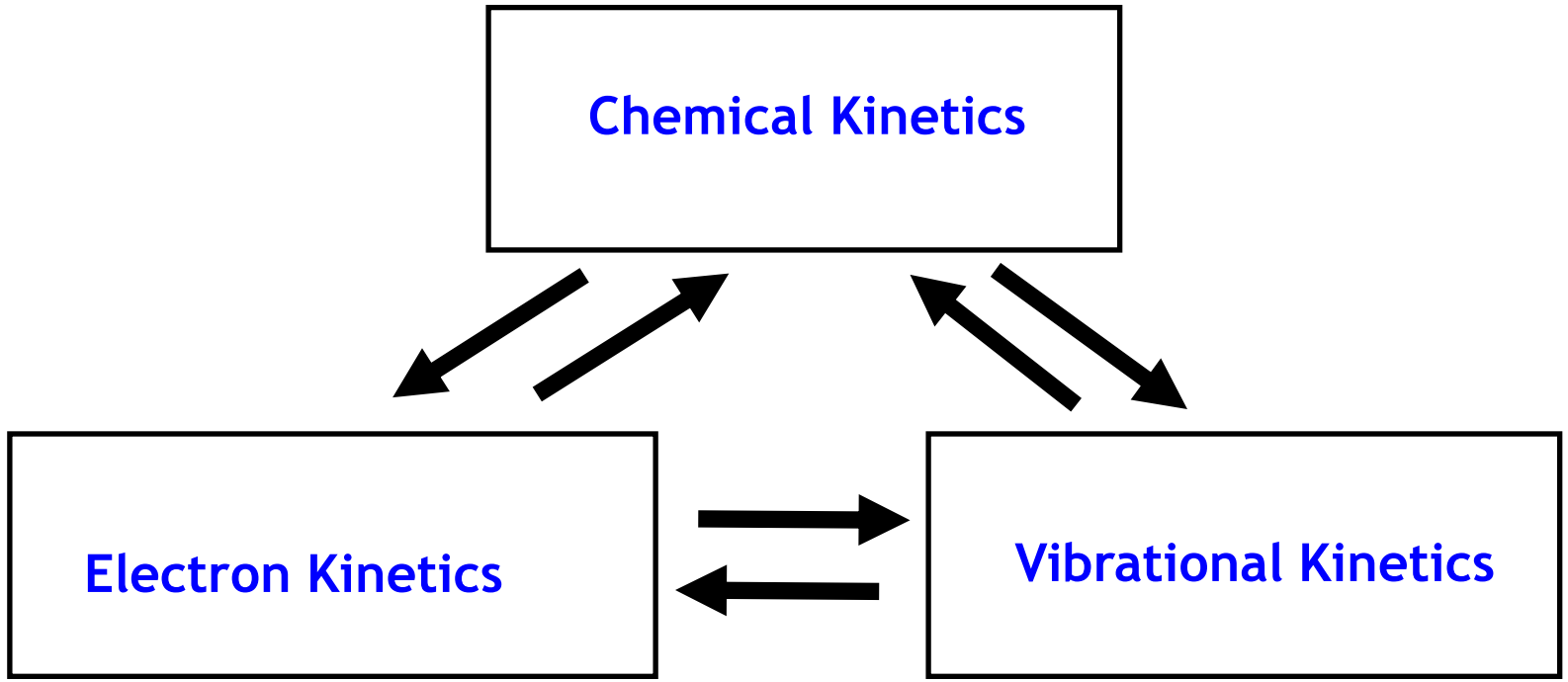
Chemical Kinetics
Electron Kinetics
Vibrational Kinetics

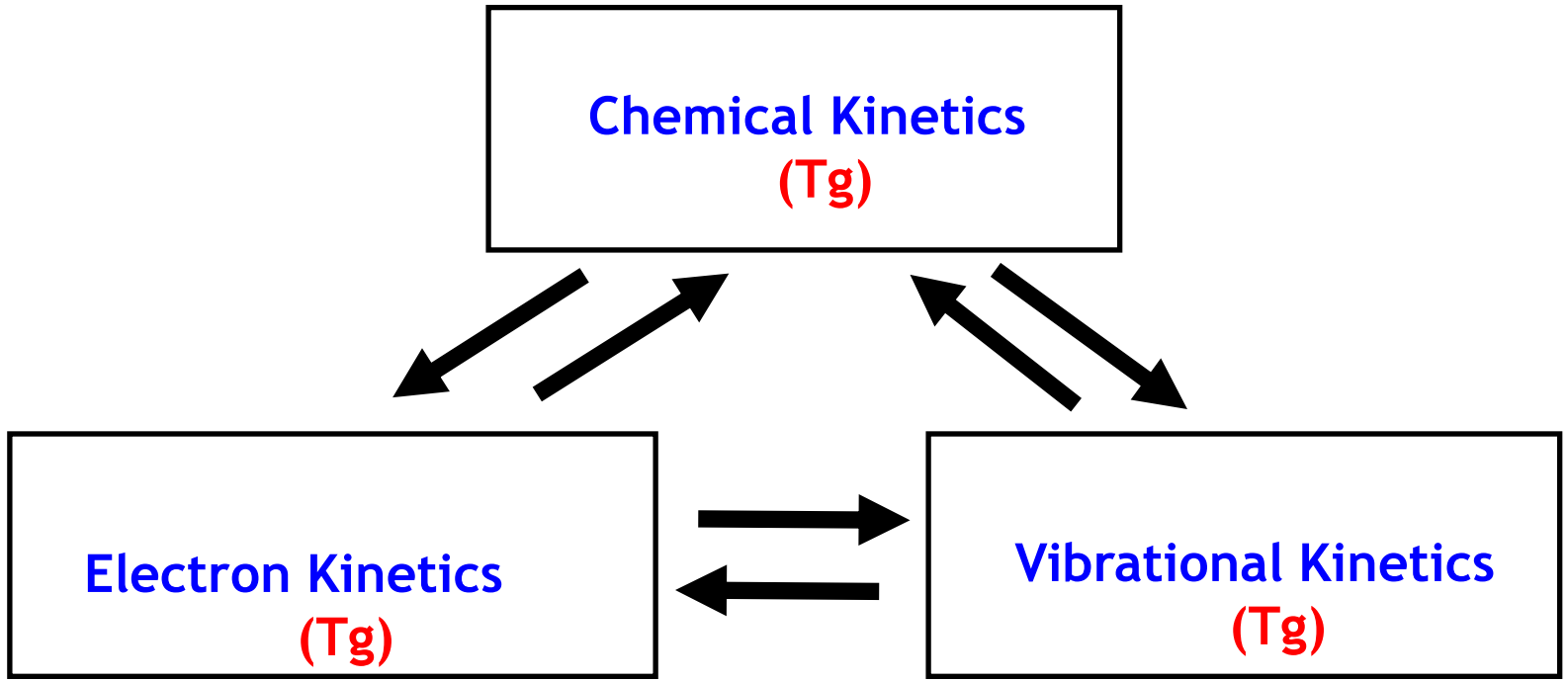
Chemical Kinetics
(Tg)
Electron Kinetics
(Tg)
Vibrational Kinetics
(Tg)

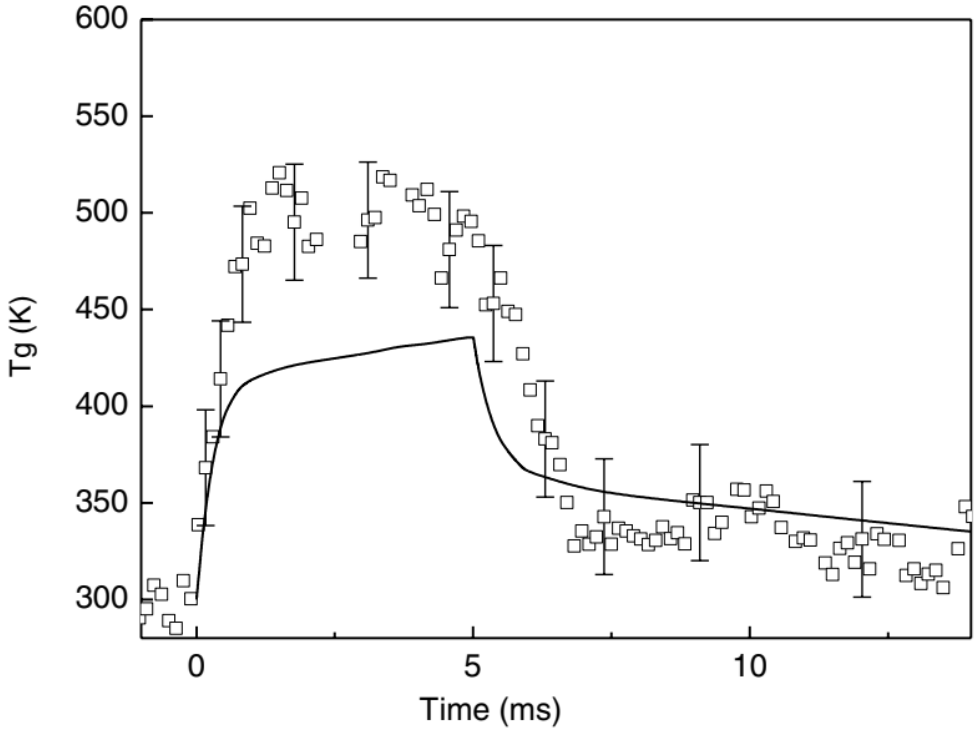

$80N_2$-$20\%O_2$ DC pulsed discharge

p = 1 Torr I = 150 mA R = 1 cm

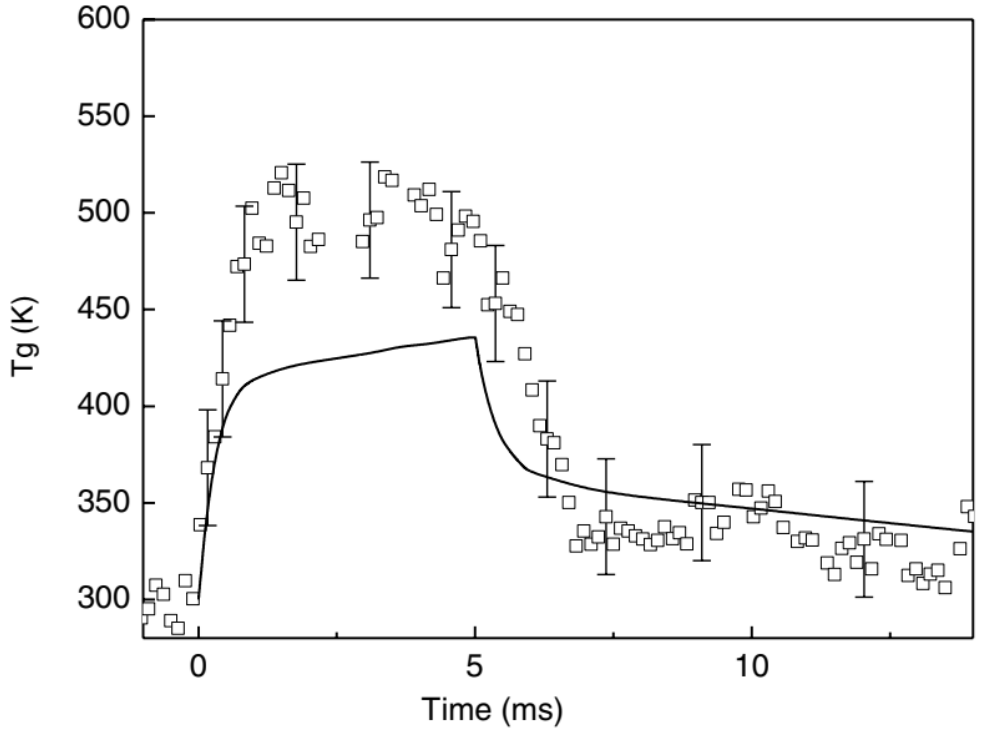

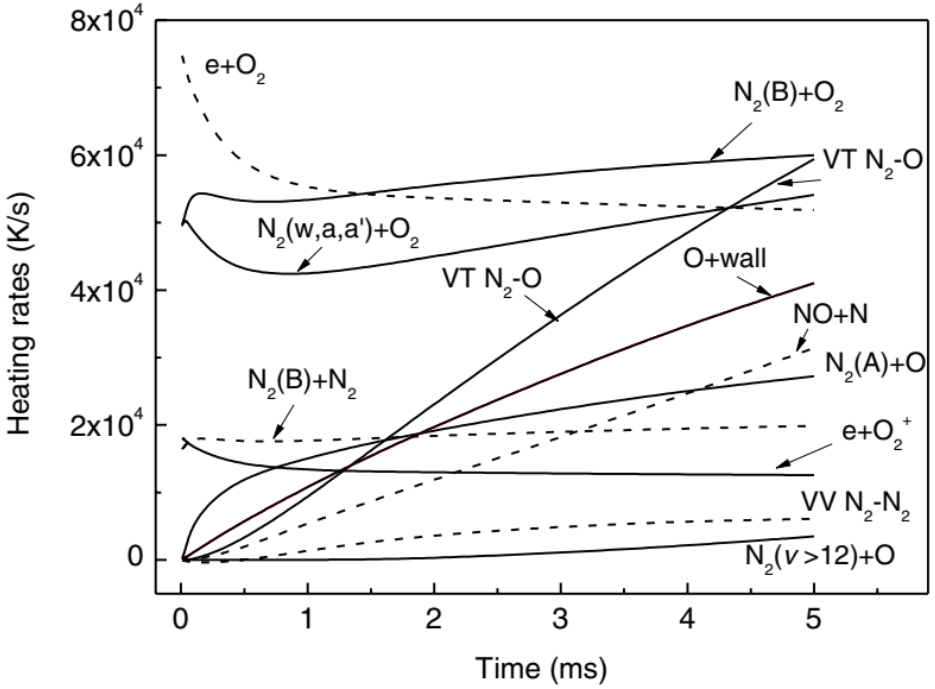

$80N_2$-$20\%O_2$ DC pulsed discharge

p = 1 Torr I = 150 mA R = 1 cm

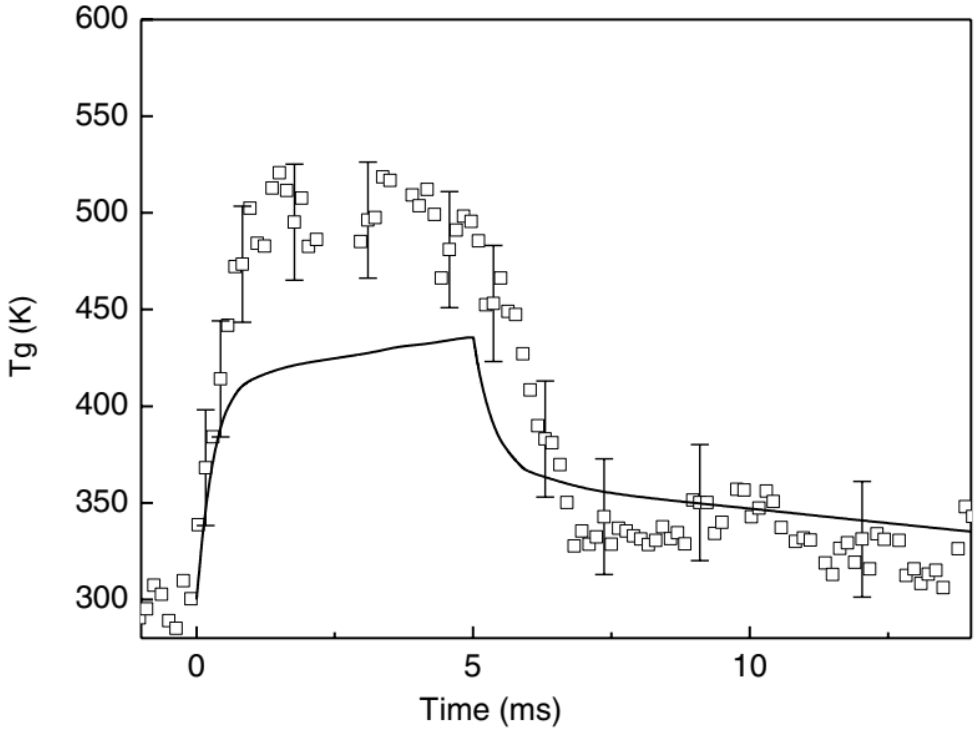

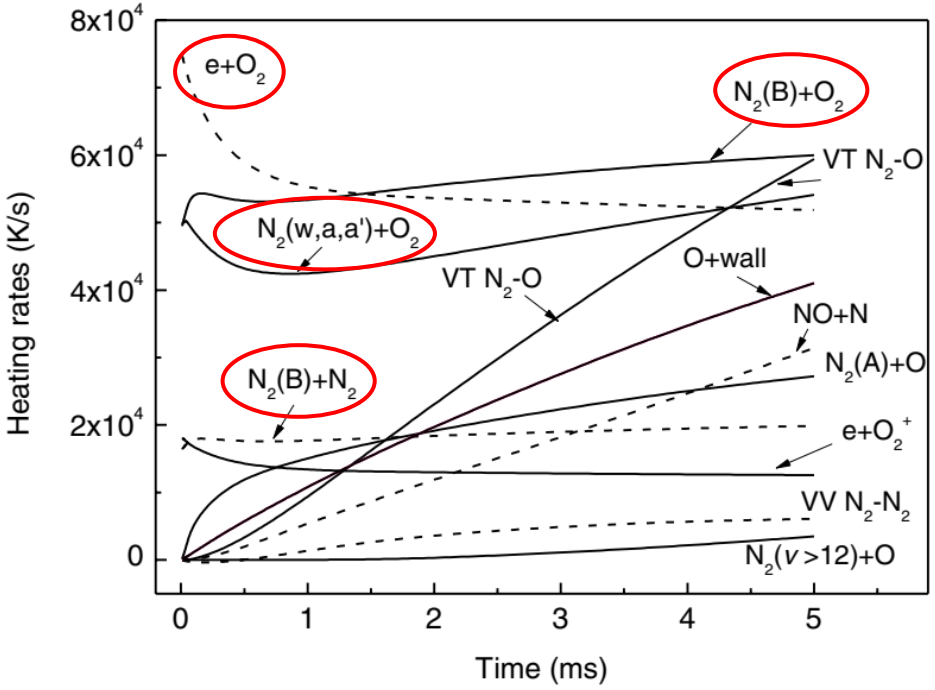

$80N_2$-$20\%O_2$ DC pulsed discharge

p = 1 Torr I = 150 mA R = 1 cm

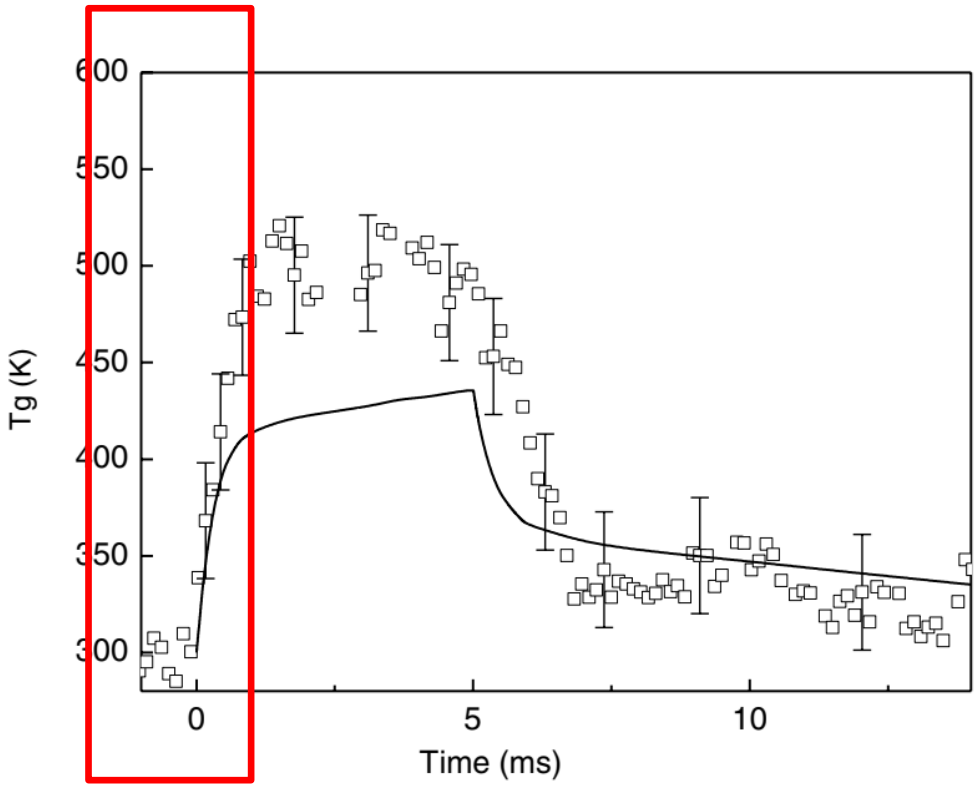

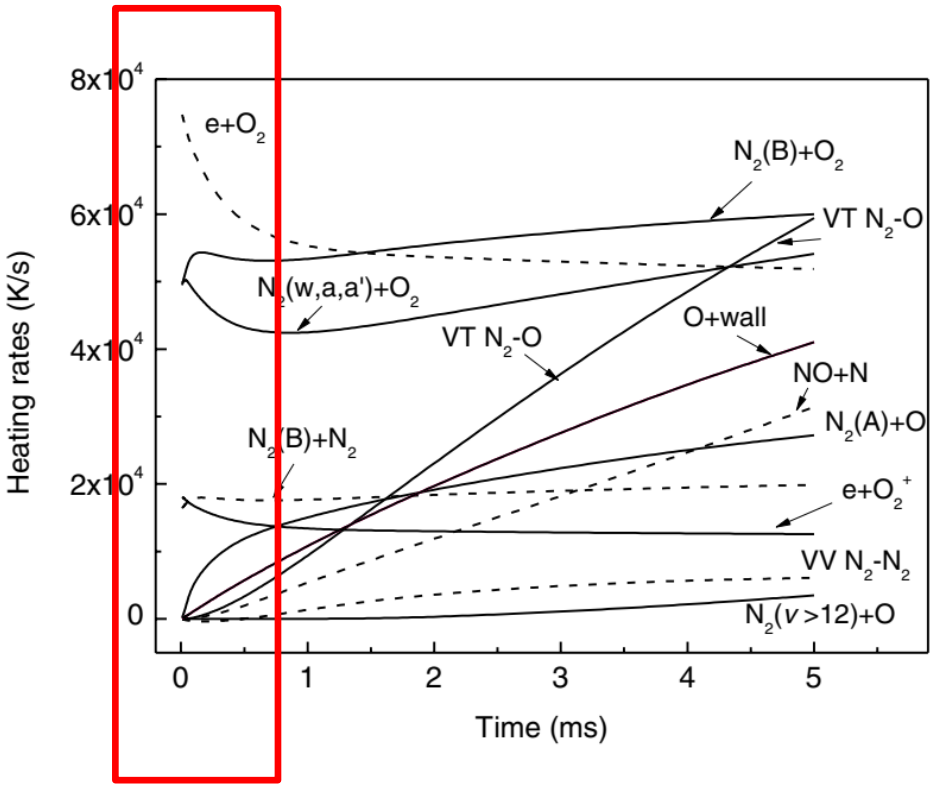

$80N_2$-$20\%O_2$ DC pulsed discharge

p = 1 Torr I = 150 mA R = 1 cm

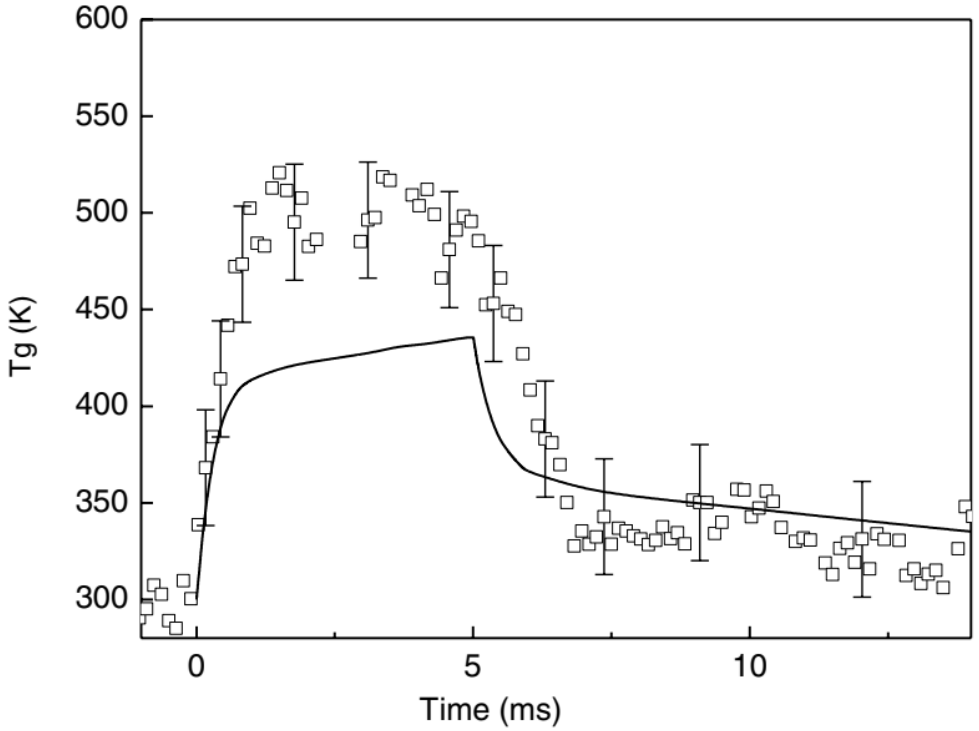

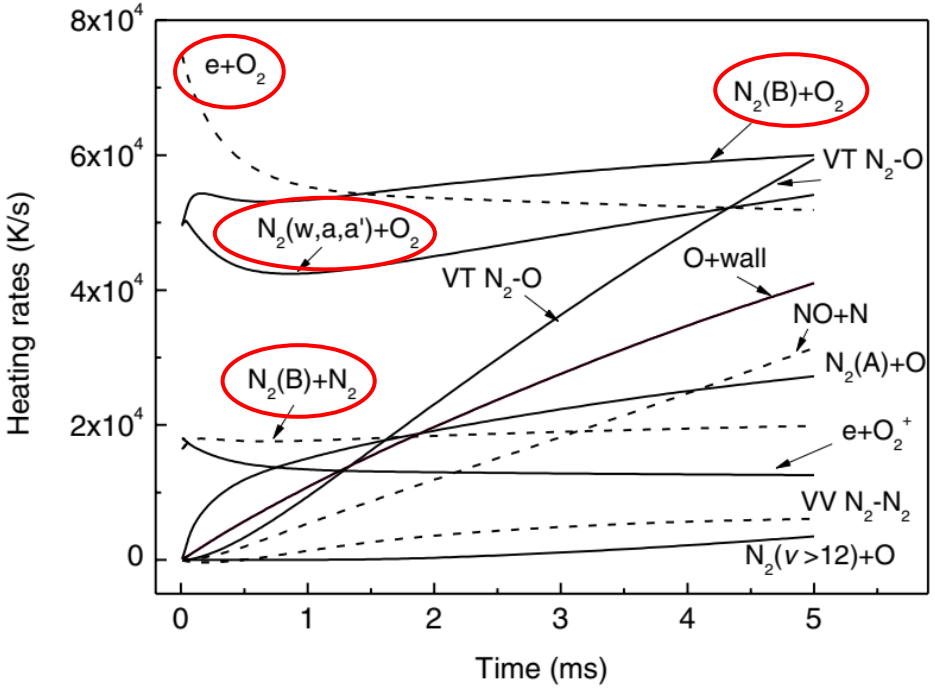

$80N_2$-$20\%O_2$ DC pulsed discharge

p = 1 Torr I = 150 mA R = 1 cm

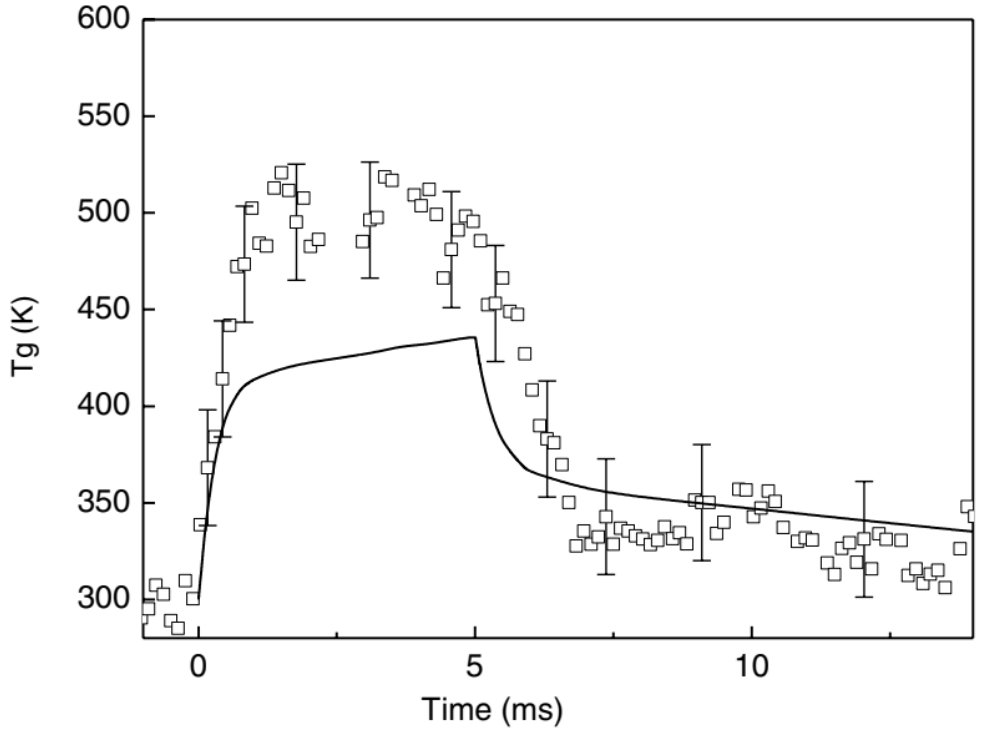

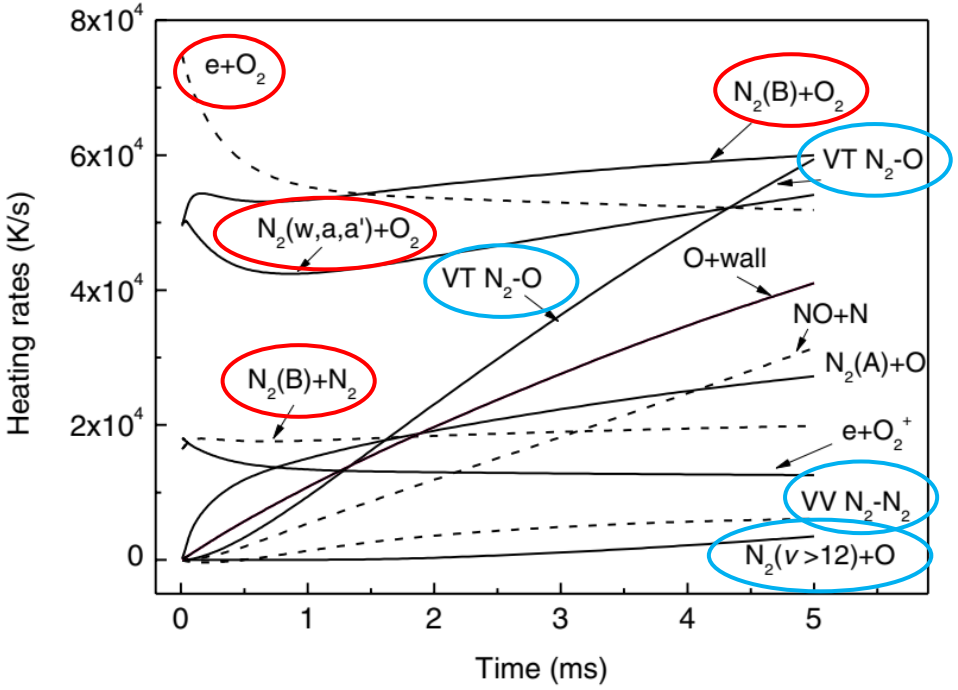

$80N_2$-$20\%O_2$ DC pulsed discharge

p = 1 Torr I = 150 mA R = 1 cm

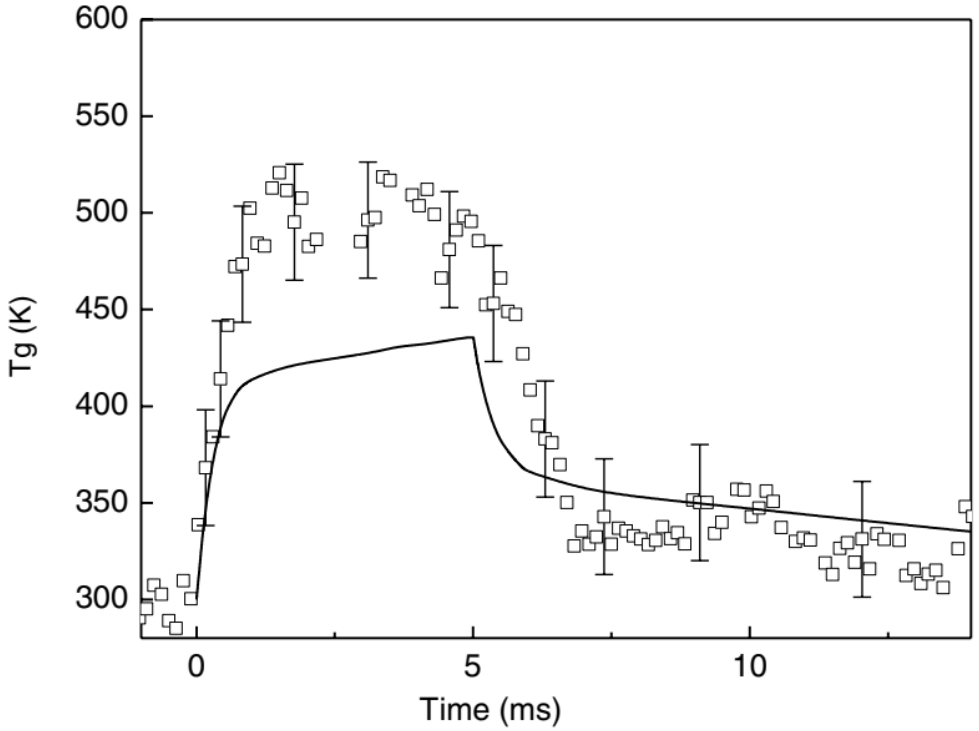

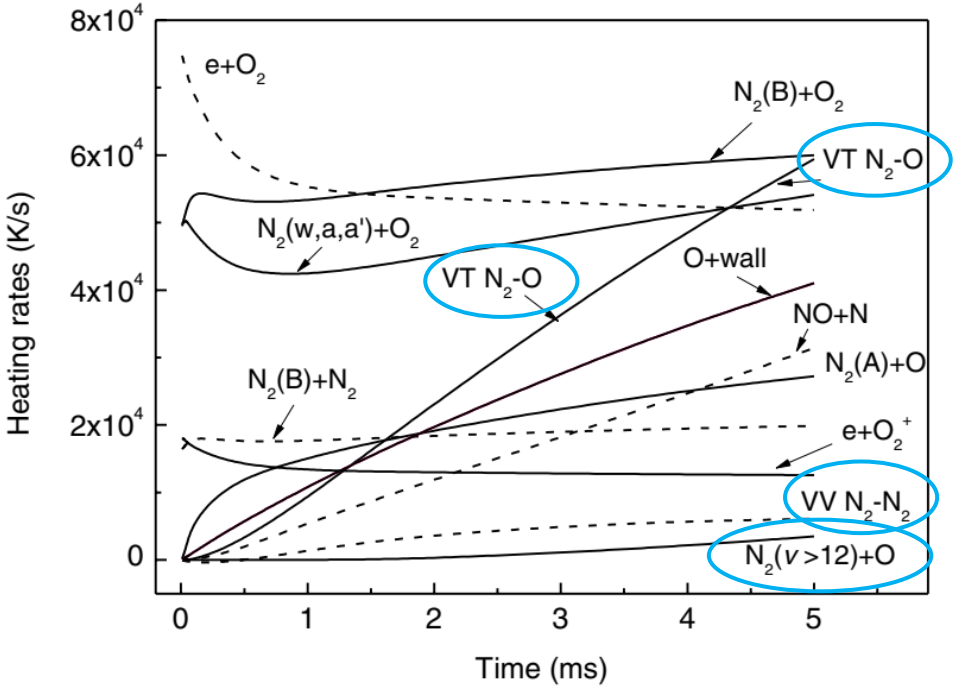

$80N_2$-$20\%O_2$ DC pulsed discharge

p = 1 Torr I = 150 mA R = 1 cm

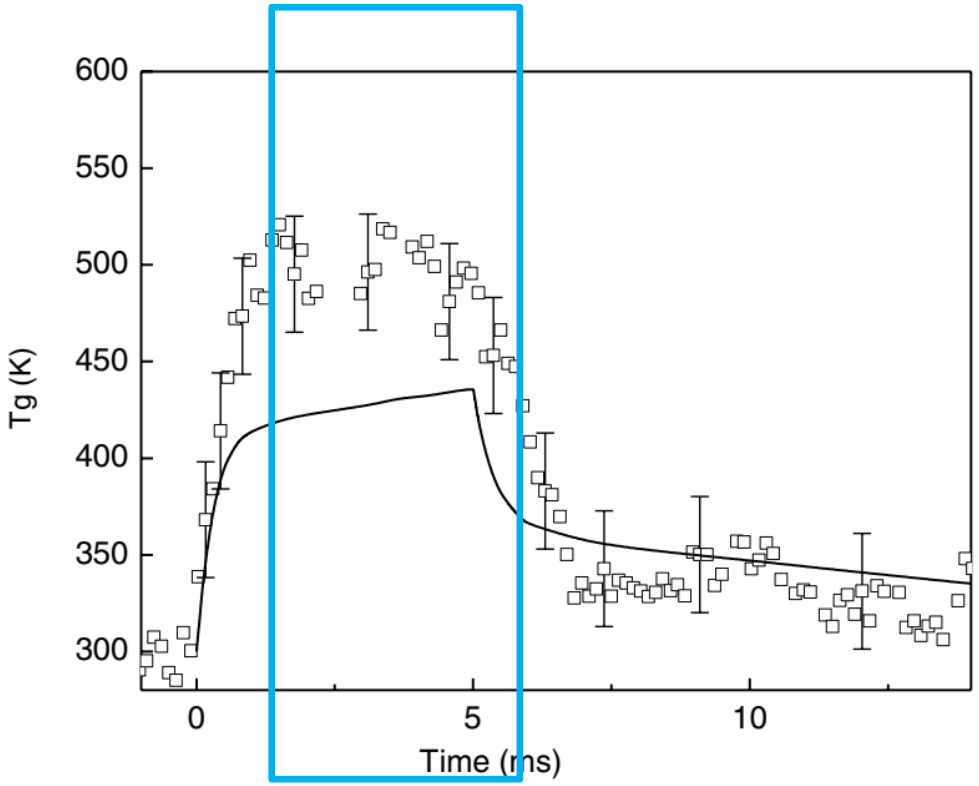

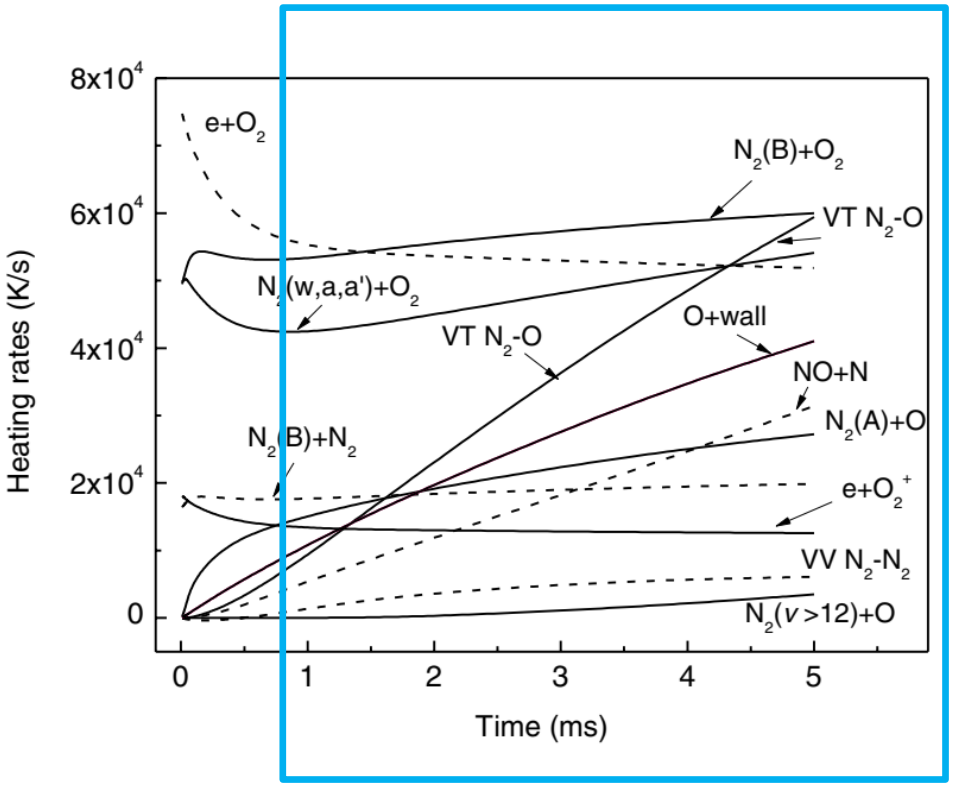

$80N_2$-$20\%O_2$ DC pulsed discharge

p = 1 Torr I = 150 mA R = 1 cm

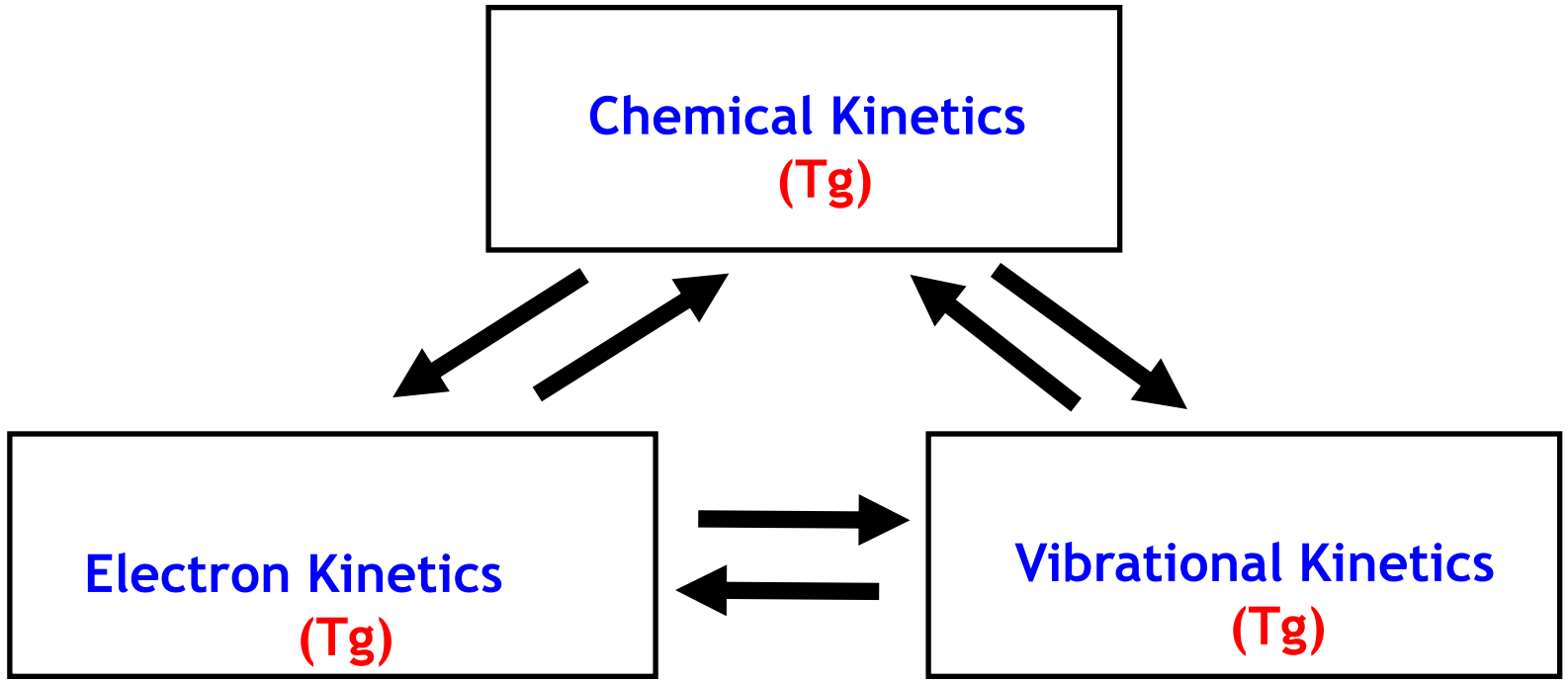
Chemical Kinetics
(Tg)
Electron Kinetics
(Tg)
Vibrational Kinetics
(Tg)

One last effect involving Tg and vibrational kinetics

DC discharge in pure N_2, 50 mA, 7.5 Torr

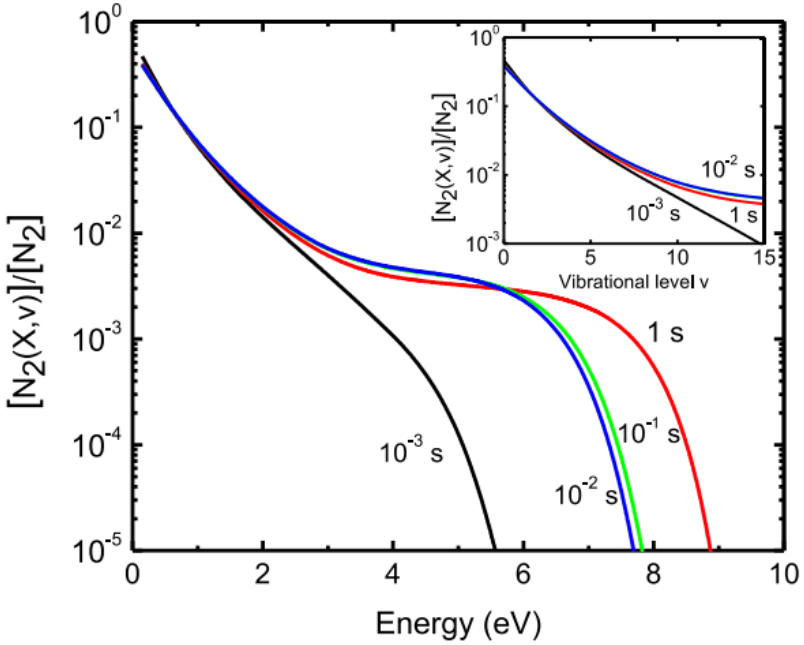

Gianpiero Colonna, Carlos D. Pintassilgo ... Eur. Phys. J. D (2021)75:183

DC discharge in pure N_2, 50 mA, 7.5 Torr

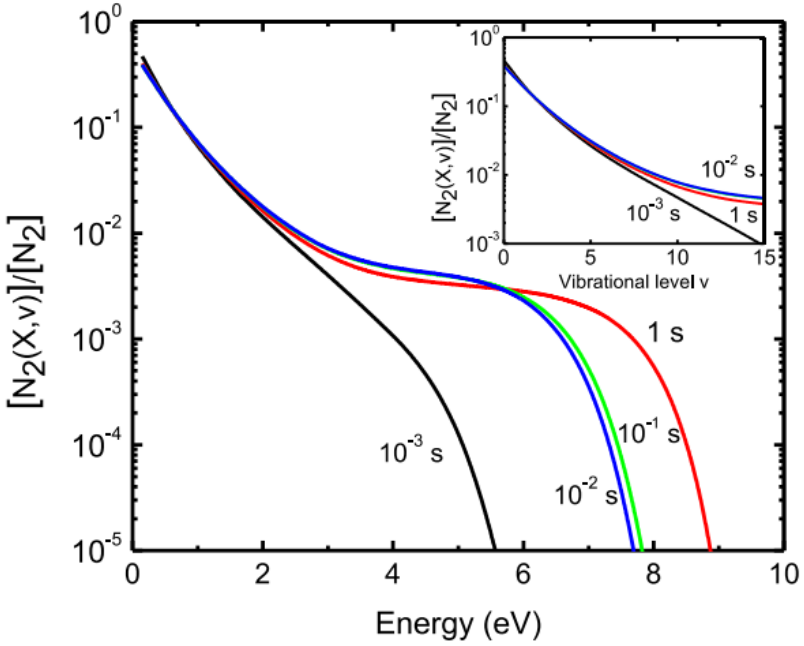

Afterglow

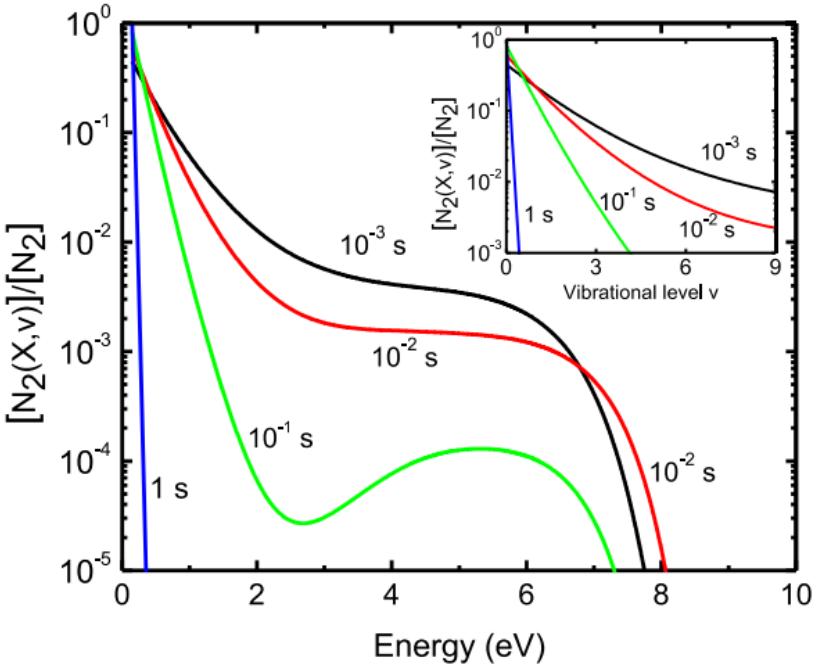

Gianpiero Colonna, Carlos D. Pintassilgo ... Eur. Phys. J. D (2021)75:183

DC discharge in pure N_2, 50 mA, 7.5 Torr

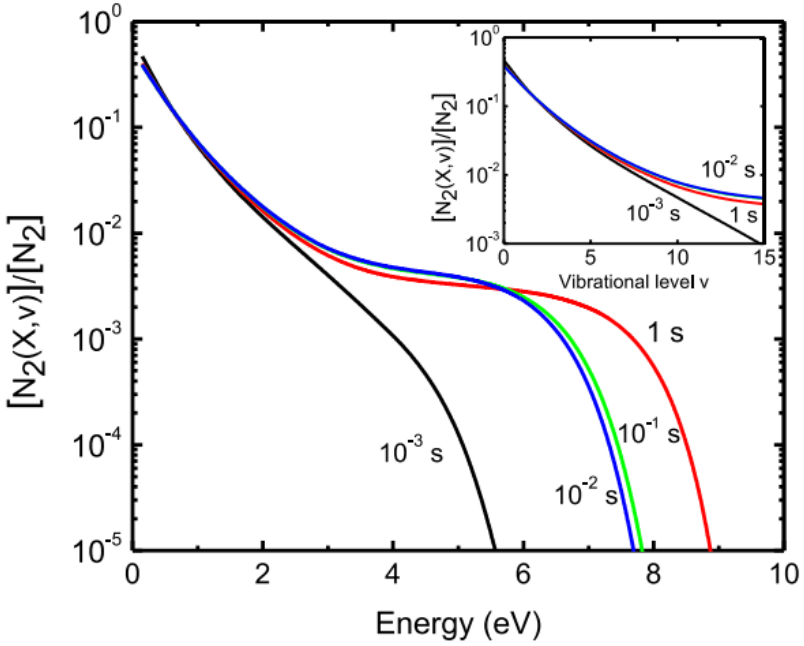

Afterglow

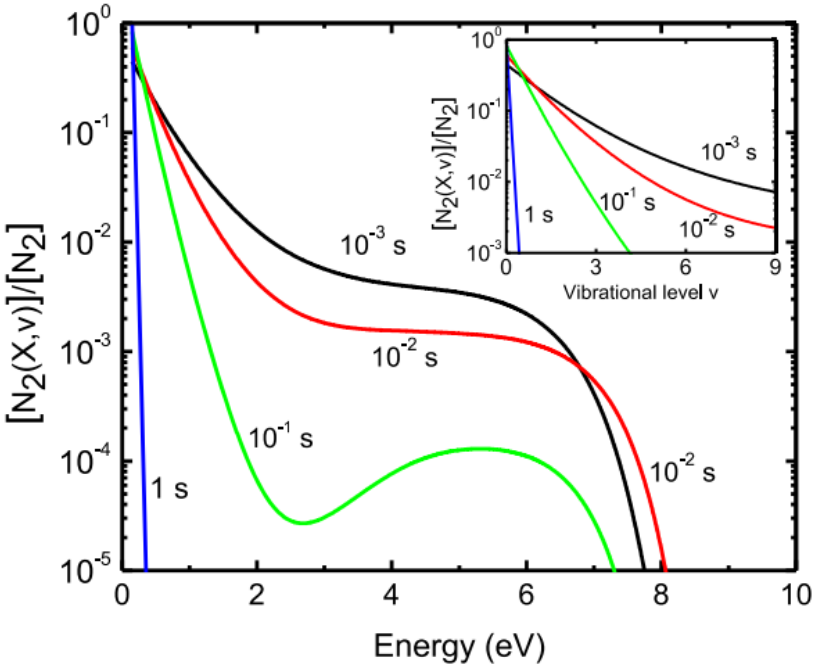

$$T_{0,1} = E_{0,1}/\ln(N_{v=0}/N_{v=1})$$ 'first level' N_2 vibrational temperature

DC discharge in pure N_2, 50 mA, 7.5 Torr

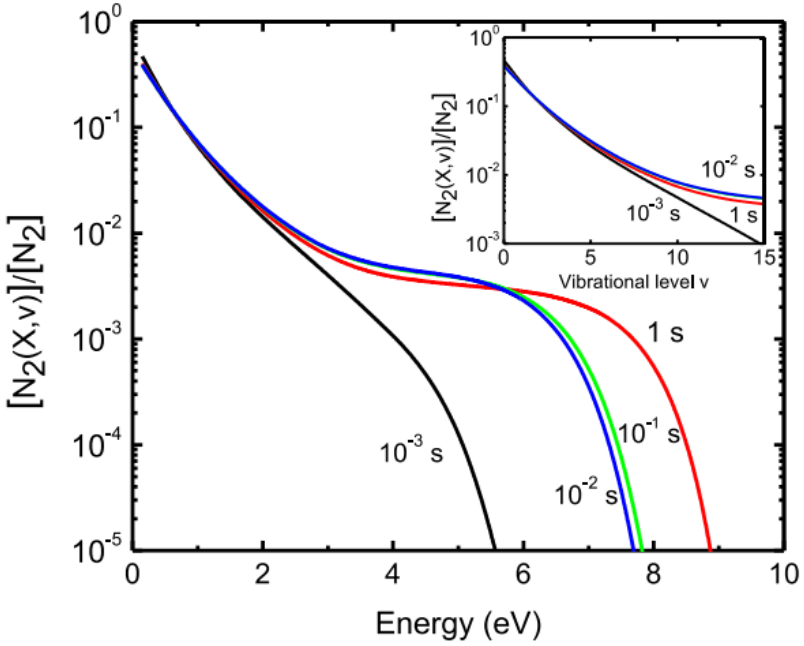

Afterglow

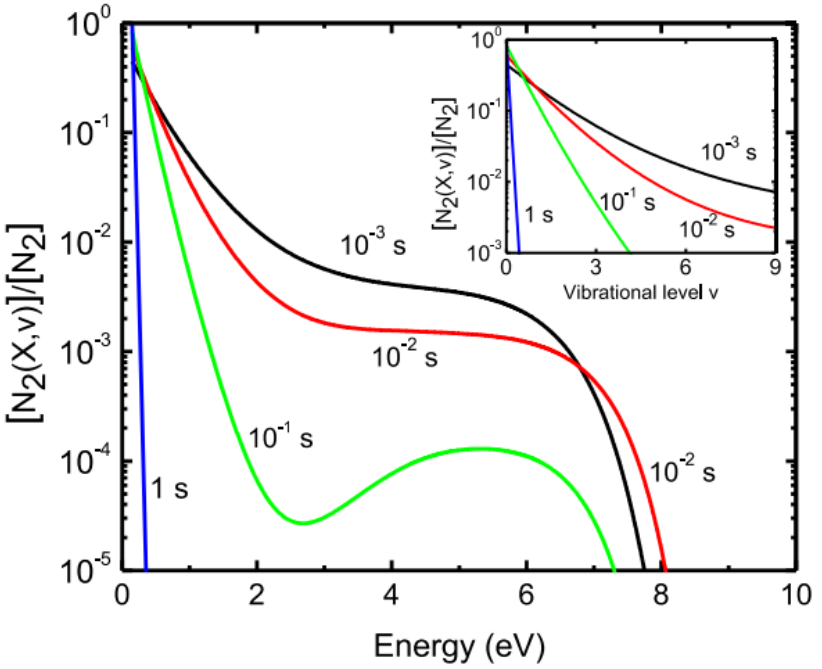

$$T_{0,1} = E_{0,1}/\ln(N_{v=0}/N_{v=1})$$ 'first level' N_2 vibrational temperature

$$\frac{\sum_v E_v N_v}{\sum_v N_v} = \frac{\sum_v E_v \exp(-E_v/k_B T_v)}{\sum_v \exp(-E_v/k_B T_v)}$$

T_v is defined as the temperature for which the average energy of the non-equilibrium vibrational distribution function (VDF) equals the one of a Boltzmann equilibrium VDF.

DC discharge in pure N_2, 50 mA, 7.5 Torr

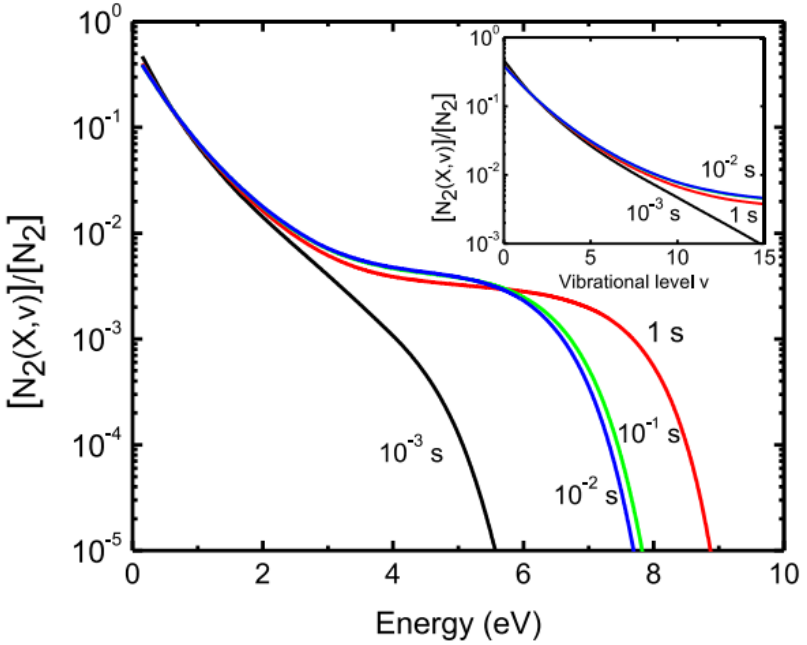

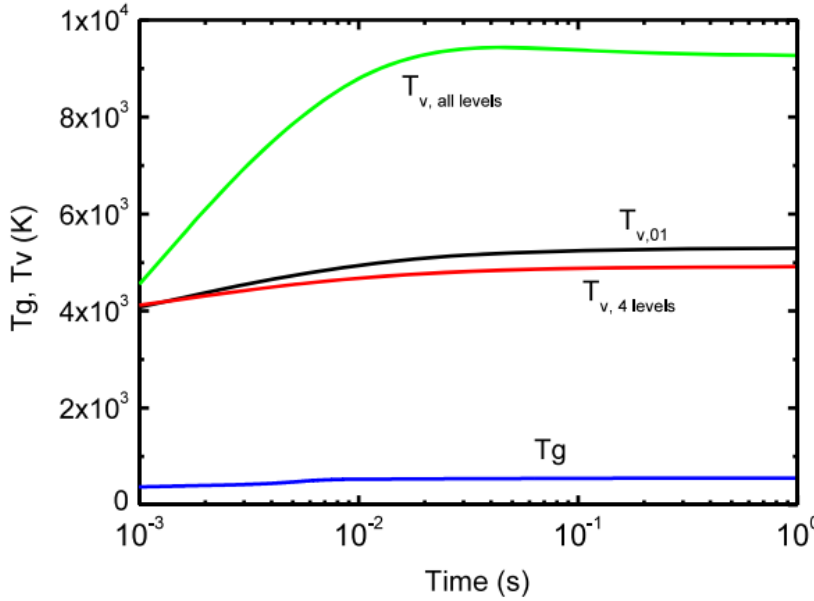

DC discharge in pure N_2, 50 mA, 7.5 Torr

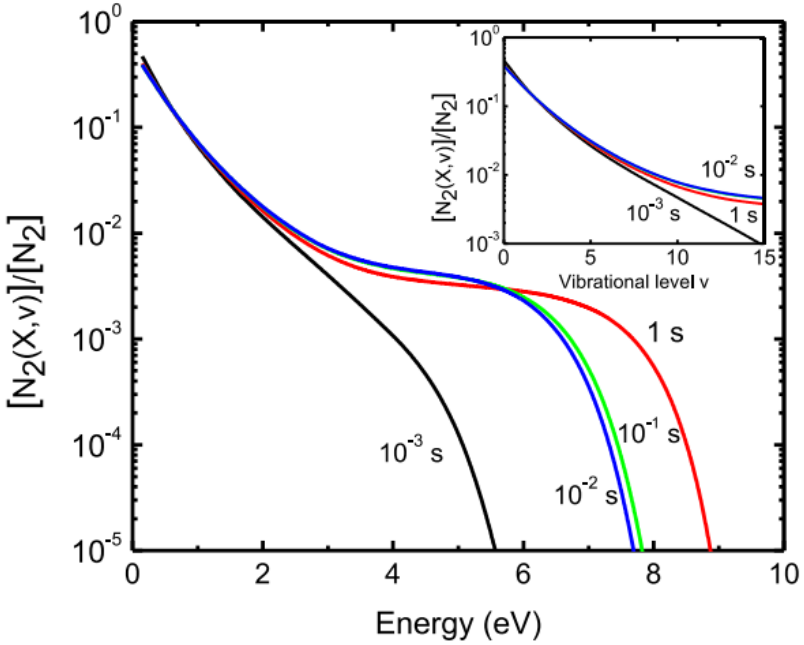

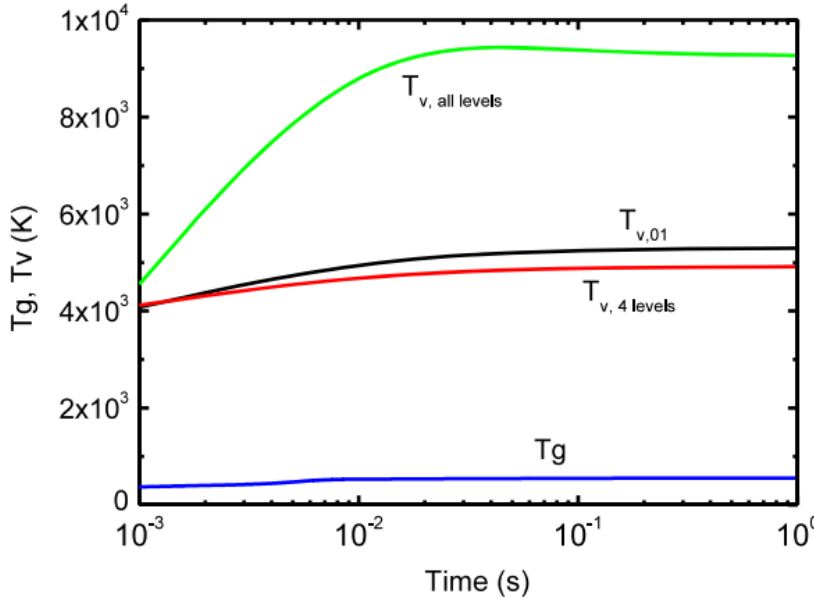

$$T_{0,1} = E_{0,1}/\ln(N_{v=0}/N_{v=1})$$

DC discharge in pure N_2, 50 mA, 7.5 Torr

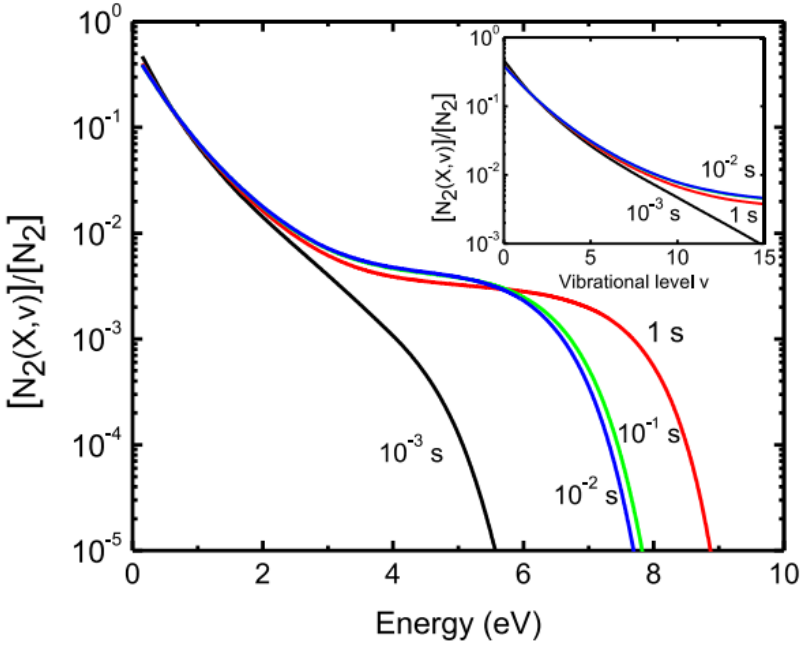

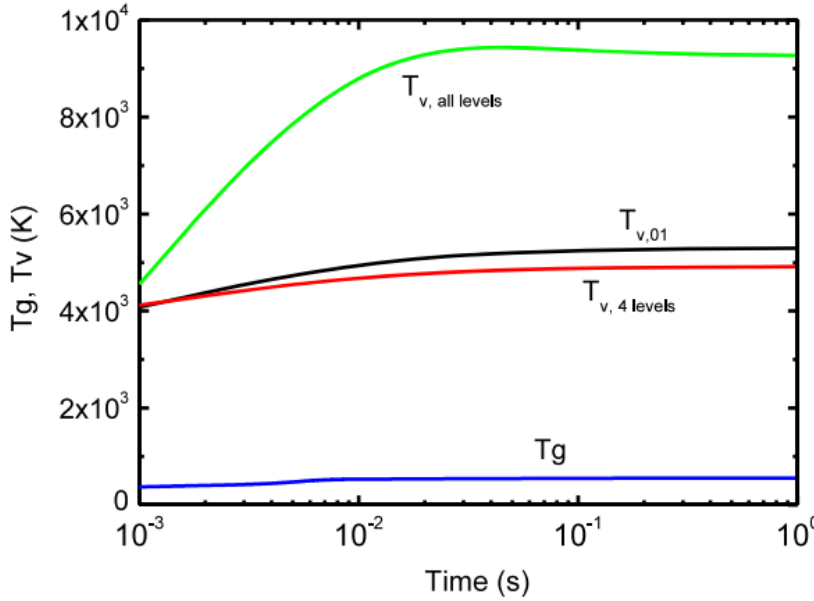

$$\frac{\sum_v E_v N_v}{\sum_v N_v} = \frac{\sum_v E_v \exp(-E_v/k_B T_v)}{\sum_v \exp(-E_v/k_B T_v)}$$

$$T_{0,1} = E_{0,1}/\ln(N_{v=0}/N_{v=1})$$

Afterglow

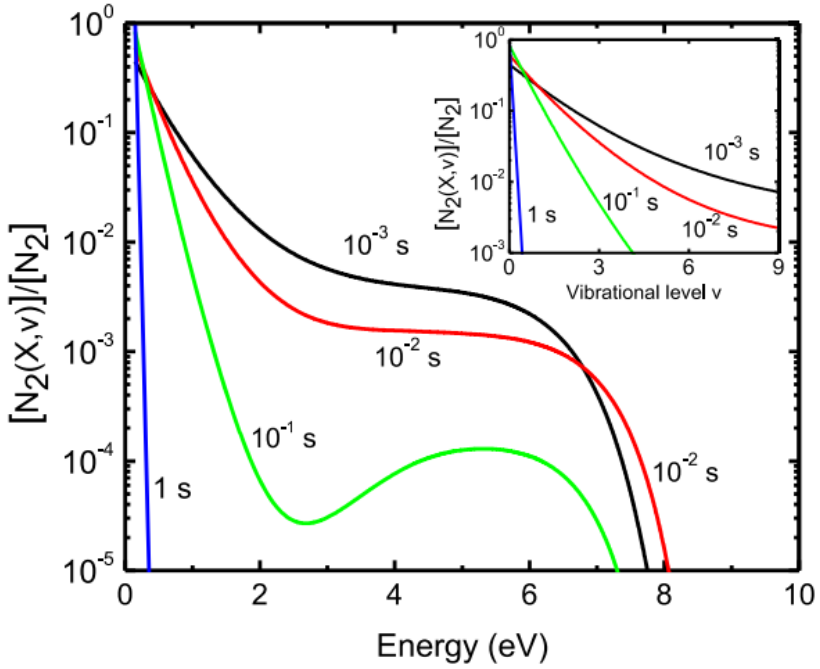
[N2(X,v)]/[N2]
Energy (eV)
10^0
10^-1
10^-2
10^-3
10^-4
10^-5
0
2
4
6
8
10
10^-3 s
10^-2 s
10^-1 s
1 s
10^-2 s
[N2(X,v)]/[N2]
Vibrational level v
0
3
6
9
10^-3 s
10^-1 s
10^-2 s
1 s

Afterglow

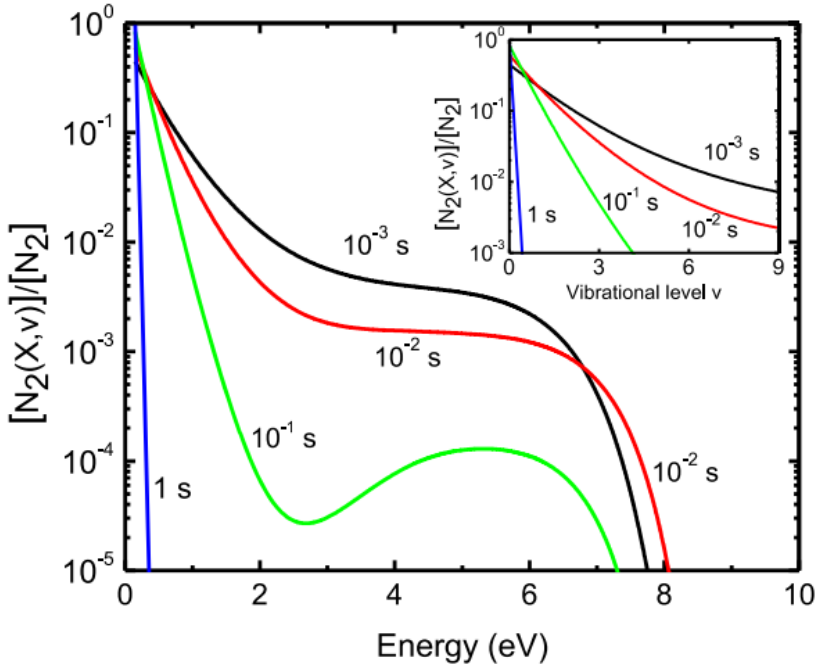

$$T_{0,1} = E_{0,1}/\ln(N_{v=0}/N_{v=1})$$

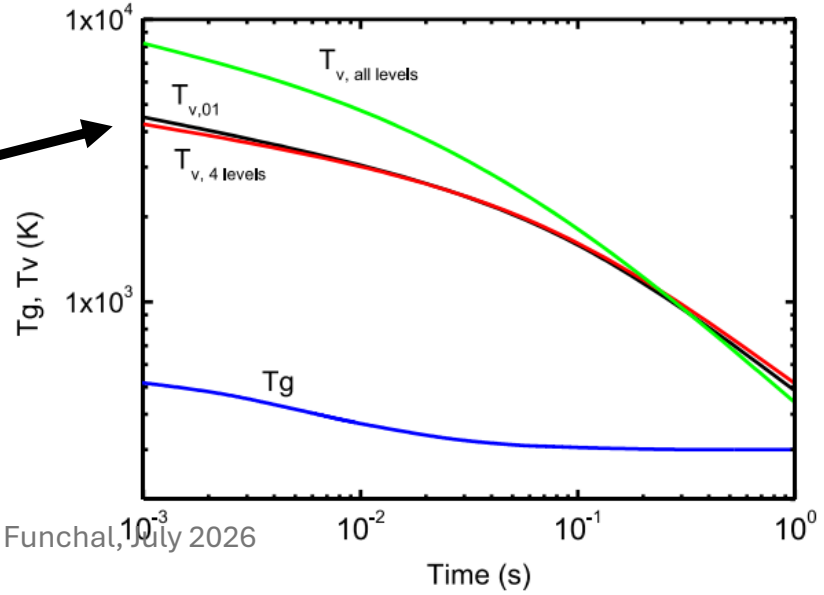

Afterglow

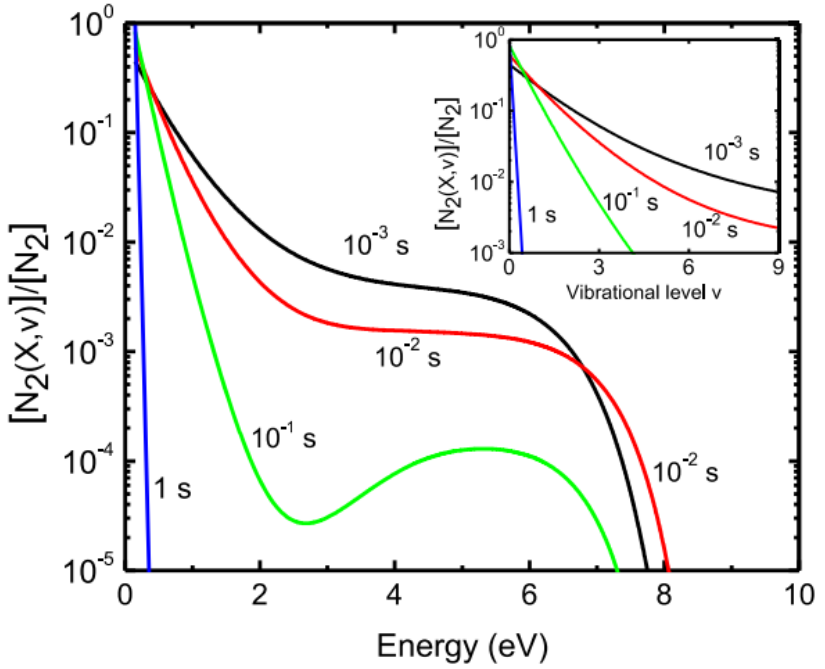

$$\frac{\sum_v E_v N_v}{\sum_v N_v} = \frac{\sum_v E_v \exp(-E_v/k_B T_v)}{\sum_v \exp(-E_v/k_B T_v)}$$

$$T_{0,1} = E_{0,1}/\ln(N_{v=0}/N_{v=1})$$

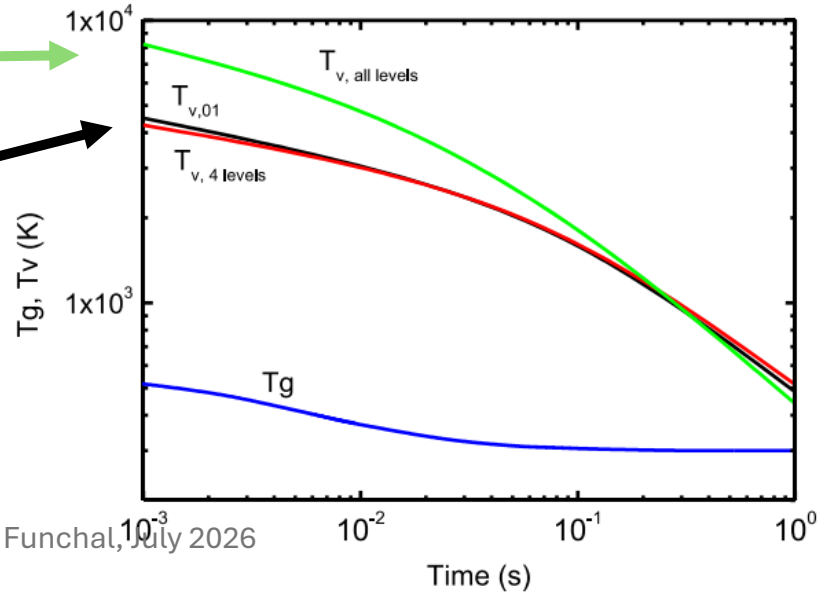

OUTLINE

Fundamentals

coupling between electron, chemical and vibrational kinetics

Typical examples

pulsed discharges (dry air, N_2)

Application to DBD discharges

N_2-O_2-H_20 plasmas (humid air)

OUTLINE

Fundamentals

coupling between electron, chemical and vibrational kinetics

Typical examples

pulsed discharges (dry air, N_2)

Application to DBD discharges

N_2-O_2-H_20 plasmas (humid air)

Plasma Chemistry and Plasma Processing
https://doi.org/10.1007/s11090-024-10484-6

ORIGINAL PAPER

Modeling Study of Chemical Kinetics and Vibrational Excitation in a Volumetric DBD in Humid Air at Atmospheric Pressure

Giacomo Pierotti[1] · Arturo Popoli[1] · Carlos Daniel Pintassilgo[2,3] · Andrea Cristofolini[1]

$78\%N_2\text{-}19\%O_2\text{-}3\%H_20$

Table 1 Species considered in the simulations. Each vibrationally-excited level is treated like a single species. $O_2(Sum)$ represents the sum of the states $O_2(A^3\Sigma_u^+)$, $O_2(C^3\Delta_u)$ and $O_2(c^1\Sigma_u^-)$

$N_2(X, 0 \le v \le 59)$, $N_2(A^3\Sigma_u^+)$, $N_2(B^3\Pi_g)$, $N_2(C^3\Pi_u)$, $N_2(a'\Sigma_u^-)$, $N_2(w^1\Delta_u)$, $N_2(a^1\Pi_g)$, N_2^+, $N_2^+(B^2\Sigma_u^+)$
$N(^4S)$, $N(^2D)$, $N(^2P)$, N^+, N_4^+, N_3^+
$O_2(X, 0 \le v \le 41)$, $O_2(a^1\Delta_g)$, $O_2(b^1\Sigma_g^+)$, $O_2(Sum)$, O_2^+, O_2^-
$O(^3P)$, $O(^1D)$, O^+, O^-, O_3, $O_3(exc)$, O_3^-, O_4^-, O_4^+
NO, $NO(A^2\Sigma^+)$, $NO(B^2\Pi)$, NO^+, NO^-, NO_2, NO_2^+, NO_2^-, $NO_2(A)$
NO_3, NO_3^-, N_2O, N_2O^+, $N_2O^-N_2O_3$, N_2O_4, N_2O_5
H_2O, H_2O^+, H_3O^+, H, H^+, H^-, OH, OH^+, OH^-, H_2, H_2^+, H_3^+, HO_2, H_2O_2
HNO, HNO_2, HNO_3, e

$$N_2(v > 12) + O(^3P) \longrightarrow NO + N(^4S)$$

$$O_2(v > 1) + N(^4S) \longrightarrow NO + O(^3P)$$

$E/N = 150\text{Td}$, $n_e = 10^{19}\text{m}^{-3}$ and $t_{\text{disch}} = 50\text{ns}$.

$t_{\text{aft}} = 10^{-5}\text{s}$ and $t_{\text{aft}} = 10^{-6}\text{s}$

$E/N = 150\text{Td}$, $n_e = 10^{19}\text{m}^{-3}$ and $t_{\text{disch}} = 50\text{ns}$. $t_{\text{aft}} = 10^{-5}\text{s}$ and $t_{\text{aft}} = 10^{-6}\text{s}$

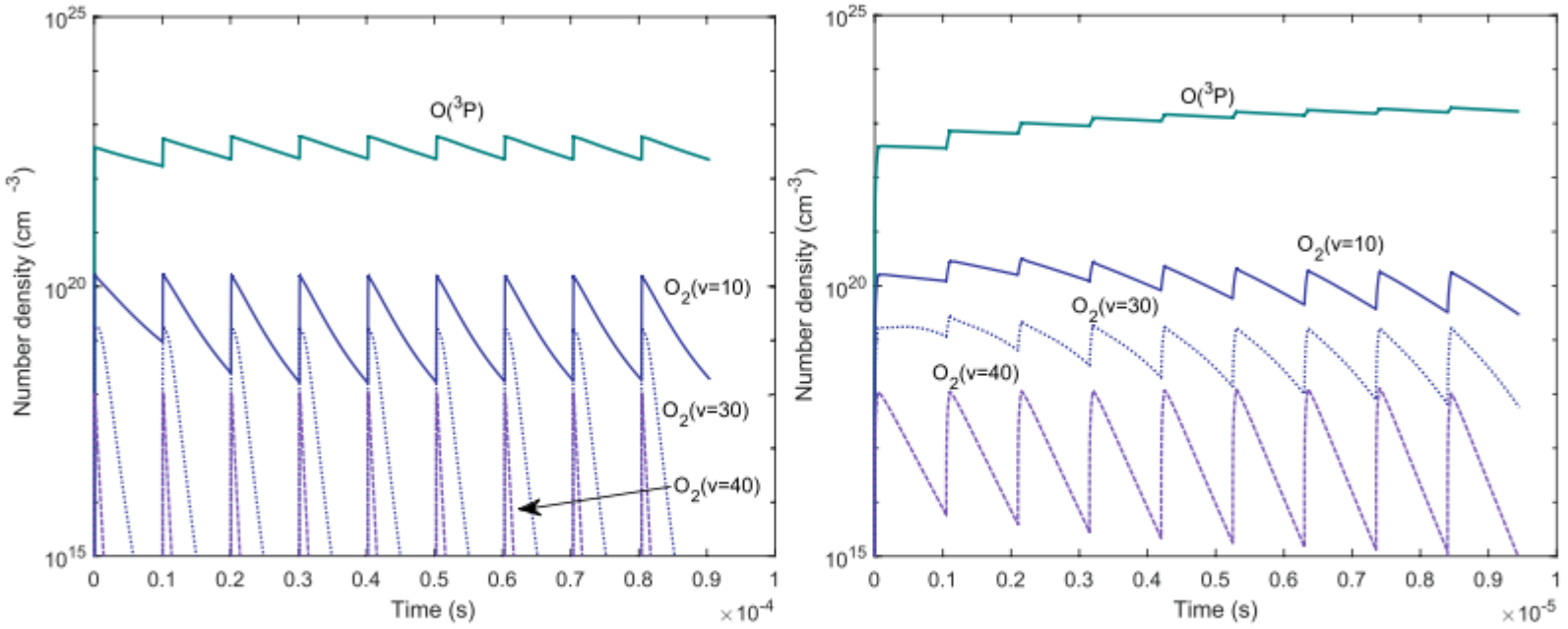

(a) $t_{\text{aft}} = 10^{-5}\,\text{s}$ (b) $t_{\text{aft}} = 10^{-6}\,\text{s}$

Figure 2: O(^{3}P), O_2(v=10), O_2(v=30) and O_2(v=40) for two afterglow durations.

$E/N = 150\text{Td}$, $n_e = 10^{19}\text{m}^{-3}$ and $t_{\text{disch}} = 50\text{ns}$. $t_{\text{aft}} = 10^{-5}\text{s}$ and $t_{\text{aft}} = 10^{-6}\text{s}$

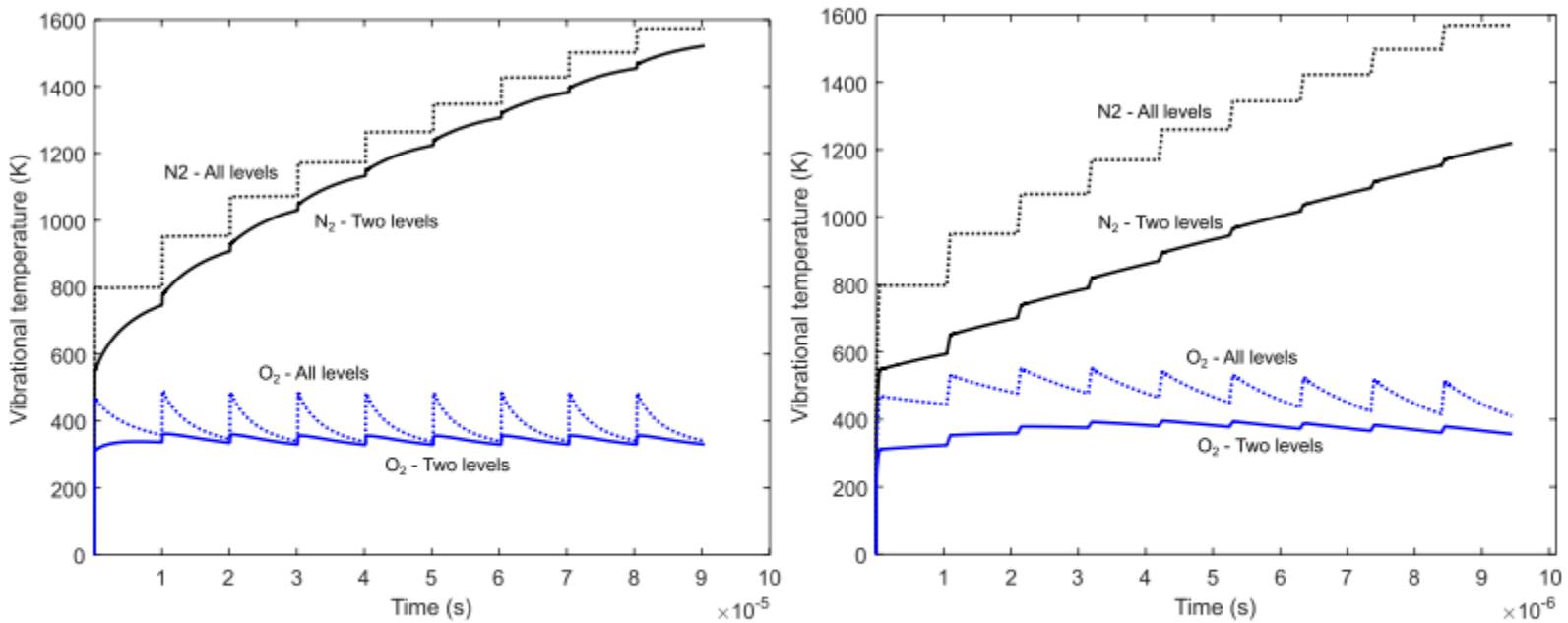

(a) $t_{\text{aft}} = 10^{-5}\,\text{s}$ (b) $t_{\text{aft}} = 10^{-6}\,\text{s}$

Fig. 3 *Two-level* vibrational temperatures (via Eq. (12)) of O_2 and N_2 considering two different afterglow times

Table 2 Reaction rates in m^{-3}/s and relative contribution of reaction (10) $O_2(v > 1) + N(^4S) \longrightarrow NO + O(^3P)$ on NO and $O(^3P)$ production and on $N(^4S)$ destruction for the two considered values of t_{aft}

	First afterglow phase		Last afterglow phase	
	$t_{aft} = 10^{-6}$s	$t_{aft} = 10^{-5}$s	$t_{aft} = 10^{-6}$s	$t_{aft} = 10^{-5}$s
Reaction rate of (10)	1.00×10^{25}	6.70×10^{23}	1.28×10^{25}	2.20×10^{23}
Contribution to $N(^4S)$	6.5%	3.5%	2.2%	1.0%
Contribution to $O(^3P)$	4.7%	0.35%	0.29%	0.2%
Contribution to NO	5.4%	1.5%	0.38%	0.1%

Table 2 Reaction rates in m^{-3}/s and relative contribution of reaction (10) $O_2(v > 1) + N(^4S) \longrightarrow NO + O(^3P)$ on NO and $O(^3P)$ production and on $N(^4S)$ destruction for the two considered values of t_{aft}

	First afterglow phase		Last afterglow phase	
	$t_{aft} = 10^{-6}$s	$t_{aft} = 10^{-5}$s	$t_{aft} = 10^{-6}$s	$t_{aft} = 10^{-5}$s
Reaction rate of (10)	1.00×10^{25}	6.70×10^{23}	1.28×10^{25}	2.20×10^{23}
Contribution to $N(^4S)$	6.5%	3.5%	2.2%	1.0%
Contribution to $O(^3P)$	4.7%	0.35%	0.29%	0.2%
Contribution to NO	5.4%	1.5%	0.38%	0.1%

users of global models typically employ one of the following approaches to estimate $E(t)/N$:

- Calculate $E(t)/N$ (and, if necessary, the electron number density) by ensuring consistency with the experimentally measured electrical power absorbed by the device [42, 47].
- Use an equivalent electric circuit approach (see, e.g. [41, 48]) to derive $E(t)/N$ from the applied voltage $v(t)$.
- Incorporate experimental data directly describing the behavior of the electric field, as implemented in this work.

users of global models typically employ one of the following approaches to estimate $E(t)/N$:

- Calculate $E(t)/N$ (and, if necessary, the electron number density) by ensuring consistency with the experimentally measured electrical power absorbed by the device [42, 47].
- Use an equivalent electric circuit approach (see, e.g. [41, 48]) to derive $E(t)/N$ from the applied voltage $v(t)$.
- Incorporate experimental data directly describing the behavior of the electric field, as implemented in this work.

users of global models typically employ one of the following approaches to estimate $E(t)/N$:

- Calculate $E(t)/N$ (and, if necessary, the electron number density) by ensuring consistency with the experimentally measured electrical power absorbed by the device [42, 47].
- Use an equivalent electric circuit approach (see, e.g. [41, 48]) to derive $E(t)/N$ from the applied voltage $v(t)$.
- Incorporate experimental data directly describing the behavior of the electric field, as implemented in this work.

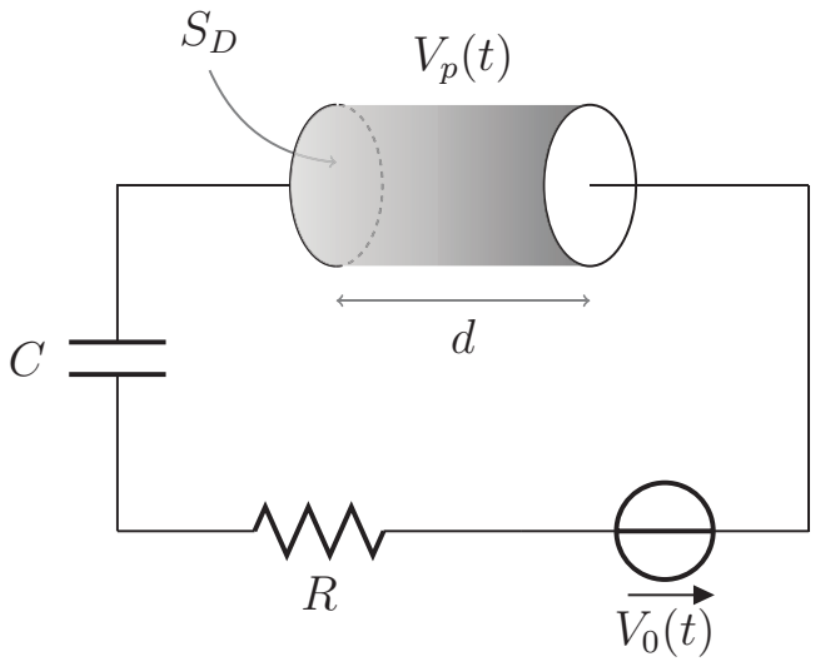

Figure 1. Circuit diagram.

A good approximation of a DBD can be made
by considering a capacitor (paralell-plate configuration)
in series in the circuit

Reduced field computed via equivalent circuit approach (within Merlino plasma global model) – atmospheric pressure air, f = 10^4 s^{-1}, V_0 = 10 kV, d = 10^{-3} m. See *Plasma Chem Plasma Process* **44**, 1575–1594 (2024). https://doi.org/10.1007/s11090-024-10484-6

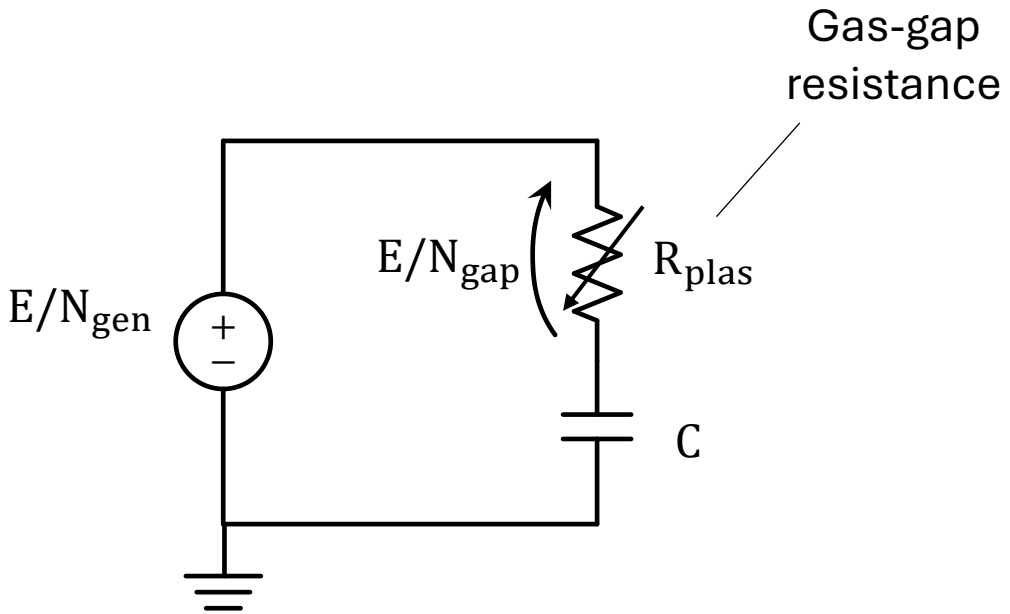

Fig. 5 DBD equivalent electric circuit

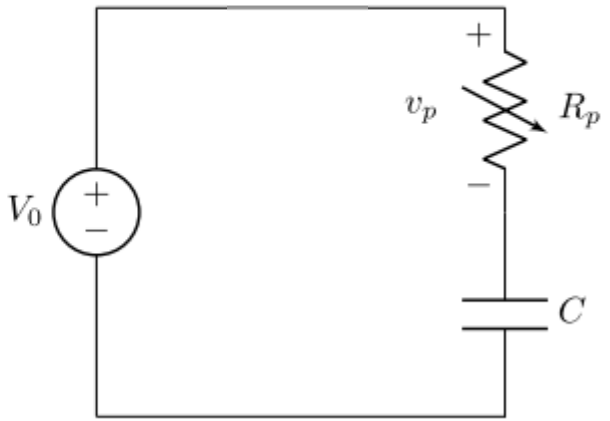

$$V_0 - v_p - v_C = 0$$

$$E_0 - E_p - \frac{v_C}{d} = 0$$

Fig. 5 DBD equivalent electric circuit

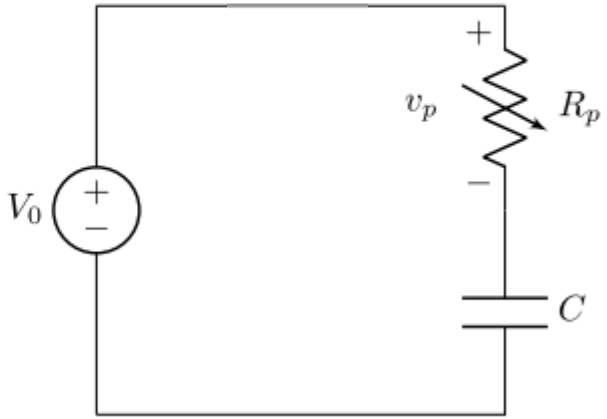

$$V_0 - v_p - v_C = 0$$

$$i = qn_e\mu_e E_p S_{\text{eff}}$$

$$i = C\frac{dv_C}{dt}$$

$$E_0 - E_p - \frac{v_C}{d} = 0$$

Fig. 5 DBD equivalent electric circuit

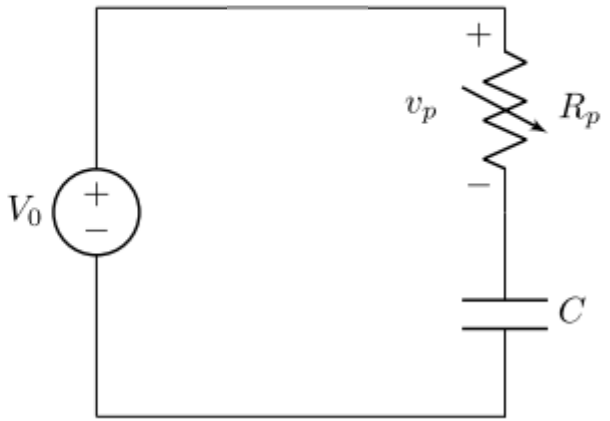

$$V_0 - v_p - v_C = 0$$

$$i = qn_e\mu_e E_p S_{\text{eff}}$$

$$i = C\frac{dv_C}{dt}$$

$$E_0 - E_p - \frac{v_C}{d} = 0$$

$$\frac{\mathrm{d}E_p}{\mathrm{d}t} = \frac{\mathrm{d}E_0}{\mathrm{d}t} - \frac{1}{d}\frac{\mu q n_e E_p S_{\text{eff}}}{C}.$$

Fig. 5 DBD equivalent electric circuit

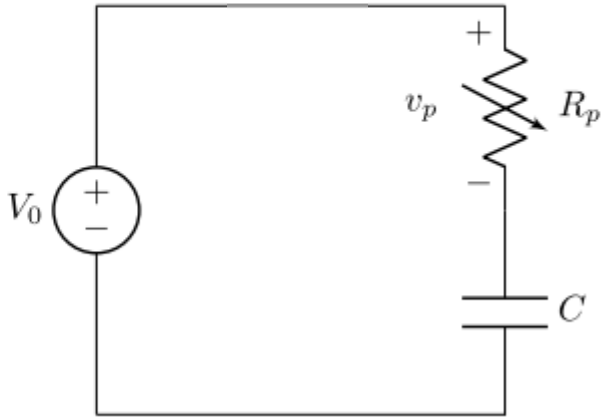

$$V_0 - v_p - v_C = 0$$

$$i = qn_e\mu_e E_p S_{\text{eff}}$$

$$i = C\frac{dv_C}{dt}$$

$$E_0 - E_p - \frac{v_C}{d} = 0$$

$$\frac{\mathrm{d}E_p}{\mathrm{d}t} = \frac{\mathrm{d}E_0}{\mathrm{d}t} - \frac{1}{d}\frac{\mu q n_e E_p S_{\text{eff}}}{C}.$$

Fig. 5 DBD equivalent electric circuit

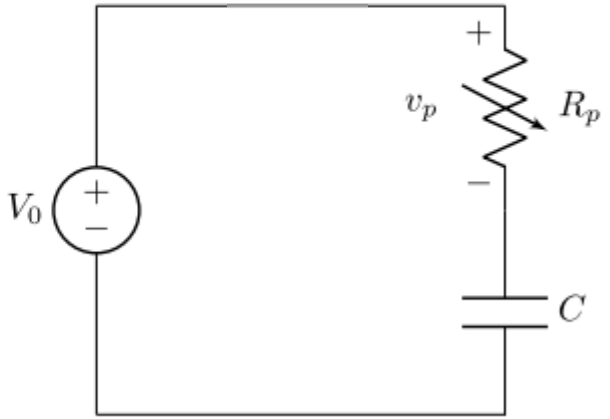

$$V_0 - v_p - v_C = 0$$

$$i = qn_e\mu_e E_p S_{\text{eff}}$$

$$i = C\frac{dv_C}{dt}$$

$$E_0 - E_p - \frac{v_C}{d} = 0$$

$$\frac{\mathrm{d}E_p}{\mathrm{d}t} = \frac{\mathrm{d}E_0}{\mathrm{d}t} - \frac{1}{d}\frac{\mu q n_e E_p S_{\text{eff}}}{C}.$$

C, S_{eff} and d can be used to define $C_0 = \frac{Cd}{S_{\text{eff}}}$.

Pierotti et al *Plasma Chem Plasma Process* **44**, 1575–1594 (2024)

Fig. 5 DBD equivalent electric circuit

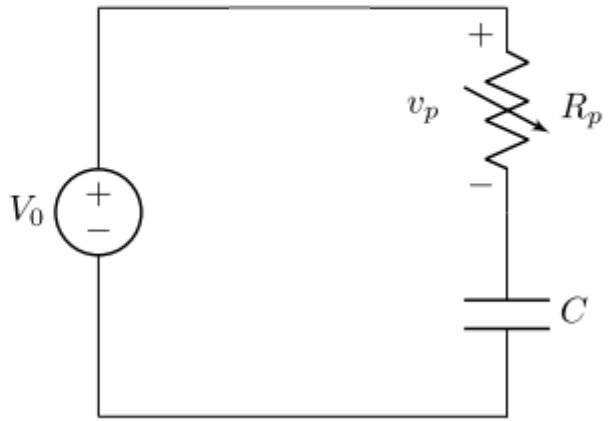

$$V_0 - v_p - v_C = 0$$

$$i = qn_e\mu_e E_p S_{\text{eff}}$$

$$i = C\frac{dv_C}{dt}$$

$$E_0 - E_p - \frac{v_C}{d} = 0$$

$$\frac{\mathrm{d}E_p}{\mathrm{d}t} = \frac{\mathrm{d}E_0}{\mathrm{d}t} - \frac{1}{d}\frac{\mu q n_e E_p S_{\text{eff}}}{C}.$$

C, S_{eff} and d can be used to define $C_0 = \frac{Cd}{S_{\text{eff}}}$.

Input parameters: 10 kV

Three different input power densities:

$P_1 = 2.7\text{x}10^6\ \text{W/m}^3$; f= 10 kHz; $C_0 = 10^4\ \varepsilon_0\ (\text{F/m})$

$P_2 = 1.35\text{x}10^5\ \text{W/m}^3$; f= 10 kHz; $C_0 = 500\ \varepsilon_0\ (\text{F/m})$

$P_3 = 1.45\text{x}10^3\ \text{W/m}^3$; f= 5 kHz; $C_0 = 10\ \varepsilon_0\ (\text{F/m})$

Fig. 5 DBD equivalent electric circuit

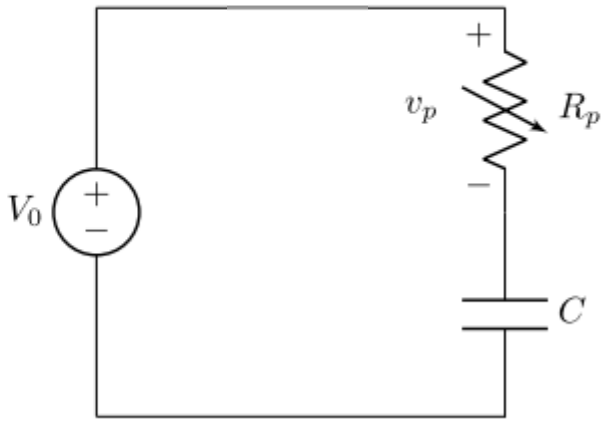

$$\frac{dn_1}{dt} = \sum_j \left[(a_{1j}^R - a_{1j}^L) k_j \prod_l n_l \right]$$

$$\vdots$$

$$\frac{dn_n}{dt} = \sum_j \left[(a_{nj}^R - a_{nj}^L) k_j \prod_l n_l \right]$$

$$\frac{dE_p}{dt} = \frac{dE_0}{dt} - \frac{1}{d} \frac{\mu q n_e E_p S_{\text{eff}}}{C}.$$

C, S_{eff} and d can be used to define $C_0 = \frac{Cd}{S_{\text{eff}}}$.

Input parameters: 10 kV

Three different input power densities:

$P_1 = 2.7 \times 10^6$ W/m^3 ; f= 10 kHz; $C_0 = 10^4\ \varepsilon_0$ (F/m)

$P_2 = 1.35 \times 10^5$ W/m^3 ; f= 10 kHz; $C_0 = 500\ \varepsilon_0$ (F/m)

$P_3 = 1.45 \times 10^3$ W/m^3 ; f= 5 kHz; $C_0 = 10\ \varepsilon_0$ (F/m)

Reduced field computed via equivalent circuit approach (within Merlino plasma global model) – atmospheric pressure air, f = 10^4 s^{-1}, V_0 = 10 kV, d = 10^{-3} m. See *Plasma Chem Plasma Process* **44**, 1575–1594 (2024). https://doi.org/10.1007/s11090-024-10484-6

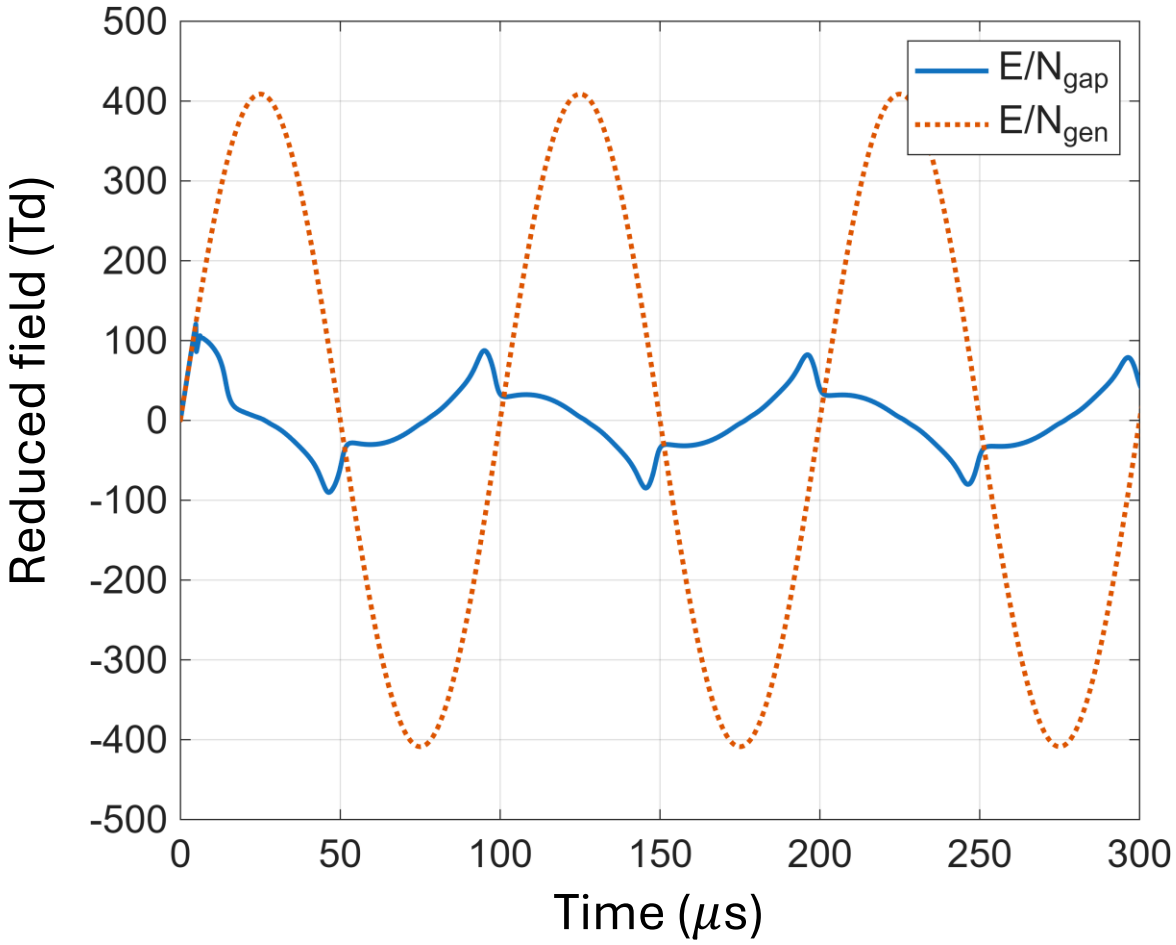

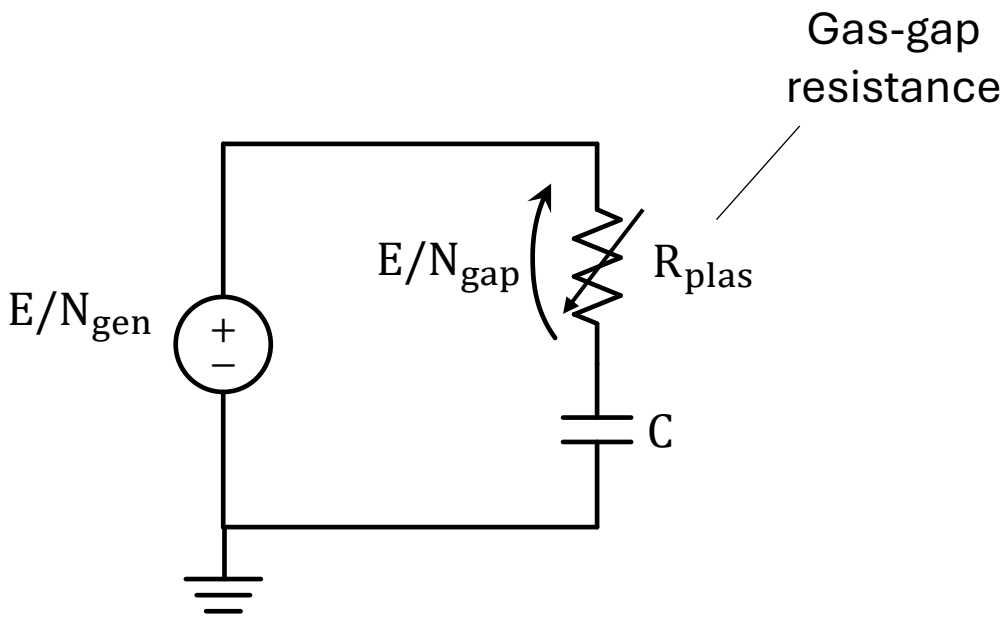

Capacitive charging and plasma conduction screen the imposed field and produce a phase lead of the effective gap field E/N_{gap}

Pierotti et al *Plasma Chem Plasma Process* **44**, 1575–1594 (2024)

Fig. 7 Electrons number density during the last time period of the considered voltage source for all the levels of input power density.*T* indicates the period of the voltage source in each simulations

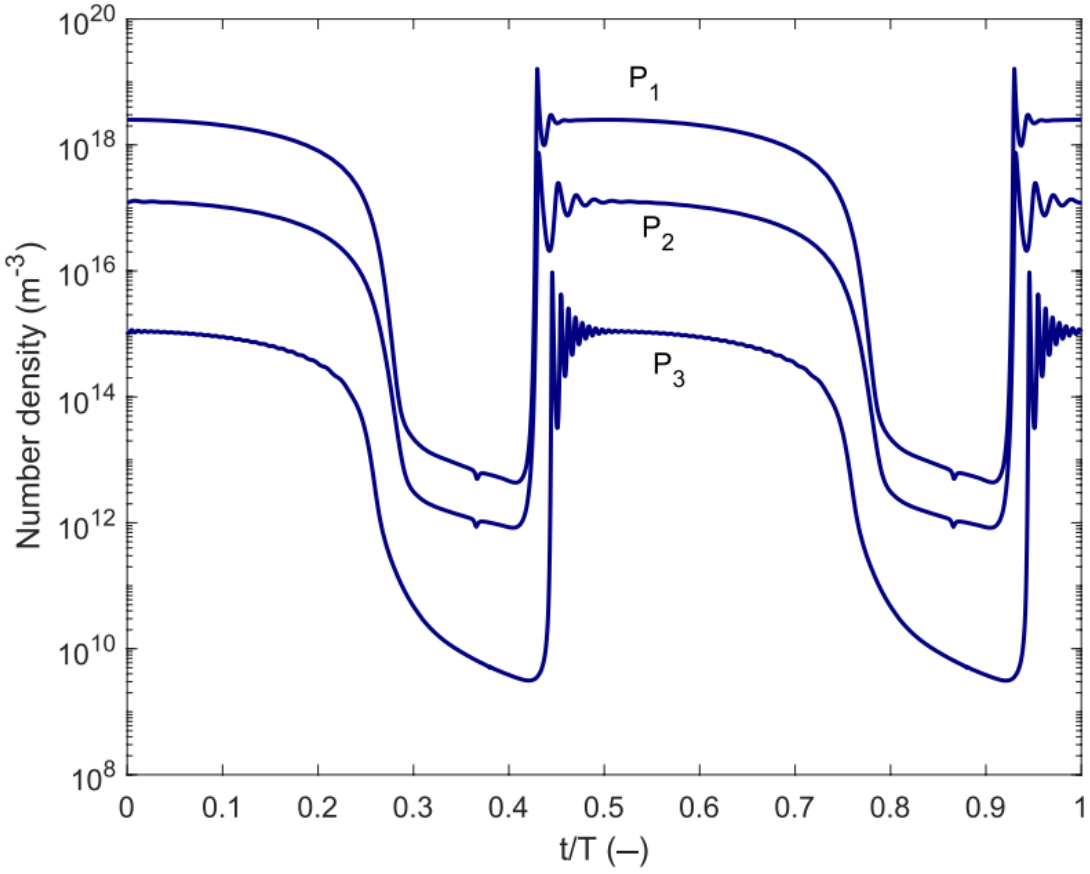

P_1 = 2.7x10^6 W/m^3 ; f= 10 kHz; C_0= 10^4 ε_0 (F/m)

P_2 = 1.35x10^5 W/m^3 ; f= 10 kHz; C_0= 500 ε_0 (F/m)

P_3 = 1.45x10^3 W/m^3 ; f= 5 kHz; C_0= 10 ε_0 (F/m)

Results obtained using the MERLINO code developed at the University of Bologna, where the rate coefficients of the electron impact reactions are obtained from LoKI -B for different values of the reduced electric field.

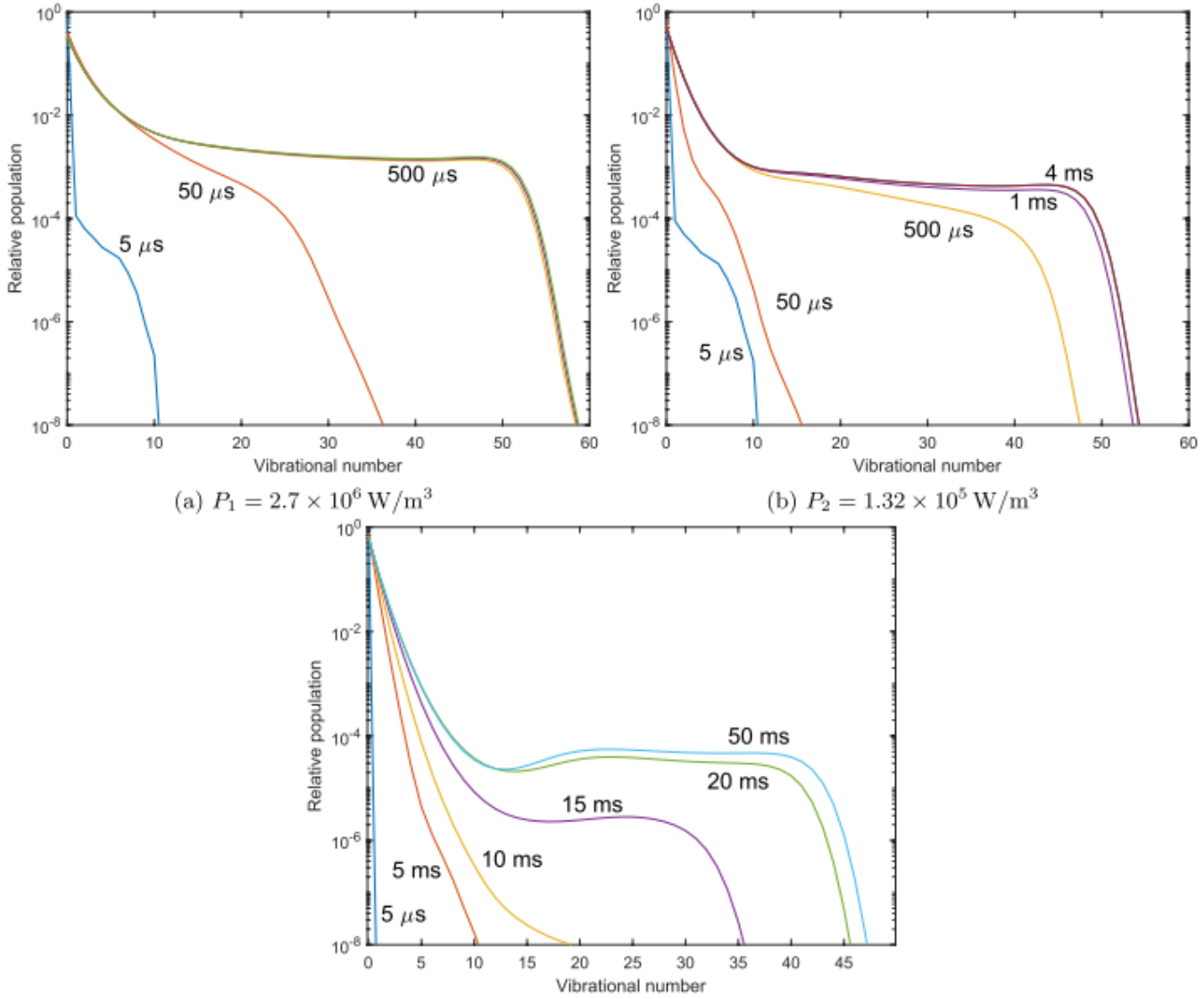

(a) $P_1 = 2.7 \times 10^6\ \mathrm{W/m^3}$

(b) $P_2 = 1.32 \times 10^5\ \mathrm{W/m^3}$

(c) $P_3 = 1.45 \times 10^3\ \mathrm{W/m^3}$

Fig. 8 Temporal evolution of N_2 VDF for the the input power densities considered in this work

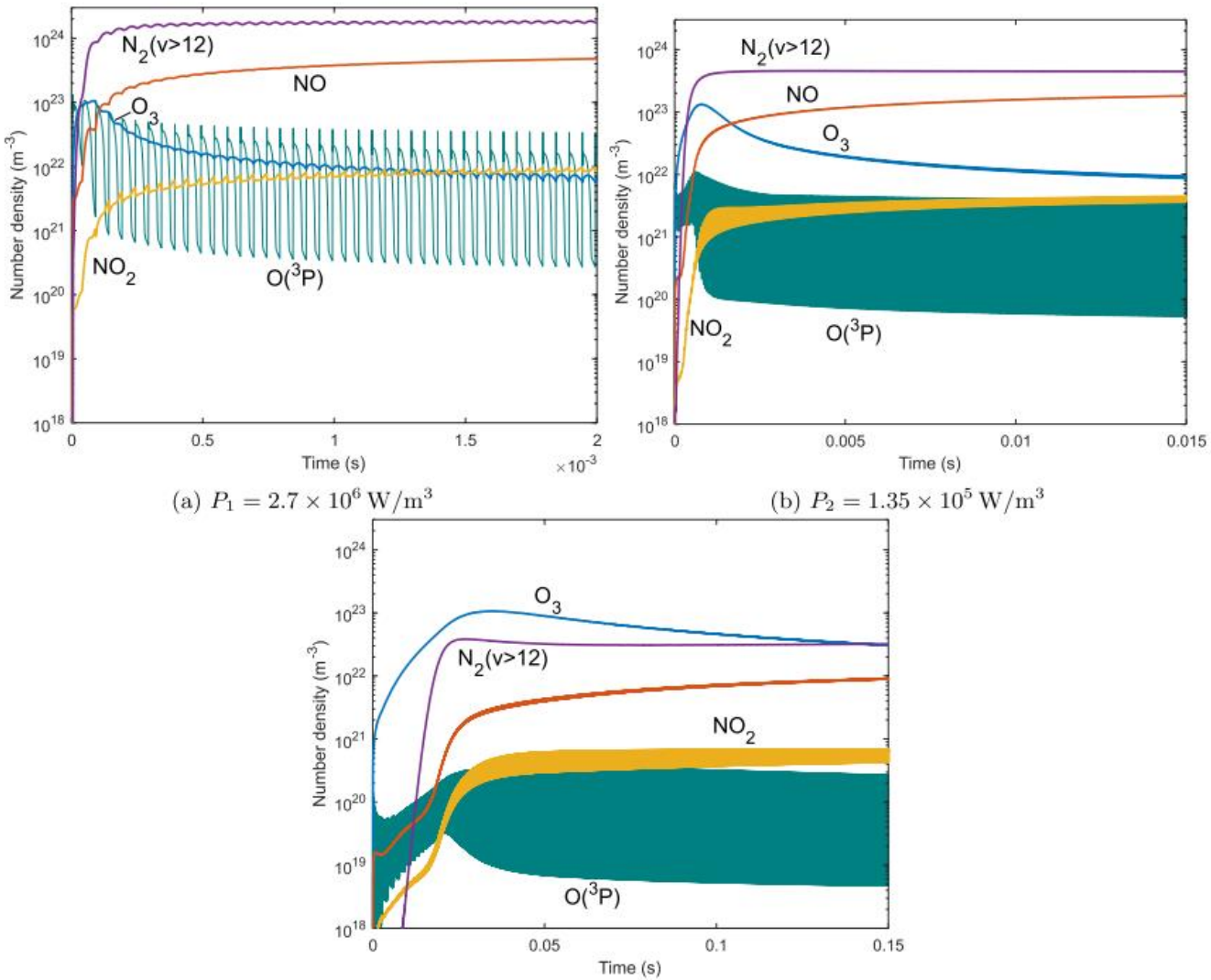

Fig. 6 Behavior of O_3, NO, NO_2, $O(^3P)$ and $N_2(v > 12)$ number densities for the considered input power levels

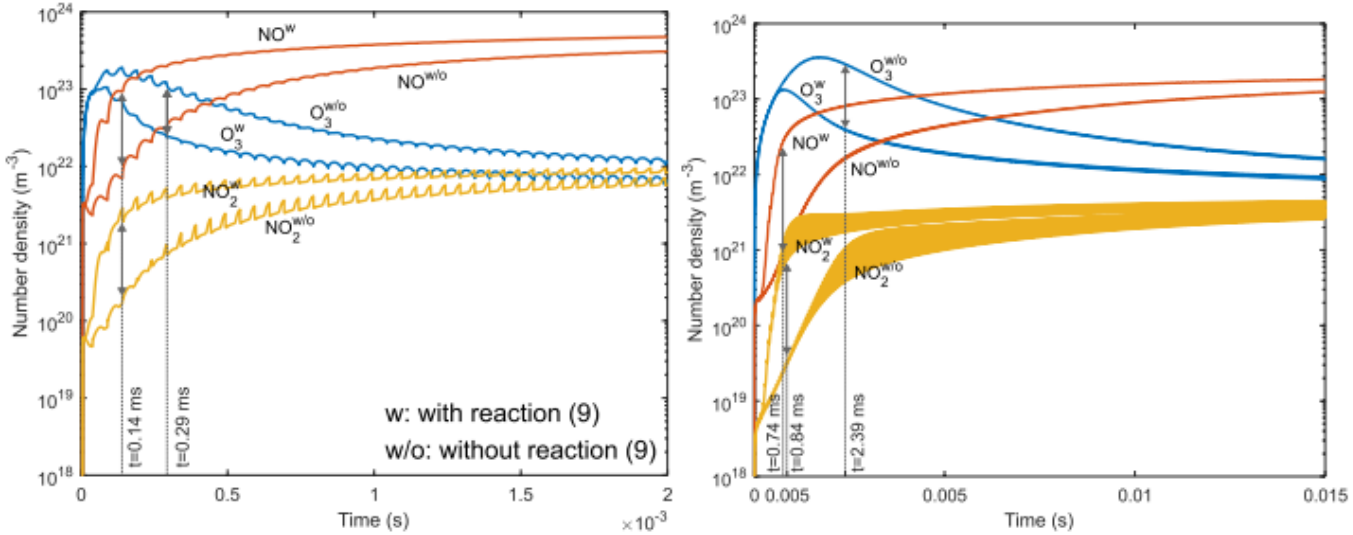

(a) $P_1 = 2.7 \times 10^6\ \mathrm{W/m^3}$

(b) $P_2 = 1.35 \times 10^5\ \mathrm{W/m^3}$

(c) $P_3 = 1.45 \times 10^3\ \mathrm{W/m^3}$

Fig. 11 Comparison between O_3, NO and NO_2 behavior for different levels of input power densities with and without reaction $N_2(v > 12) + O(^3P) \longrightarrow NO + N(^4S)$ (9). The arrows in figure and the corresponding time values indicate the instant at which the values of Table 4 are calculated

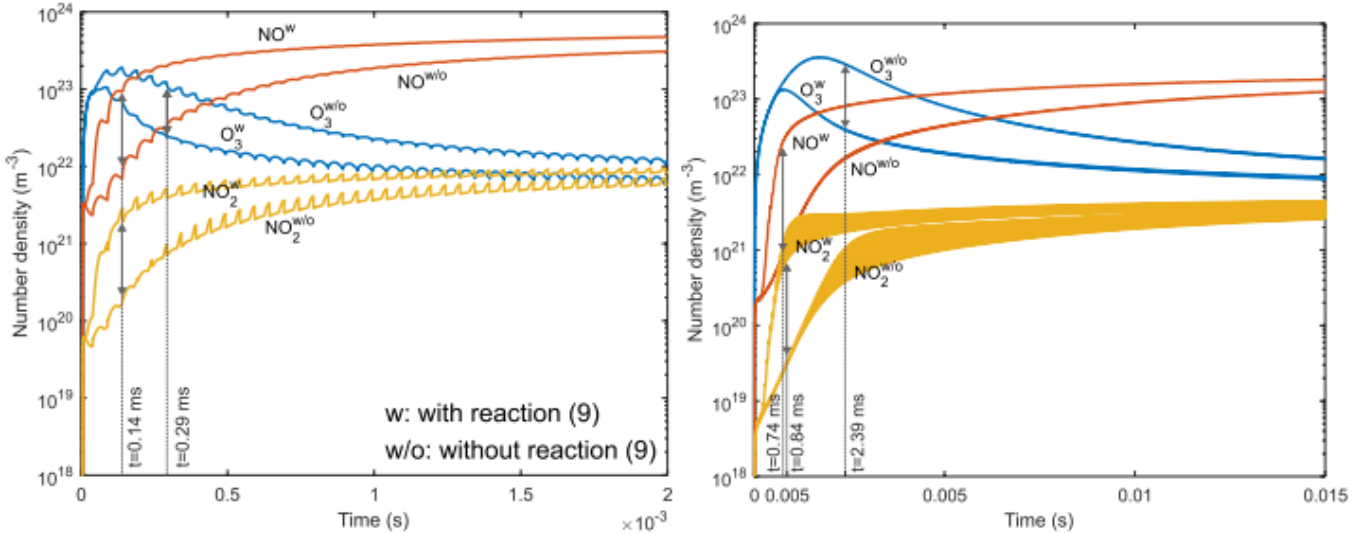

(a) $P_1 = 2.7 \times 10^6\ \mathrm{W/m^3}$

(b) $P_2 = 1.35 \times 10^5\ \mathrm{W/m^3}$

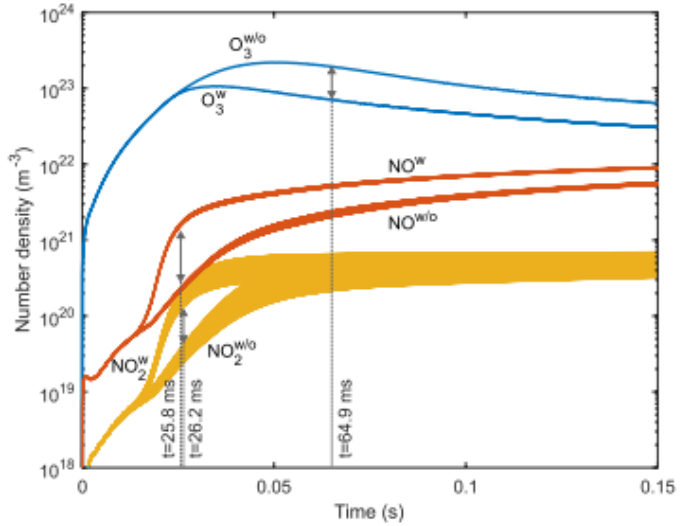

(c) $P_3 = 1.45 \times 10^3\ \mathrm{W/m^3}$

Fig. 11 Comparison between O_3, NO and NO_2 behavior for different levels of input power densities with and without reaction $N_2(v > 12) + O(^3P) \longrightarrow NO + N(^4S)$ (9). The arrows in figure and the corresponding time values indicate the instant at which the values of Table 4 are calculated

OPEN ACCESS
IOP Publishing
Plasma Sources Science and Technology
Plasma Sources Sci. Technol. **34** (2025) 105012 (21pp)
https://doi.org/10.1088/1361-6595/ae0765

Nanosecond-pulsed volume DBD plasma in saturated humid air: a combined experimental and computational study using EFISH and LIF

Lorenzo Ibba[1,*], Giacomo Pierotti[2], Arturo Popoli[2], Domenico Aceto[3], Carlos D Pintassilgo[4,5], Andrea Cristofolini[2], Paolo F Ambrico[3] and Ivo Furno[1]

$78\%N_2\text{-}19\%O_2\text{-}3\%H_2O$

users of global models typically employ one of the following approaches to estimate $E(t)/N$:

- Calculate $E(t)/N$ (and, if necessary, the electron number density) by ensuring consistency with the experimentally measured electrical power absorbed by the device [42, 47].
- Use an equivalent electric circuit approach (see, e.g. [41, 48]) to derive $E(t)/N$ from the applied voltage $v(t)$.
- Incorporate experimental data directly describing the behavior of the electric field, as implemented in this work.

users of global models typically employ one of the following approaches to estimate $E(t)/N$:

- Calculate $E(t)/N$ (and, if necessary, the electron number density) by ensuring consistency with the experimentally measured electrical power absorbed by the device [42, 47].
- Use an equivalent electric circuit approach (see, e.g. [41, 48]) to derive $E(t)/N$ from the applied voltage $v(t)$.
- Incorporate experimental data directly describing the behavior of the electric field, as implemented in this work.

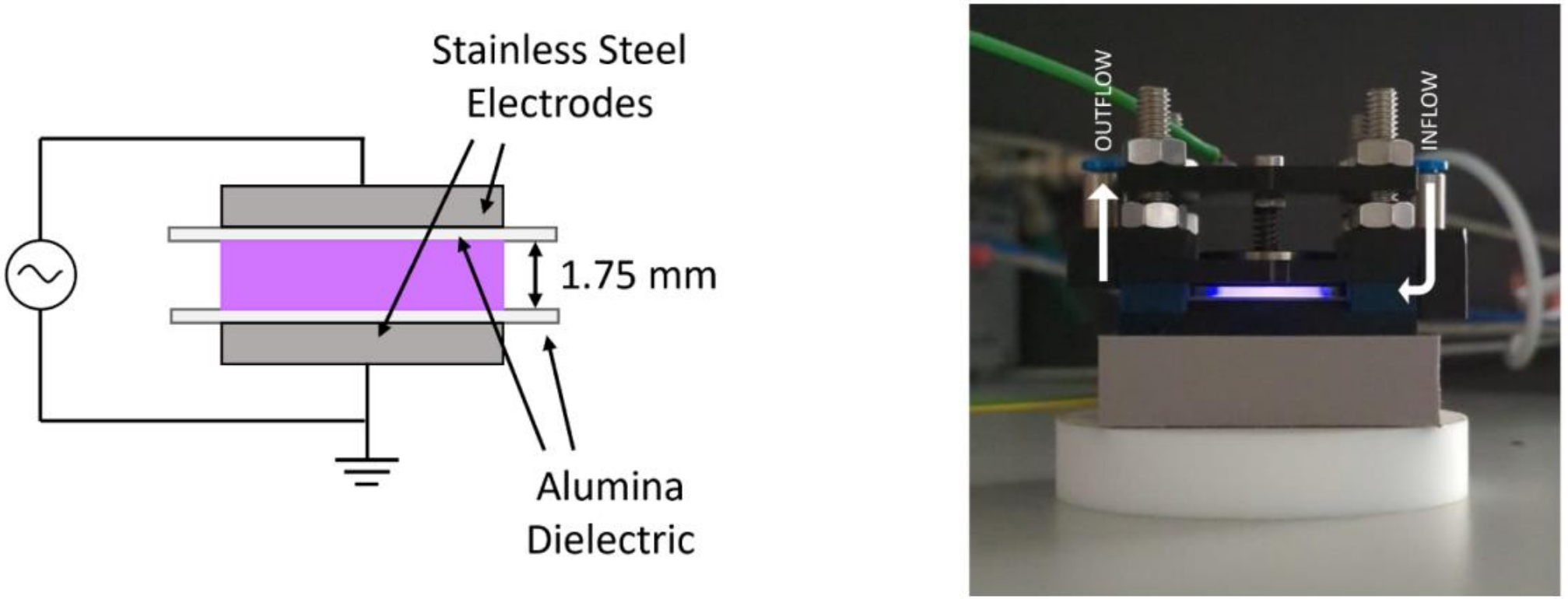

(a) (b)

Figure 1. (a) Schematic of the VDBD components. (b) Picture of the operating VDBD with the schematics of the inflow and outflow positions.

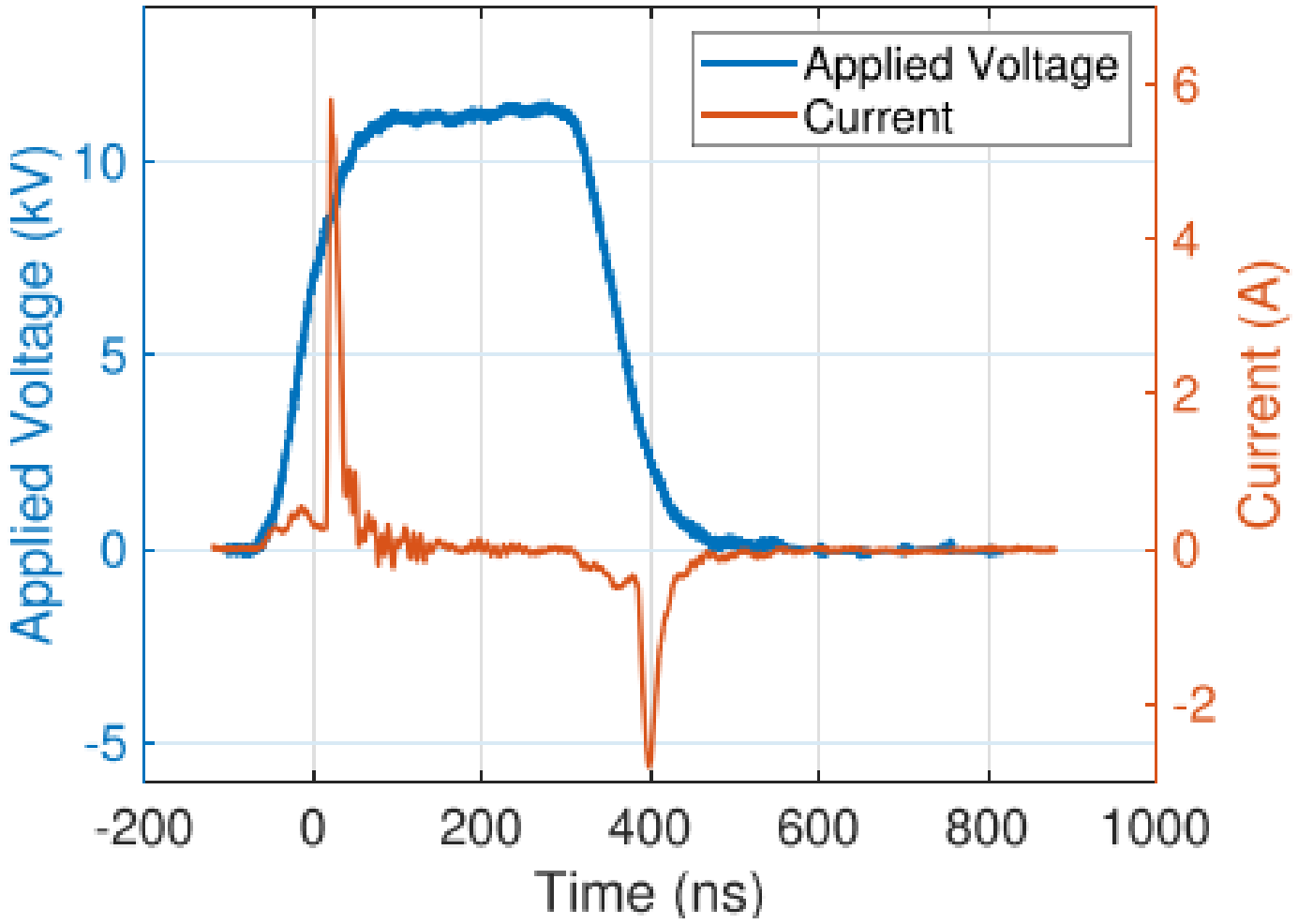

200 ns HV pulse at approximately 11.6 kV

Repetition frequency of 1 kHz

Rise/fall time of approximately 50 ns

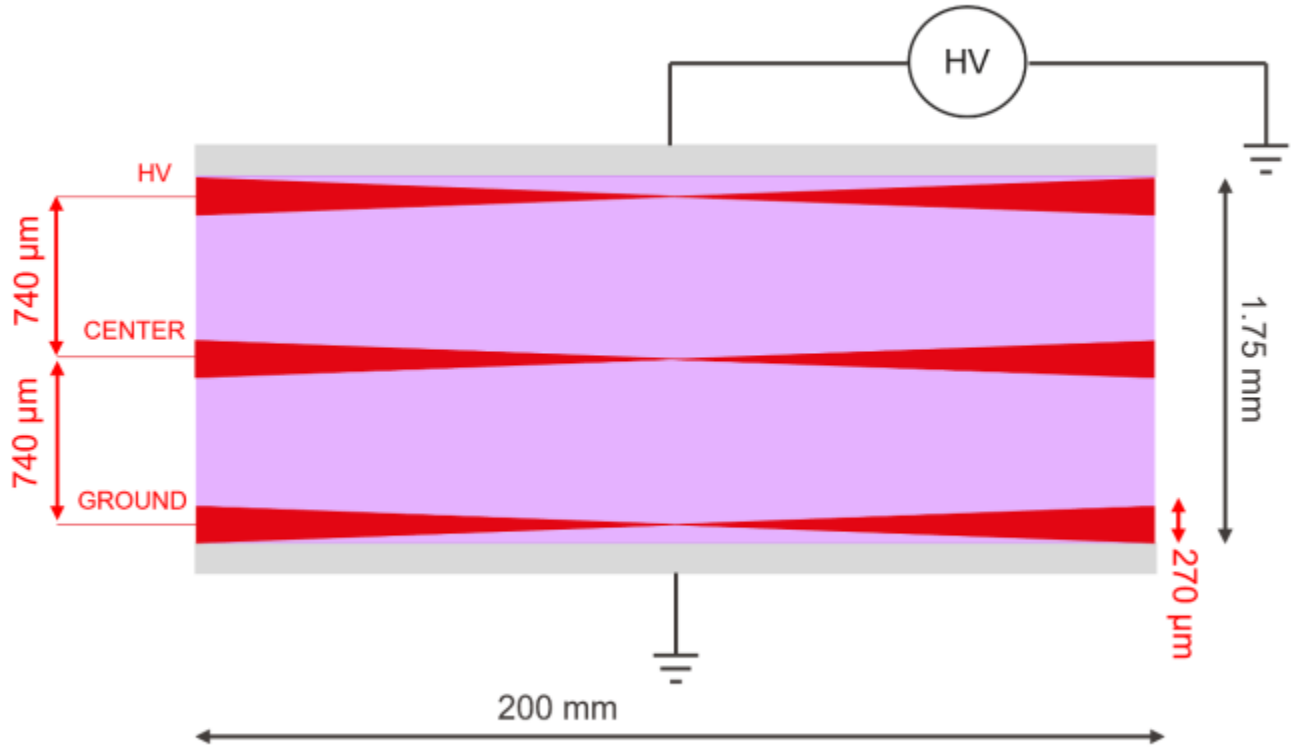

Figure 8. Position of the laser beam passing in the inter-electrode gap of the VDBD. The scheme shows the three distinct positions used for the EFISH measurements: Center, HV and Ground. The diagram also highlights that the beam width at the edge of the VDBD electrode measures approximately 270 μm.

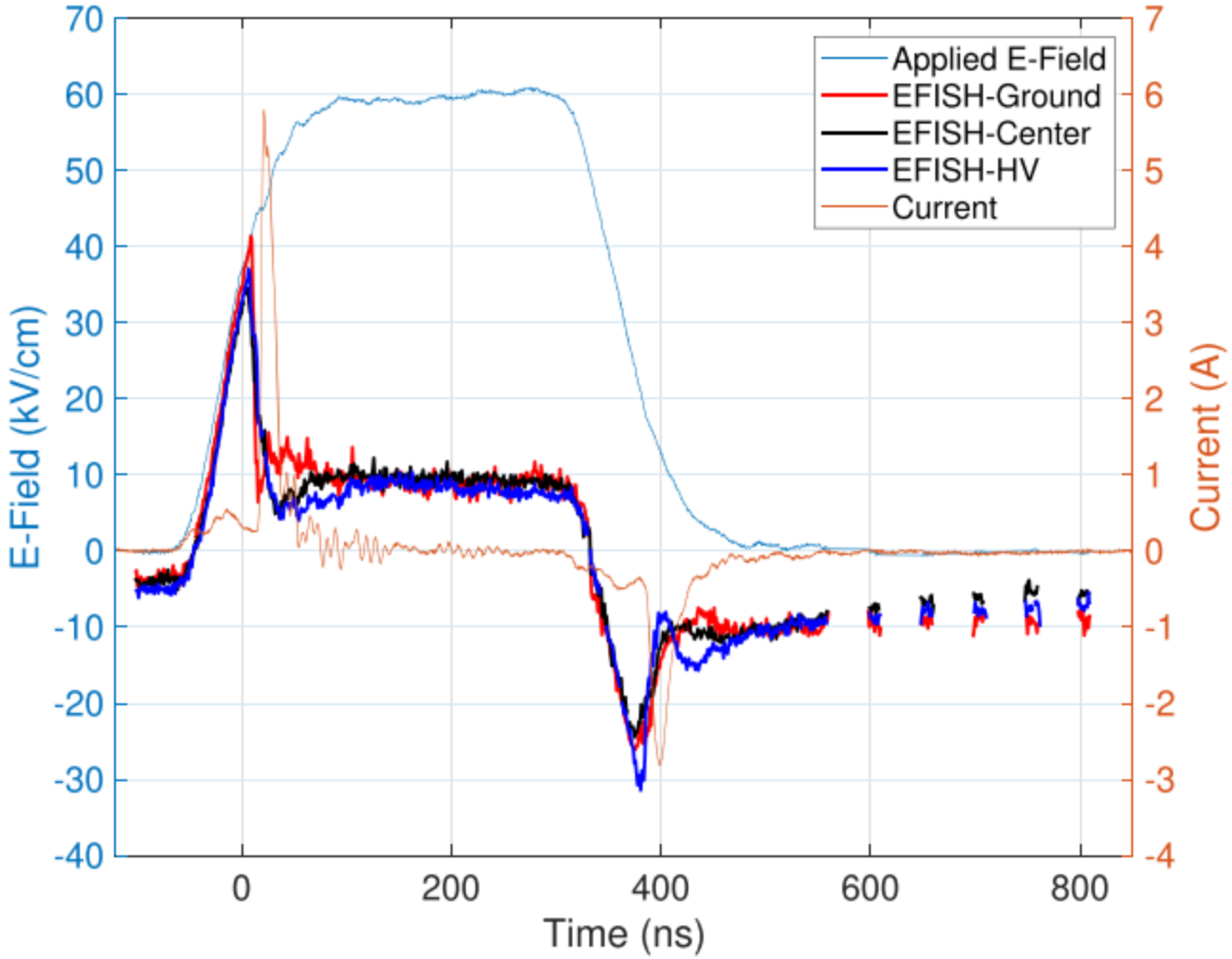

Figure 9. Calibrated and binned over 1 ns intervals EFISH measurements at the three different positions, namely Ground, Center and HV, within the inter-electrode gap of the VDBD. The applied electric field and the current are also reported.

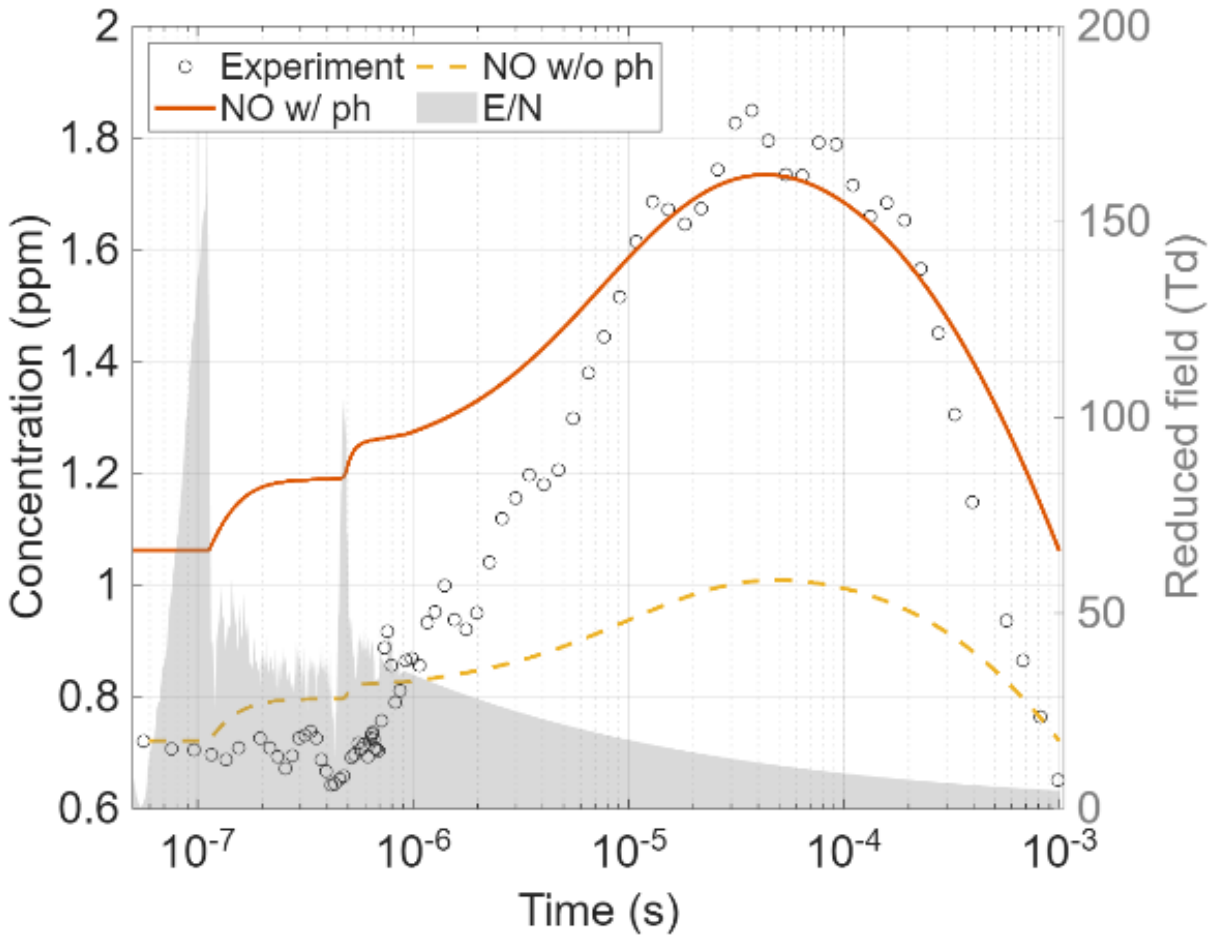

Modelling results obtained using the MERLINO code developed at the University of Bologna, where the rate coefficients of the electron impact reactions are obtained from LoKI -B for different values of the measured reduced electric field (in gray).

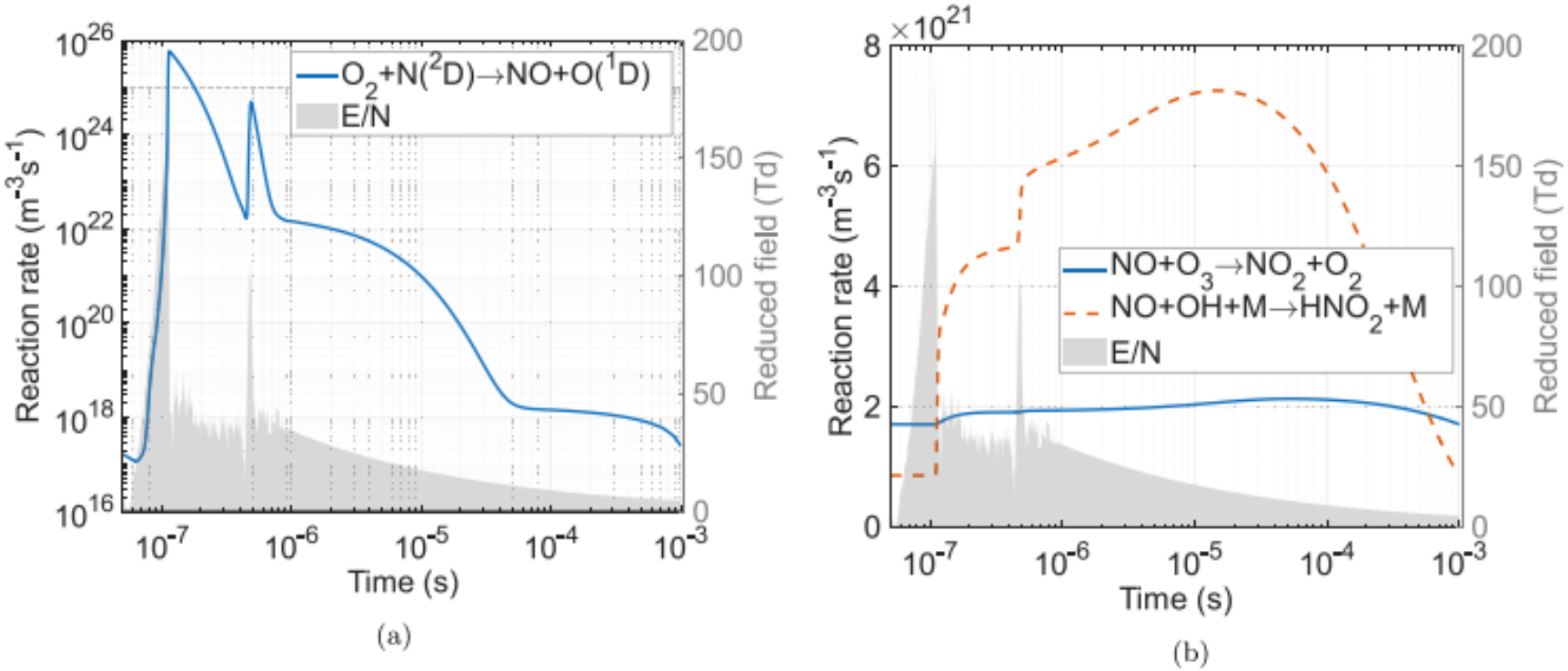

Figure 13. (a) Reaction rates for the main formation (a) and loss (b) mechanisms of NO. M represents N_2, O_2 and H_2O; E/N is the reduced electric field used in the simulation, inferred from EFISH measurements.

Modelling results obtained using the MERLINO code developed at the University of Bologna, where the rate coefficients of the electron impact reactions are obtained from LoKI -B for different values of the measured reduced electric field (in gray).

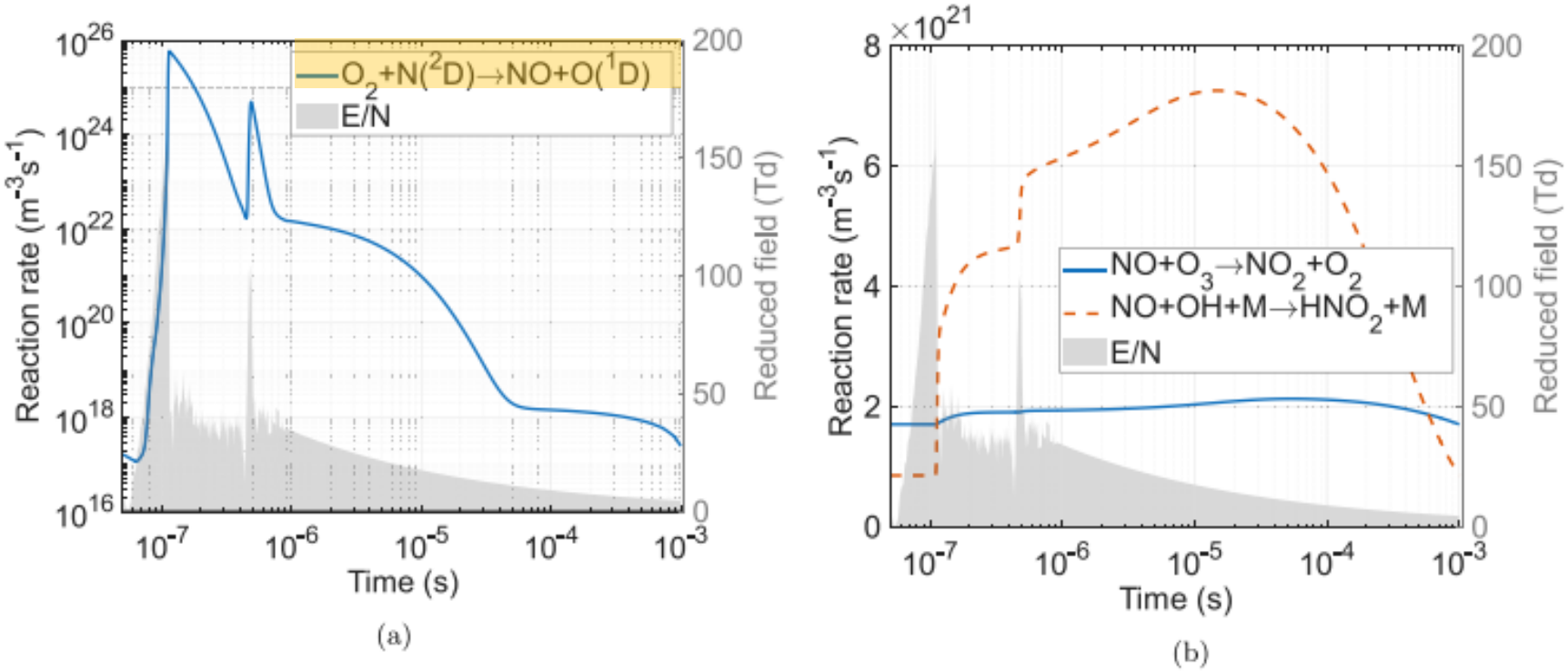

Figure 13. (a) Reaction rates for the main formation (a) and loss (b) mechanisms of NO. M represents N_2, O_2 and H_2O; E/N is the reduced electric field used in the simulation, inferred from EFISH measurements.

Modelling results obtained using the MERLINO code developed at the University of Bologna, where the rate coefficients of the electron impact reactions are obtained from LoKI -B for different values of the measured reduced electric field (in gray).

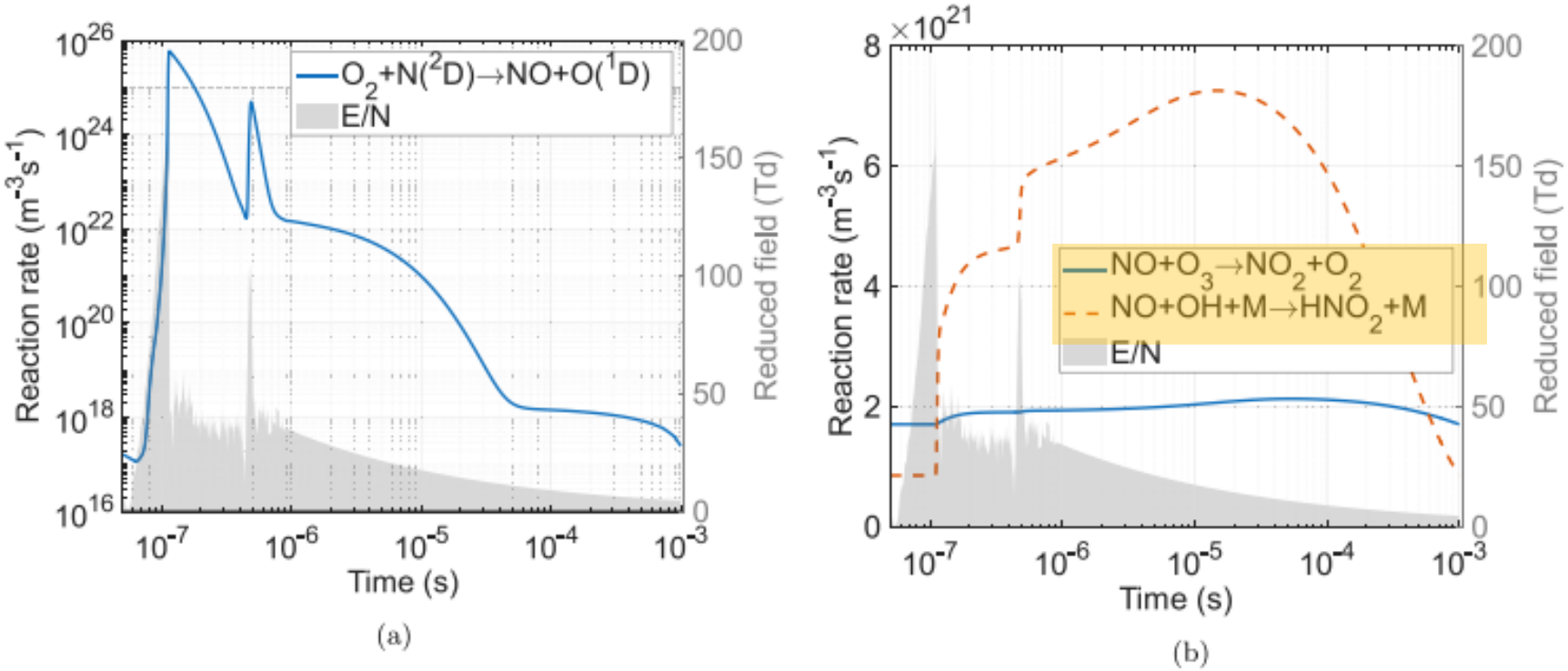

Figure 13. (a) Reaction rates for the main formation (a) and loss (b) mechanisms of NO. M represents N_2, O_2 and H_2O; E/N is the reduced electric field used in the simulation, inferred from EFISH measurements.

Modelling results obtained using the MERLINO code developed at the University of Bologna, where the rate coefficients of the electron impact reactions are obtained from LoKI -B for different values of the measured reduced electric field (in gray).

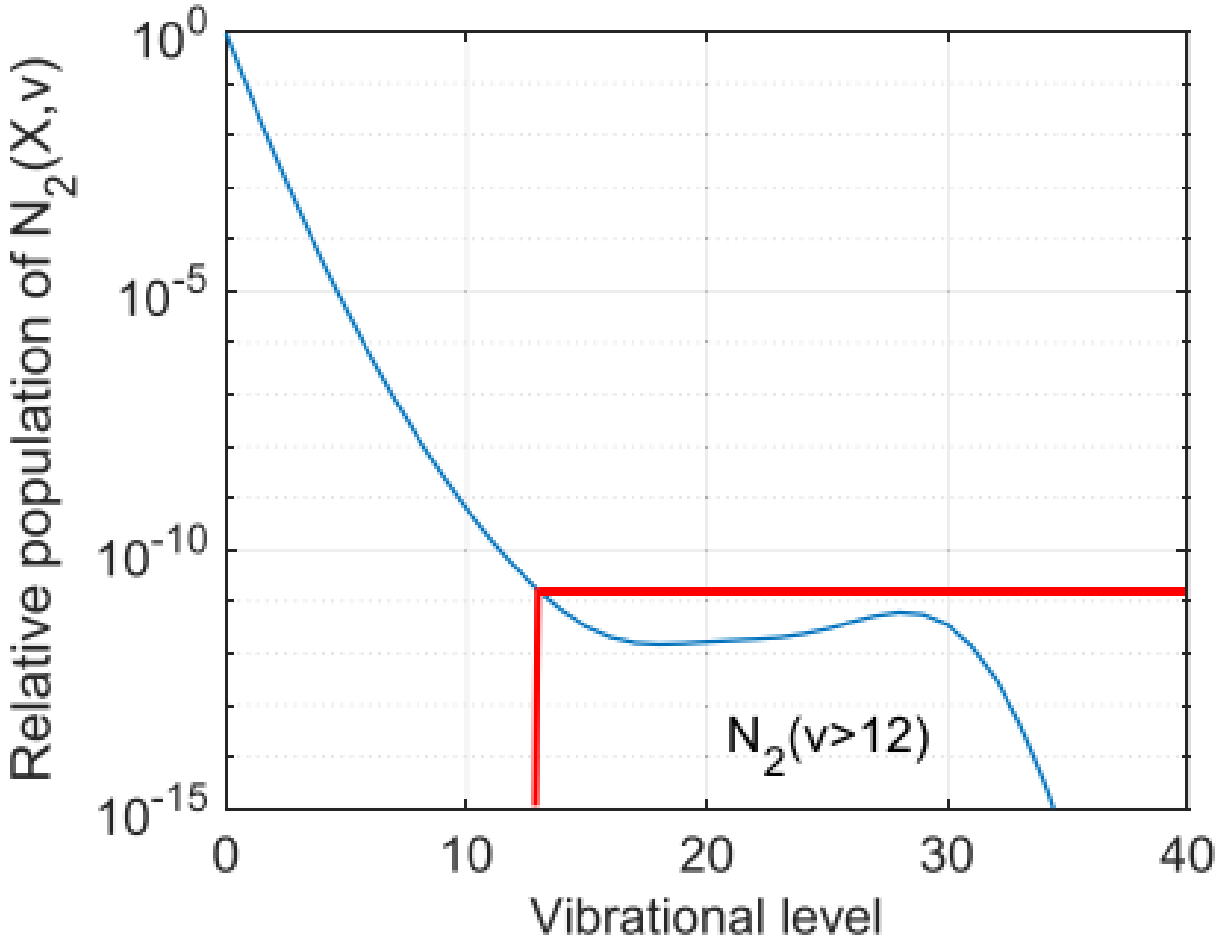

Figure 14. Vibrational distribution function of N_2 molecules immediately before the ignition of a voltage pulse. The part of the VDF contributing to NO formation is highlighted in red.

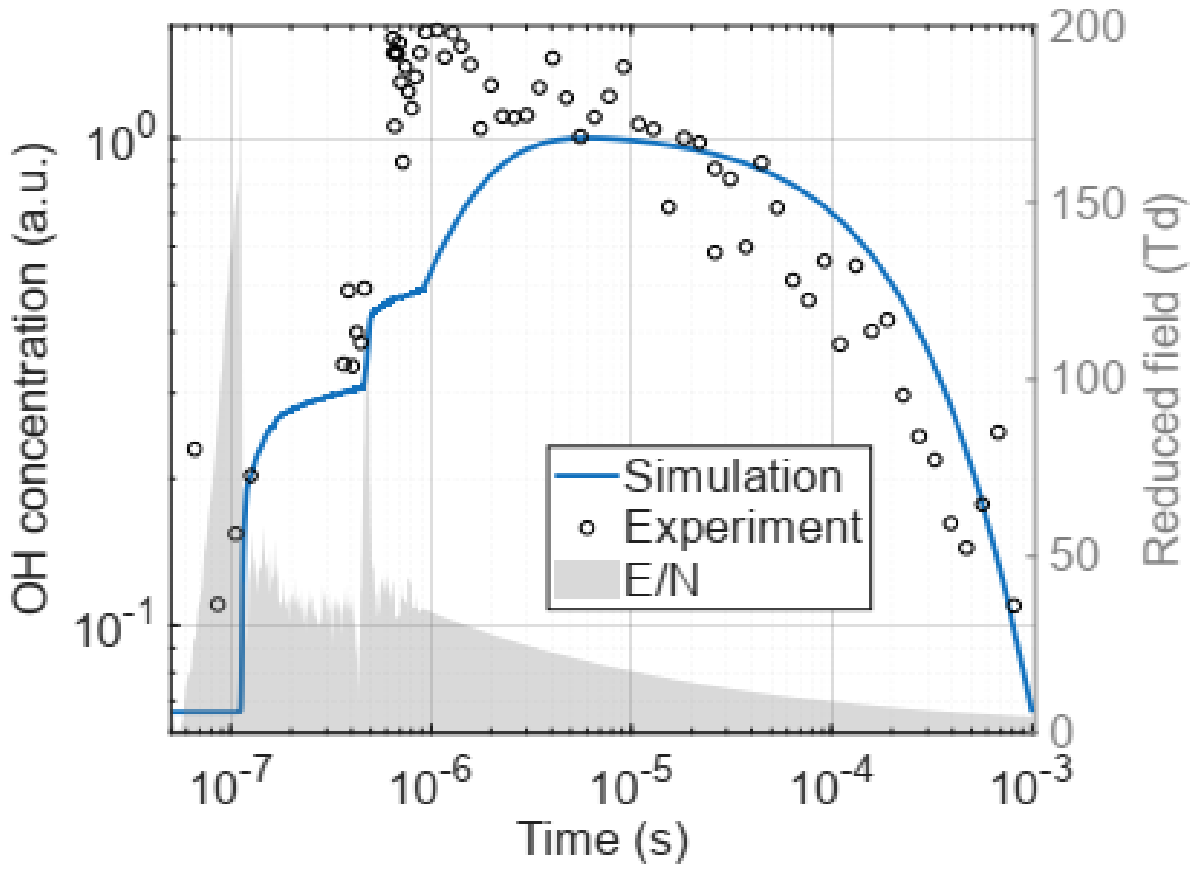

Modelling results obtained using the MERLINO code developed at the University of Bologna, where the rate coefficients of the electron impact reactions are obtained from LoKI -B for different values of the measured reduced electric field (in gray).

OH creation:

$O(^1D) + H_2O \rightarrow 2OH$

$N(^2D) + H_2O \rightarrow OH + NH$

with a minor contribution:

$e + H_2O \rightarrow e + OH + H$

$OH^- + O_3 \rightarrow O_3^- + OH$

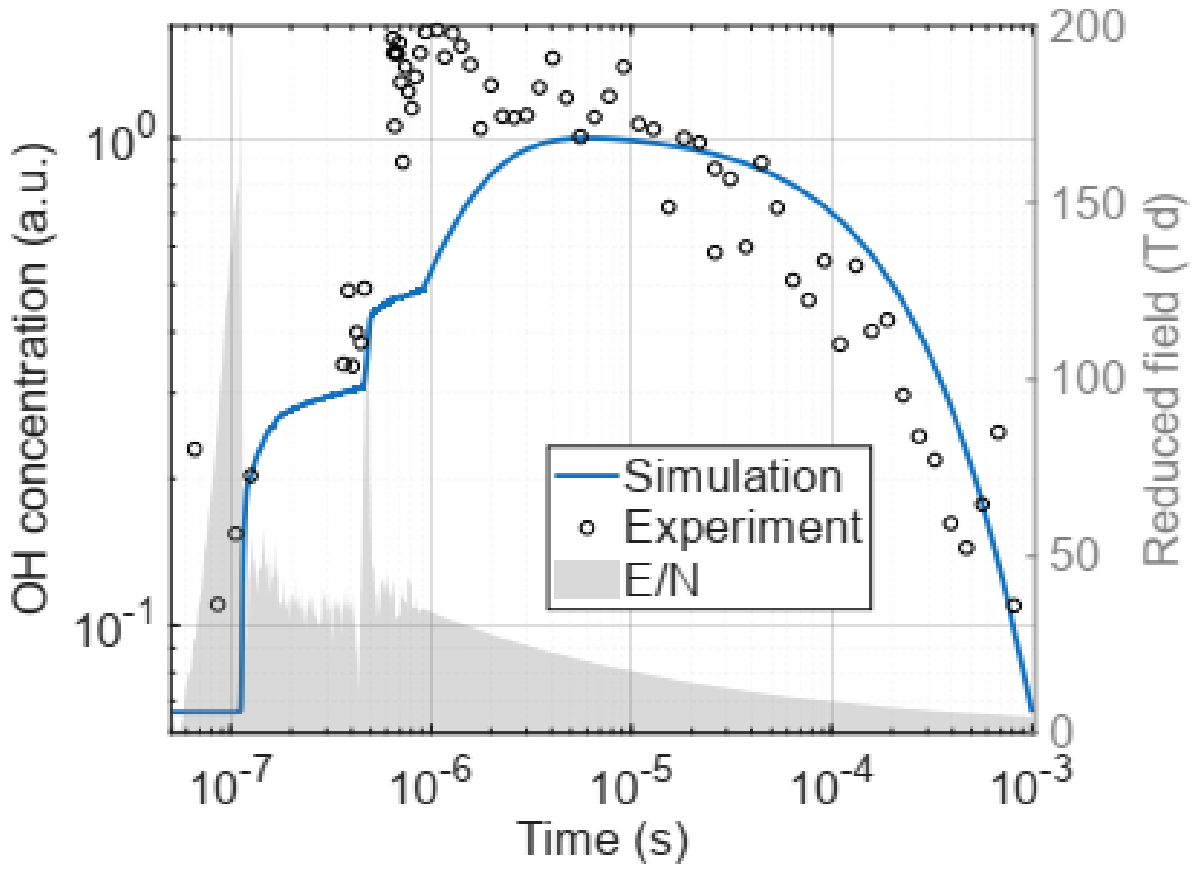

Modelling results obtained using the MERLINO code developed at the University of Bologna, where the rate coefficients of the electron impact reactions are obtained from LoKI -B for different values of the measured reduced electric field (in gray).

OH creation:

$O(^1D) + H_2O \rightarrow 2OH$

$N(^2D) + H_2O \rightarrow OH + NH$

with a minor contribution:

$e + H_2O \rightarrow e + OH + H$

$OH^- + O_3 \rightarrow O_3^- + OH$

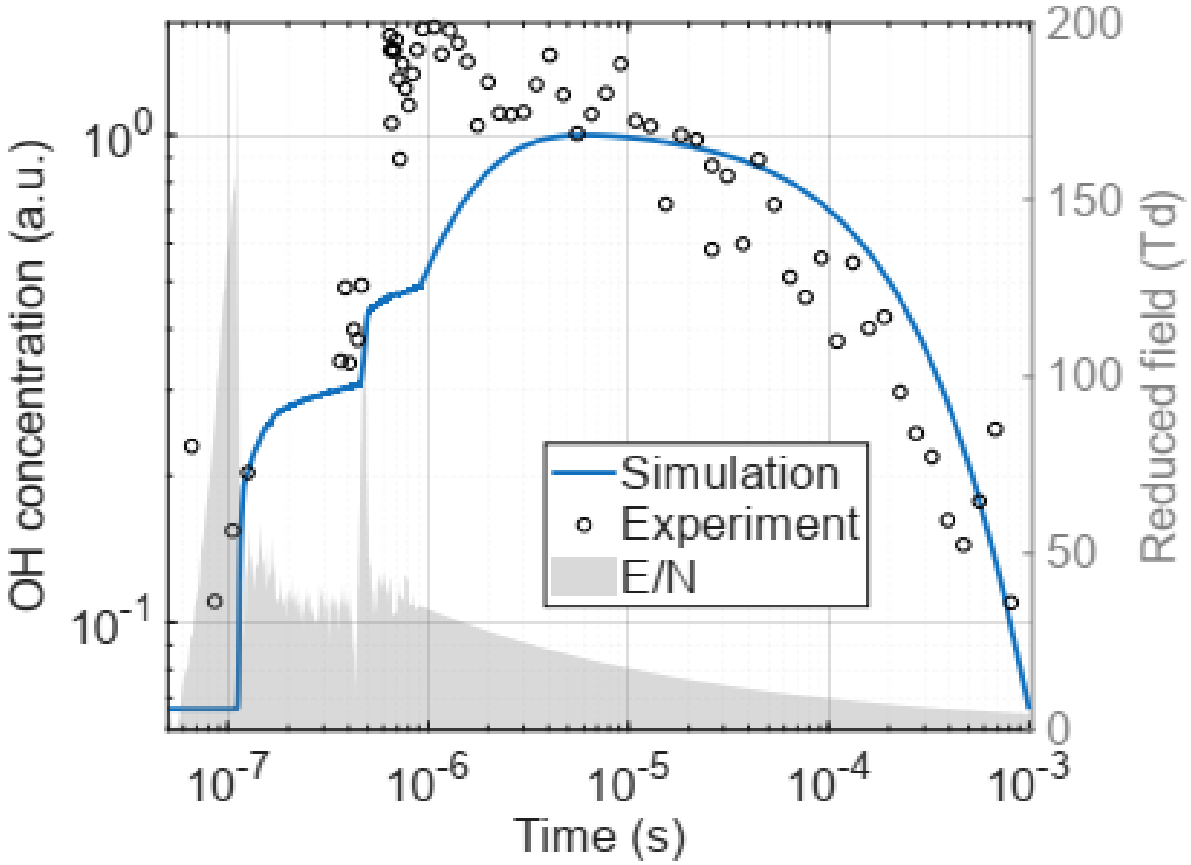

OH losses:

For shorter times, after ignition:

$O(^3P) + OH \rightarrow H + O_2$

For longer times:

$OH + HO_2 \rightarrow O_2 + H_2O$

$OH + NO_2 + (M) \rightarrow HNO_3 + (M)$

$O_3 + OH \rightarrow HO_2 + O_2$

$OH + HNO_2 \rightarrow NO_2 + H_2O$

Modelling results obtained using the MERLINO code developed at the University of Bologna, where the rate coefficients of the electron impact reactions are obtained from LoKI -B for different values of the measured reduced electric field (in gray).

Thank you for your attention !!

Funding institution

doi.org/10.54499/2022.04128.PTDC

QUESTIONS ?